

ARMY RESEARCH LABORATORY

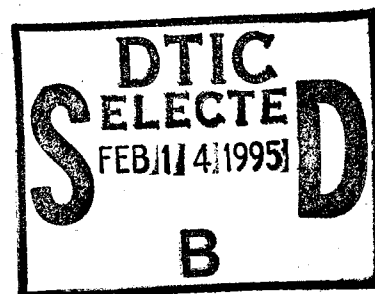


# Fractography of Advanced Structural Ceramics: Results From The VAMAS Round Robin Exercise

Jeffrey J. Swab and George Quinn

ARL-TR-656

December 1994



19950206 228

Approved for public release; distribution unlimited.

The findings in this report are not to be construed as an official Department of the Army position unless so designated by other authorized documents.

Citation of manufacturer's or trade names does not constitute an official endorsement or approval of the use thereof.

Destroy this report when it is no longer needed. Do not return it to the originator.

# REPORT DOCUMENTATION PAGE

Form Approved  
OMB No. 0704-0188

Public reporting burden for this collection of information is estimated to average 1 hour per response, including the time for reviewing instructions, searching existing data sources, gathering and maintaining the data needed, and completing and reviewing the collection of information. Send comments regarding this burden estimate or any other aspect of this collection of information, including suggestions for reducing this burden, to Washington Headquarters Services, Directorate for Information Operations and Reports, 1215 Jefferson Davis Highway, Suite 1204, Arlington, VA 22202-4302, and to the Office of Management and Budget, Paperwork Reduction Project (0704-0188), Washington, DC 20503.

1. AGENCY USE ONLY (Leave blank)		2. REPORT DATE December 1994	3. REPORT TYPE AND DATES COVERED Final Feb. 93 - June 94	
4. TITLE AND SUBTITLE Fractography of Advanced Structural Ceramics: Results From the VAMAS Round Robin Exercise			5. FUNDING NUMBERS	
6. AUTHOR(S) Jeffrey J. Swab and *George D. Quinn				
7. PERFORMING ORGANIZATION NAME(S) AND ADDRESS(ES) Army Research Laboratory Watertown, MA 02172-0001 AMSRL-MA-CA			8. PERFORMING ORGANIZATION REPORT NUMBER  ARL-TR-656	
9. SPONSORING/MONITORING AGENCY NAME(S) AND ADDRESS(ES) VAMAS (Versailles Project on Advanced Materials and Standardization)			10. SPONSORING/MONITORING AGENCY REPORT NUMBER  VAMAS Technical Report #19	
11. SUPPLEMENTARY NOTES  *George D. Quinn, National Institute of Standards and Technology, Gaithersburg, MD 20899				
12a. DISTRIBUTION/AVAILABILITY STATEMENT  Approved for public release; distribution unlimited.			12b. DISTRIBUTION CODE	
13. ABSTRACT (Maximum 200 words)  SEE REVERSE				
14. SUBJECT TERMS  Advanced Ceramics, Fractography, Fracture Mechanics, Fracture Origins			15. NUMBER OF PAGES 141	
			16. PRICE CODE	
17. SECURITY CLASSIFICATION OF REPORT Unclassified	18. SECURITY CLASSIFICATION OF THIS PAGE Unclassified	19. SECURITY CLASSIFICATION OF ABSTRACT Unclassified	20. LIMITATION OF ABSTRACT UL	

## ***Abstract***

Fractography of ceramic specimens and components is critical to the design and future use of ceramic materials in commercial applications. In 1992 the U.S. Department of Defense released Military Handbook 790 "Fractography and Characterization of Fracture Origins in Advanced Structural Ceramics" which furnished guidelines for the comprehensive interpretation of ceramic fractographic information. Even with the release of this handbook there were still some issues which warranted further study.

A round robin exercise sponsored by the Versailles Project on Advanced Materials and Standards (VAMAS) was conducted to determine the applicability of the handbook and to attempt to clarify any ambiguous sections or issues. The exercise was divided into three topics. Topic #1 addressed the detection and interpretation of machining damage on photographs of ceramic specimens. Topic #2 dealt with the fractographic analysis of ceramic specimens. Topic #3 was optional, and asked the participants to perform fractography on a ceramic material of their choice.

The results from Topic #1 showed that there are problems in detecting and interpreting machining damage in advanced ceramics. These problems stem from a lack of understanding of how machining damage can manifest itself in various ceramic materials. Topic #2 indicated that the guidelines and characterization scheme outlined in the handbook are adequate to completely characterize fracture origins in ceramics but some refinements are necessary. There was a good to excellent consensus in origin characterization in many cases. The instances where concurrence was not forthcoming helped the organizers understand where improvements to MIL HDBK-790 should be made and also highlighted the key steps that are integral to a proper fractographic evaluation.

This report summarizes the results from this round robin exercise, identifies areas of concern which require further study, provides amendments that will be made to the handbook and evaluates each of the round robin participants fractographic analysis.



## Preface

Scientists and engineers in the ceramic community traditionally have used the terms "flaw" or "defect" to describe the fracture initiation site in ceramics and other brittle materials. These terms are used in the context of fracture mechanics whereby a singularity or microstructural irregularity acts as a stress raiser from which fracture commences. It should be understood that the use of these terms does not imply that a ceramic product has been prepared improperly or is somehow defective.

The general user community might be better served if the terms "fracture origin" or "origin" are used instead. Therefore, we have refrained from using the terms "flaw" or "defect" wherever possible in this report, except in instances where they are included in direct quotations from the round robin participants or as part of a referenced document.

Jeffrey J. Swab  
George D. Quinn

<b>Accession For</b>	
NTIS GRA&I	<input checked="checked" type="checkbox"/>
DTIC TAB	<input type="checkbox"/>
Unannounced	<input type="checkbox"/>
Justification	
By	
Distribution	
Availability Codes	
Dist	Avail and/or Special

## **Contents**

Preface .....	i
Introduction .....	1
Questionnaire - Participants Background Information .....	4
<b>Topic #1: Characterization of Machining Damage .....</b>	<b>9</b>
Objective .....	9
Background .....	9
Machining Damage .....	9
Estimating the Fracture Origin Size .....	9
Estimating the Fracture Mirror Size .....	10
Approach .....	10
Instructions .....	12
Results .....	12
Overall Comments .....	12
Photograph Set #1: Zirconia/Alumina Composite (TSZ-14) ..	12
Photograph Set #2: Silicon Nitride (SN-5) .....	18
Photograph Set #3: Alumina (RR8) .....	22
Discussion .....	27
Conclusion .....	36
<b>Topic #2: Characterization of Fracture Origins in Specimens .....</b>	<b>38</b>
Objective .....	38
Background .....	38
Approach .....	38
Instructions .....	39
Results and Discussion .....	39
Specimen 1: Large Grains in Alumina w/SiC Whiskers .....	39
Specimen 2: Handling Damage in Alumina .....	49
Specimen 3: Pore in Zirconia .....	52
Specimen 4: Pit in Silicon Carbide .....	58
Specimen 5: Machining Damage in Silicon Nitride .....	62
Specimen 6: Porous Seam or Porous Region in .....	69
Titanium Diboride	
Summary .....	73
Conclusions .....	74
<b>Topic #3: Participants' Evaluation of Their Own Material .....</b>	<b>77</b>
Objective .....	77
Approach .....	77
Instructions .....	77
Discussion .....	77

Participant 2 - $\beta$ -Silicon Carbide .....	77
Participant 6 - Silicon Nitride .....	81
Participant 10 - Silicon Nitride w/Titanium Nitride .....	81
Participant 11 - Silicon Nitride and Alumina .....	87
Synopsis .....	95
General Conclusions.....	95
Amendments to MIL HDBK-790 .....	95
Proposed Future Work.....	97
Acknowledgments .....	97
References .....	98
Appendices .....	102
1: Instructions for the Round Robin.....	102
2: Factors Which Complicate the Comparison of the Measured ..... Fracture Origin Size to the Fracture Mechanics Size Estimate	108
3: Synopses of Laboratory Responses, Topics #1 and #2.....	119

### ***Figures***

1. Relationship of fractographic analysis with mechanical property .....2  
testing and statistical analysis.
  
- 1.1. Schematic diagram of how the shape factor (Y) varies at the ..... 11  
depth and surface as the shape of a surface-located origin changes  
from a semicircle to an elongated semiellipse. The shape factor is  
determined by the Newman-Raju<sup>12</sup> analysis. It is assumed that the  
cracks are small relative to the specimen thickness. Note that the  
maximum stress intensity factor is at the surface intersection of the  
semicircular precrack, but for semiellipses, it shifts to the deepest part  
of the precrack periphery and becomes larger in magnitude as the  
semiellipse becomes elongated.
  
- 1.2. The three pairs of photographs for Set #1 (TSZ-14) which ..... 13  
were provided to the participants. "T" denotes the tensile surface.
  
- 1.3. High magnification photographs of one half of the fracture ..... 16  
surface from Set #1 (TSZ-14). A) Unmarked. B) The organizers  
outlined two possible semicircular origins. Arrows indicate possible  
striations on tensile surface. C) The organizers outlined a possible  
semielliptical origin. "T" denotes the tensile surface.

- 1.4. The three pairs of photographs for Set #2 (SN-5) which were ..... 19  
provided to the participants. "T" denotes the tensile surface.
- 1.5. High magnification photographs of one half of the fracture ..... 21  
surface from Set #2 (SN-5). A) Unmarked. B) The organizers  
outlined three possible semicircular origins. Arrows indicate possible  
striations on tensile surface. C) The organizers outlined a possible  
semielliptical origin. "T" denotes the tensile surface.
- 1.6. The three pairs of photographs for Set #3 ( $\text{Al}_2\text{O}_3$ -RR8) which ..... 23  
were provided to the participants. "T" denotes the tensile surface and  
"Ch" the chamfer.
- 1.7. High magnification photographs of one half of the fracture ..... 26  
surface from Set #3 ( $\text{Al}_2\text{O}_3$ -RR8). A) Unmarked. B) Three stages  
of fracture are outlined by the organizers. Stage 1 is transgranular  
fracture, Stage 2 is subcritical crack growth and Stage 3 is fast fracture.  
Open arrows indicate the irregular section of the chamfer. "T" denotes  
the tensile surface and "Ch" the chamfer.
- 1.8. Schematic example of the effect of crack nesting on the ..... 31  
stress intensity experienced by a crack.
- 2.1.1. Example of Large Grains in Specimen 1: Alumina/SiC ..... 40  
(whiskers). Mating halves of the primary fracture surface are shown.  
"T" denotes the tensile surface.
- 2.1.2. Photographs of large grain fracture origin in specimen 1 from ..... 42  
participant 2 specimen set. A) Participants' photograph. B) Organizers'  
photograph. "T" denotes the tensile surface in B).
- 2.1.3. Optical photograph of alumina grains as the fracture origin in ..... 44  
specimen #1. Origin appears as a dark spot when viewed optically.  
(Arrow added by the organizers.)
- 2.1.4. Photographs of large grain origin in specimen 1 from ..... 45  
participant 4. A) and B) are the participants' photographs. Large grains  
can be seen in B). C) Organizers' photograph. "T" denotes the tensile  
surface. D) Participants' photograph of the possible machining damage.  
(Arrows in B and D were added by the organizers. The handwritten notes  
are the participants comments.)
- 2.1.5. Two of participant 18's photographs of the origin in specimen 1. .... 47  
The origin is clearly located at the surface.

- 2.1.6. Organizers' SEM photograph showing several clusters of large ..... 48 alumina grains in specimen 1. "T" denotes the tensile surface.
- 2.2.1. Example of Handling Damage in Specimen 2: Alumina. .... 51 "T" denotes the tensile surface.
- 2.2.2. Participant 16's photograph of one of the mating halves of the ..... 51 primary fracture surface in specimen 2. The arrow was added by the organizers and points out the scratch (HD<sup>s</sup>) on the tensile surface.
- 2.3.1. Example of a Pore in Specimen 3: Zirconia. "T" denotes the ..... 53 tensile surface.
- 2.3.2. SEM photographs of the pore in specimen 3 from the set sent ..... 55 to participant 3. A) Organizers' photograph. "T" denotes the tensile surface. B) Participant 3's photograph. "+" indicates the "globule" where EDS was done.
- 2.3.3. Participant 5's SEM photograph of the origin in specimen 3. .... 56 Is this a pore or porous region?
- 2.3.4. SEM photographs of specimen 3 from the set sent to participant .... 57 18. A) Participant 18's photograph. The participant used hand drawn arrows to show the pore. B) SEM photograph taken by the organizers' prior to sending the specimen to the participant. C) Organizers' SEM photograph of the fracture origin after it was characterized by the participant and returned to the organizers. Black arrow indicates the pore and white arrow shows where the piece was removed. "T" denotes the tensile surface.
- 2.3.5. SEM photograph, from participant 7, of a pore located at the side .. 59 of the flexure specimen. Appropriate location: Volume (V)\*. \* located at the side of the specimen approximately 175  $\mu\text{m}$  beneath the tensile surface.
- 2.4.1. Example of Pits in Specimen 4: Silicon Carbide. Mating halves ... 61 of the primary fracture surface are shown. "T" denotes the tensile surface.
- 2.4.2. A) Participant 2's SEM photograph of the pit in specimen 4. .... 63 Arrows added by the organizers. B) SEM photograph of a surface void from Military Handbook 790, Figure 33, page 40. Note the similarity.

2.5.1. Example of Machining Damage in Specimen 5: Silicon Nitride. ....	65
Mating halves of the primary fracture surface are shown. "T" denotes the tensile surface.	
2.5.2. Optical photograph from participant 4, of machining related .....	66
chipping on the chamfer of specimen 5. Arrows were added by the organizers.	
2.5.3. SEM photographs of specimen 5. A) Participant 10's .....	68
photograph. B) Organizers' photograph. Arrows point out the machining damage on the tensile surface. "T" denotes the tensile surface.	
2.6.1. Example of Porous Seam/Porous Region in Specimen 6: .....	70
Titanium Diboride. Mating halves of the primary fracture surface are shown. "T" denotes the tensile surface.	
2.6.2. SEM photographs of specimen 6. A) Participant 15's .....	71
photograph. B) Organizers' photographs of the mating halves of the primary fracture surface. The photographs in B) indicate that this origin is a porous region (PRV) and not an agglomerate (AV). "T" denotes the tensile surface.	
2.7. Fractography is like assembling a jigsaw puzzle, if a few key .....	75
pieces are missing then the picture cannot be understood.	
3.1. Participant 2's Weibull plot for a $\beta$ -SiC. See Table 3.1 for the .....	79
individual data.	
3.2. Example of the fracture origin, pore (PV), seen in the $\beta$ -SiC .....	80
analyzed by Participant 2. A) 70X. B) 600X.	
3.3. Combined Weibull plot of surface, internal and chamfer failures .....	83
from the room temperature flexure of the HIPed $\text{Si}_3\text{N}_4$ examined by Participant 6. See Table 3.2 for the individual data.	
3.4. Examples of the fracture origins seen in the HIPed $\text{Si}_3\text{N}_4$ .....	84
analyzed by Participant 6. A) Specimen LP-37, Surface at surface?	
B) Specimen LP-29, Chip located at the edge. C) Specimen LP2-26, Inclusion located in the volume.	
3.5. Weibull plot of room temperature strength data generated by .....	86
participant 10 on a $\text{Si}_3\text{N}_4/\text{TiN}$ material. Plot shows two possible origin populations. See Table 3.3 for the individual data.	

- 3.6. Example of an origin in a  $\text{Si}_3\text{N}_4/\text{TiN}$  specimen. Labeled by .....88  
participant 10 as a crack.
- 3.7. Example of an origin in a  $\text{Si}_3\text{N}_4/\text{TiN}$  specimen. Labeled by .....89  
participant 10 as a porous region.
- 3.8. Fracture origin in specimen 2 for a  $\text{Si}_3\text{N}_4/\text{TiN}$  specimen. Labeled ....90  
by participant 10 as machining damage.
- 3.9. Origins in a sintered-SiC from participant 11. A) Optical .....91  
photograph taken at 25X using grazing incident illumination. B)  
and C) Optical photographs of the mating halves of the fracture  
surface showing the origin. Taken at 100X under mixed lighting.  
Note large grains with river lines.
- 3.10. Origins in an alumina from participant 11. A) Optical .....93  
photograph of the mating halves of the primary fracture surface,  
taken at 25X using grazing incident illumination. B) and C) Optical  
photographs of the mating halves of the fracture surface showing  
the origin. Taken at 100X under mixed lighting.
- A2.1 Slow crack growth may cause an origin to grow. Fracture .....114  
occurs when the crack has extended to the critical size which should be  
the same as the size predicted from fracture mechanics ( $c_{\text{calc}}$ ). If the  
SCG zone is not detected, then it will appear that  $c_{\text{calc}}$  is larger than  $c_{\text{meas}}$ .
- A2.2 A origin can link-up with other discontinuities or with a free .....115  
surface. The calculated size ( $c_{\text{calc}}$ ) will be larger than the size of the  
original or initially-obvious origin feature ( $c_{\text{meas}}$ ).
- A2.3 Nested, overlapping cracks can lead to a reduction in the stress .....116  
intensity (Y) at any single crack. In this case  $c_{\text{calc}}$  will underestimate  
the crack size measured on the fracture surface.
- A2.4 Staggered or aligned cracks can cause the stress intensity (Y) to ....116  
be magnified at the fracture origin.  $c_{\text{calc}}$  will overestimate the measured  
crack size ( $c_{\text{meas}}$ ).
- A2.5 Discontinuities in the vicinity of the fracture origin can increase or ...117  
decrease the stress intensity (Y) and result in  $c_{\text{calc}}$  being either and  
over- or underestimate of  $c_{\text{meas}}$ .
- A2.6 The origin may be truncated on the fracture surface, and its size .....118  
( $c_{\text{meas}}$ ) may be underestimated during the fractographic analysis.

## ***Tables***

1.	Round Robin Participants .....	3
Q.1	Participants' Fractographic Experience Level .....	5
Q.2	Participants' Fractographic Experience with Ceramic Materials .....	6
1.1	Participants' Results from Photograph Set #1: Zirconia/Alumina .... (TSZ-14)	14
1.2	Participants' Results from Photograph Set #2: Silicon Nitride .....	20
	(SN-5)	
1.3	Participants' Results from Photograph Set #3: Alumina (RR-8) .....	24
1.4	Mirror Constants for the Three Ceramics in Topic #1 .....	35
1.5	Mirror Size Ranges for the Three Ceramic Specimens in .....	35
	Topic #1	
2.1	Participants' Results from Specimen #1: Large Grains in .....	41
	Alumina w/SiC whiskers	
2.2	Participants' Results from Specimen #2: Handling Damage in .....	50
	Alumina	
2.3	Participants' Results from Specimen #3: A Pore in Zirconia .....	54
2.4	Participants' Results from Specimen #4: A Pit in Silicon Carbide ...	60
2.5	Participants' Results from Specimen #5: Machining Damage in .....	67
	Silicon Nitride	
2.6	Participants' Results from Specimen #6: A Porous Seam or .....	72
	Porous Region in Titanium Diboride	
2.7	Concurrence with Organizers' Evaluation .....	73
3.1	Strength and Fractographic Information for the $\beta$ -SiC Examined .....	78
	by Participant 2	
3.2	Strength and Fractographic Information for the HIPed $\text{Si}_3\text{N}_4$ .....	82
	Examined by Participant 6	



**3.3 Strength and Fractographic Information for a  $\text{Si}_3\text{N}_4/\text{TiN}$  Material ...85**  
**Tested and Examined by Participant 10**

## ***Introduction***

The release of Military Handbook 790 "Fractography and Characterization of Fracture Origins in Advanced Structural Ceramics" (MIL HDBK-790) by the Department of Defense in July 1992 marked the most comprehensive effort to date to standardize the fractographic analysis of advanced ceramics materials. Details on MIL HDBK-790 and the considerations that went into it can be found in references 1 and 2. The objectives of MIL HDBK-790 are two-fold. First, it acts as an educational tool for scientists/engineers venturing into fractography of ceramics for the first time and second, it provides an efficient and consistent methodology to locate and characterize fracture origins in this class of materials.

The fundamentals of fractography of ceramics and glasses are well documented<sup>3-9</sup> but analysis can be interpretive and dependent on the fractographic experience level of the analyst. MIL HDBK-790 attempts to rationalize and guide fractographic analysis of ceramics which will lead to more consistency and clarity in the interpretation and characterization of fracture origins.

The handbook also serves as a bridge between mechanical testing standards and statistical analysis standards to permit comprehensive interpretation of the data for design, Figure 1. Although the procedures described in MIL HDBK-790 are primarily for the analysis of mechanical test specimens loaded in so-called "fast fracture," they can be extended to include other modes of loading and are relevant to component failure analysis.

Painstaking efforts were taken to develop a handbook which addressed the concerns of all types of ceramic engineers (processing, R&D, testing and design) as well as the concerns of those involved in quality control, materials research and development, and design applications. Input from colleagues in these various disciplines was immensely helpful in the formation of this handbook. However, there were still some issues which warranted additional study in order to lead to improvements in the handbook. The ultimate test comes with the use of the handbook and its characterization scheme. To this end, a round robin exercise was organized through the auspices of VAMAS (Versailles Project on Advanced Materials and Standardization). The exercise was designed to evaluate the applicability of the handbook to a range of ceramics, to determine whether the participants could reach a consensus on the characterization of fracture origins, and to solicit suggestions and refinements to the handbook.

There were a total of seventeen agencies/institutes/laboratories which participated in this round robin exercise, Table 1. This group included eight government agencies, one academic institute and eight industrial participants. Eight nations were represented. The exercise was divided into three topics. Topic #1 addressed the detection and interpretation of machining damage on

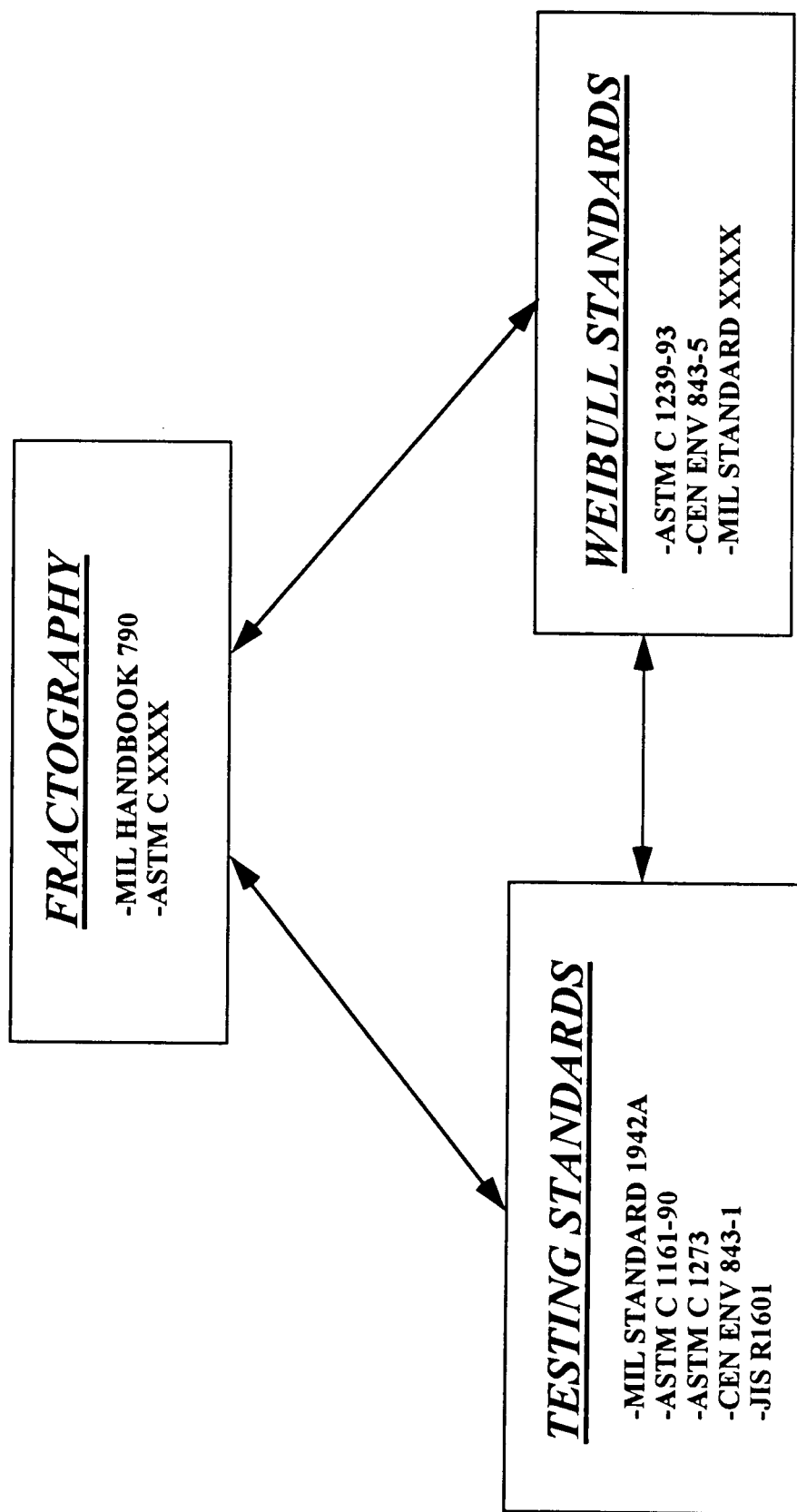


Figure 1. Relationship of fractographic analysis with mechanical property testing and statistical analysis.

photographs of ceramic specimens. Topic #2 dealt with the fractographic analysis of ceramic specimens. Topic #3 was optional, and asked the participants to perform fractography on a ceramic material of their choice.

Table 1.  
**ROUND ROBIN PARTICIPANTS**

<u>COUNTRY</u>	<u>AGENCY</u>	<u>INVESTIGATOR</u>	<u>AFFILIATION*</u>
Belgium	VITO	Dr. W. Vandermeulen	I
France	Desmarquest	Dr. B. Cales	I
Germany	BAM Berlin	Dr. C. Ullner	G
	KfK Karlsruhe	Dr. D. Munz & Dr. T. Fett	G
	FhG Fraunhofer	Dr. T. Hollstein	I
Netherlands	JRC Petten	Dr. M. Steen & Dr. P. Moretto	G
United Kingdom	National Physical Laboratory	Dr. R. Morrell	G
	Morgan Materials Technology Ltd	Mr. R. Stannard	I
USA	NASA-Lewis Research Center	Mr. J. Salem	G
	Allied Signal/Garrett Auxiliary Power	Mr. H. Fang & Dr. J. Wimmer	I
	Alfred University	Dr. J. Varner	A
	Oak Ridge National Laboratory	Dr. K. Breder	G
	Osram-Sylvania	Ms. G. Meyers	I
	W.R. Grace & Co.	Dr. R. Rice	I
	Eaton Corporation	Mr. J. Edler	I
Switzerland	EMPA	Mr. J. Kübler	G
Sweden	SP Boras	Dr. L. Carlsson	G

\* G - Government; I - Industry; A - Academia

The following report outlines the round robin exercise, provides an analysis of the results, describes possible refinements to the handbook, and identifies issues which must be resolved. Each round robin topic is addressed separately within the report but a final section summarizes the overall conclusions and outlines further actions to be taken.

## ***Questionnaire - Participants' Background Information***

Each participant was asked to fill out a questionnaire to provide essential background information on their level of fractographic experience as well as the ceramic materials and fractographic procedures typically used in their laboratory. A copy of the entire questionnaire is shown in Appendix 1 and a synopsis of the information is given below.

*What is the Fractographers' Fractographic Experience?* Since fractography can be interpretive, fractographic skill requires not only a comprehensive understanding of the fundamentals of fractography but hands-on experience as well. Fractography is a continual learning experience and the success of finding and accurately characterizing fracture origins is a function of this experience level.

It was important in this exercise to know the level of experience of each participant. The combined fractographic experience of the participants was over 149 years but as can be seen in Table Q.1 the experience level varies significantly with each participant. Prior to this exercise one participant had never performed fractography, while three others had a year or less of fractographic experience with ceramic materials. At the other extreme, one participant had 27 years of experience, albeit with glasses, while another had 35 years of experience with ceramics and glasses. Eight participants had between 5 and 10 years of experience. The median amount of experience per participant was slightly less than 9 years. It is interesting to note that one participant with 15 years of experience considered himself an "intermittent amateur".

Six participants listed a "combined" experience level. It should be pointed out that one individual with 10 years of fractographic experience is significantly different from several individuals with 10 years of experience between them.

*What is the Fractographers' Experience with Particular Ceramic Materials?* The conduciveness of the ceramic to fractographic analysis varies with each material. Dense, fine-grained or amorphous ceramics are very amenable to fractography since they typically leave distinct fracture markings (mirror and hackle) which will aid in locating the fracture origin. On the other hand, porous or coarse-grained ceramics and lower-energy ceramic fractures will be less conducive because the mirror and hackle are difficult to properly identify if they even exist. In some instances, especially in very strong ceramics, the fracture origin may be extremely small and difficult to differentiate from the normal microstructural features or a critical piece of the fracture surface may have been lost during strength testing.

The participants were asked to indicate their familiarity with a variety of advanced structural ceramics. (Since the handbook is applicable to simple

ceramic composites such as whisker- and particulate-reinforced composites these were included in the ranking.) As can be seen in Table Q.2 many of the participants indicated that a majority of their fractographic experience was obtained by examining fractures in silicon nitride specimens. The least common was titanium diboride. Only four participants indicated they had any experience with this ceramic material. Whisker- and particulate-reinforced ceramics also tended to be very low on the experience list.

Table Q.1  
**PARTICIPANTS' FRACTOGRAPHIC EXPERIENCE LEVEL**

<u>No.*</u>	<u>Experience (Yrs)</u>	<u>Comments</u>
1	6.5	
2	10	
3	10+	Combined experience of 3 people
4	5.5	
5	35	
6	10+	Combined experience of 2 people
7	27	Mostly with glass
8	3	
9	1	
10	7	Investigator plus Institute experience
11	15	"Intermittent amateur"
12	0	First fractographic effort
13	0	
15	1	
16	2	Combined experience of 2 people
17	6	Combined Institute experience??
18	10	Combined Institute experience

Total Experience**	149 years
Median Experience	8.8 years
Minimum Experience	0 years
Maximum Experience	35 years

\* Participant 14 failed to report.

\*\* The organizers had more than 28 years of experience between 2 people. This value is not included in the above calculations.

*Why and How Much Fractography is Typically Done?* MIL HDBK-790 and the questionnaire list three levels of suggested fractographic sampling: Quality Control (Level 1), Materials Research & Development (Level 2), and Design (Level 3). These levels were created because it may not be feasible, practical, or even necessary to examine all fracture surfaces within a given specimen set. Quality control may only require the analysis of specimens which fracture below a given strength level. In contrast, Design might require 100% characterization

Table Q.2  
**PARTICIPANTS' FRACTOGRAPHIC EXPERIENCE WITH CERAMIC MATERIALS**

No.	Al <sub>2</sub> O <sub>3</sub>	SiC	TiB <sub>2</sub>	Si <sub>3</sub> N <sub>4</sub>	ZrO <sub>2</sub>	Whisker	Particulate	Other Comments
1	4	2	3	1	5	--	--	Whisker - Al <sub>2</sub> O <sub>3</sub> /SiC(w)
2	2	4	--	1	5	3	--	Particulate - SiC/RBSN
3	2	3	--	1	--	--	4	Whisker - Si <sub>3</sub> N <sub>4</sub> /SiC(w); Particulate - SiC/TiB <sub>2</sub>
4	2	1	7	3	6	4	5	Whisker & Particulate - Al <sub>2</sub> O <sub>3</sub>
5	1	5	6	3	4	7	2	Whisker - Si <sub>3</sub> N <sub>4</sub> /SiC(w); Particulate - SiC
6	5	2	--	1	--	3	4	Whisker - Si <sub>3</sub> N <sub>4</sub> /SiC; Other - Porcelain and glass
7	1	3	--	2	5	6	--	4
8	--	--	--	1	2	--	--	
9	2	4	--	3	1	--	--	
10	3	--	--	1	1	2	2	Whisker - Zirconia Toughened Alumina (ZTA); Particulate - ZTA, Si <sub>3</sub> N <sub>4</sub> /TiN
11	1	3	6	5	4	--	--	2
12	--	--	--	--	--	--	--	Other - glass-ceramics
13	2	3	--	1	--	--	--	First fractographic experience
15	--	1	--	2	3	--	--	
16	1	3	--	2	4	--	--	
17	1	4	--	2	3	--	4	2-3 Particulate - Tetragonal Zirconia Polycrystal (TZP); Other - SiAlON
18	--	3	--	2	--	--	--	1 Other - glasses & metals

Numbers indicate the experience level each fractographer has with a specific ceramic (1: having the most experience; --: no experience)

\* The organizers had experience with the following ceramic materials: ZrO<sub>2</sub>, Si<sub>3</sub>N<sub>4</sub>, Al<sub>2</sub>O<sub>3</sub>, SiC, Al<sub>2</sub>O<sub>3</sub>/SiC, ZTA/SiC(w), ZrO<sub>2</sub>/SiC(w), ZTA, Si<sub>3</sub>N<sub>4</sub>/SiC(fiber) and glasses.

of all identifiable fracture origins. Over half of the participants stated that Materials Research & Development was their main purpose for fractography. Two listed Quality Control and two others listed Design.

*Does the Fractographer also do the Strength Testing?* Although it is not critical to proper characterization of fracture origins, having the same person conduct the strength testing and fractographic analysis can improve the confidence of the characterization. All but one of the participants stated that they do their own strength testing. This number may be misleading since six participants responded based on their agencies experience rather than the individual's own experience. In fact one participant circled "yes" but added: "sometimes; students do much of it".

*Are Specimen Cleaned and if so How Much?* The myriad of contaminants present in a laboratory environment and the amount of handling a specimen can receive often result in the contamination of the fracture surfaces. Upon examination some of these contaminants can be inadvertently labeled as the fracture origin. Therefore cleaning can be important to fractography. All but three participants responded that cleaning is a normal part of their fractographic analysis. Some stated that they only clean "if necessary" or if they are going to examine the fracture surfaces using the Scanning Electron Microscope (SEM).

Care also has to be taken in the selection of the cleaning solution. The solution must not contaminate the surface further. When cleaning is necessary the participants responded that it is typically done in an ultrasonic bath of ethanol, methanol or acetone. Some follow the acetone cleaning with another cleaning in ethanol or methanol, or simply rinse the specimens in one of these alcohols. (When acetone dries it can leave a residual layer on the surface.) In instances where ultrasonic cleaning is deemed unnecessary, the specimens are "cleaned" with compressed air. One of the three participants who said "no" has never performed fractography prior to this exercise.

*Is Optical Fractography a Normal Part of Your Fractographic Analysis?* Over two-thirds of the participants indicated that optical microscopy is a normal part of their analysis procedure. The participant with 35 years of experience stated: "Before SEM it was my only method.". Typically a stereo or binocular microscope is used because it provides good depth of field and working distances. The purposes behind this examination are to "get acquainted" with the material, locate the primary fracture origin, observe the general fracture features, save time on the Scanning Electron Microscope (SEM) and if possible, identify the fracture origin. Three participants circled "no", but did not provide any additional information.

*Is Scanning Electron Microscopy (SEM) a Normal Part of Your Fractographic Analysis?* The SEM is one of the most powerful tools available to



a fractographer. This is especially true in the case of translucent ceramics or when fractography is required on ceramics which failed at very high stress levels (approaching or exceeding 1 GPa) where the fracture origin is extremely small. All but two participants use the SEM as a normal part of fractography. One "no" was followed by the comment "unless further identification is needed", while the other stated that "Sometimes we use both." (Optical and SEM).

*Are Specimens Coated Prior to SEM Analysis?* Only one participant circled "no". The remainder used coatings at various times. Some coated the specimens all the time while others were selective when they used coatings. In the latter case, coatings were applied only after the examination of an uncoated specimen at low acceleration voltages was fruitless. A few participants had access to a Field Emission Microscope which eliminates the need for coatings.

Typical coatings were Au, Au/Pd, and C. Other coatings mentioned were Cu and Pt. The metallic coatings were up to 200 Å thick and applied by sputtering. Carbon coatings were deposited by evaporation. The metallic coatings were applied to improve the image while a carbon coating was added when elemental analysis was required.

*Is Energy Dispersive Spectroscopy (EDS) a Normal Part of Your Fractographic Analysis?* An elemental analysis of the fracture origin and surrounding area can be extremely helpful during fractography. This is especially true when the origin is compositionally different from the normal microstructure, i.e., inclusion or the non-uniform distribution of a second phase. It was generally agreed upon by the participants that EDS is a normal part of fractography, but for some participants, only on an "as needed basis".

*Is Microstructural Analysis a Normal Part of Your Fractographic Analysis?* The information obtained from the microstructural analysis of a polished section can aid a fractographer, especially to determine if the fracture origin is part of the normal microstructural features or is an aberrant feature.

The response to this question was mixed. Six participants stated that this analysis was not a normal part of their fractographic analysis. Five others stated that they used microstructural analysis to detect pores or agglomerates, and to determine the size and shape of grains. A majority of the participants said that this analysis was done on an "as needed basis" or that it was part of the overall characterization of the material, not just for fractographic purposes.

## **Topic #1 - Characterization Of Machining Damage**

### **Topic #1: Objective**

To detect and interpret machining damage in a variety of advanced structural ceramics.

### **Topic #1: Background**

**MACHINING DAMAGE** - Machining damage can be very difficult to identify since the associated subsurface microcracking can blend into the microstructure, when viewed on the fracture surface and because there may be no discernible marks left on the machined surface(s). (Subsurface cracking often has little relationship to the final surface roughness or topography.) The latter is a consequence of the fine grinding steps involved in the last stages of normal machining processes. Since most ceramic pieces require some degree of machining, damage induced during this process can limit the strength of the final product. This will be especially true as refined or improved manufacturing techniques reduce or eliminate sintering irregularities and abnormal or gross material fracture origin types. The precision and control available in ceramic machining technology may make it possible to control the type and size of machining damage imparted to a ceramic piece. In principle, if machining damage is the controlling origin, this may create a ceramic with a known strength-limiting origin population. Therefore, the accurate characterization of machining damage will be imperative. References 10 and 11 discuss the formation of subsurface machining damage and its affects on strength.

**ESTIMATING THE FRACTURE ORIGIN SIZE** - The round robin instructions did not state explicitly that fracture mechanics should be used as an aid in identifying the origin. MIL HDBK-790 encourages the use of fracture mechanics, however, the organizers were eager to see how many participants would actually use fracture mechanics analysis. For each specimen the necessary background information, including fracture toughness, was given.

The following equations can be used to estimate the size of fracture origins and fracture mirrors as discussed in section 2.1.8 of MIL HDBK-790. Linear elastic fracture mechanics relates strength, fracture toughness and fracture origin size for an origin in a ceramic as follows:

$$K_{Ic} = Y \sigma \sqrt{c} \quad (1a)$$

where  $K_{Ic}$  is the fracture toughness,  $Y$  is a unitless shape factor for the origin which takes in to account a number of geometric factors including the severity of the crack,  $\sigma$  is the fracture stress, and  $c$  is some measure of the fracture origin size (e.g. depth).

Equation 1a can be rearranged to estimate the size of the fracture origin when the strength and fracture toughness values are known, Equation 1b .

$$c = \{K_{Ic} / (Y \sigma)\}^2 \quad (1b)$$

Compendiums and handbooks which contain Y values for a variety of cracks in various stress states are available (see references cited in Appendix 2). A Y value can be obtained from the Newman and Raju<sup>12</sup> analysis for fracture origins which are essentially semicircular or semielliptical and located at the surface. This analysis determines the Y at the surface and depth of the origin and uses the maximum value in either Equation 1a or 1b. Figure 1.1 schematically shows how this analysis applies to these geometries. In a number of examples below, Equation 1a or 1b will be applied to fracture origins. The origins will be modeled by circles, ellipses, semicircles or semiellipses, but it should be understood that these are only approximations to the real, three-dimensional origin shapes.

ESTIMATING THE FRACTURE MIRROR SIZE - Similarly an estimate of the mirror size can be made using the relationship between the mirror size and the strength of the specimen, Equation 2a,

$$r = (A/\sigma)^2 \quad (2a)$$

where r is the radius of the fracture mirror, A is the appropriate mirror constant for the specific ceramic material, and  $\sigma$  is the fracture strength at the origin in a specimen or component. Equation 2a can be rearranged to estimate the strength of the ceramic when the mirror size is known.

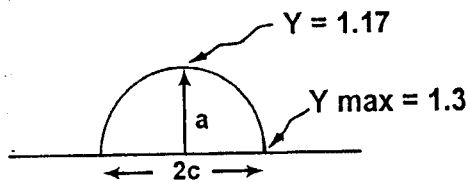
$$\sigma = A/\sqrt{r} \quad (2b)$$

Mirror constants have the same set of units (MPa\* $\sqrt{m}$ ) as fracture toughness. Since the fracture mirror is larger than the fracture origin, the mirror constant must be larger than the fracture toughness.

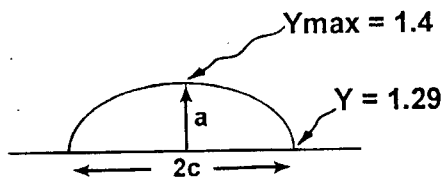
### **Topic #1: Approach**

Three identical sets of photographs were sent to the participants. Each set was of one specimen and contained three pairs of photographs, taken at different magnifications, of the mating halves of the primary fracture surface. The photograph sets were from three specimens of the following three ceramic materials:

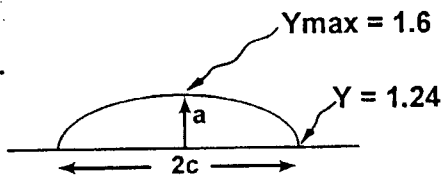
- Set #1: Zirconia/Alumina composite
- Set #2: Silicon Nitride
- Set #3: Alumina



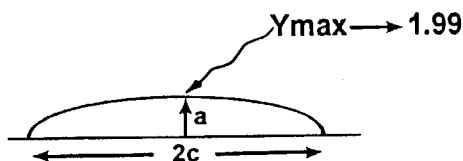
Semicircle  
 $c = a$



Semiellipse  
 $c = 1.4a$



Semiellipse  
 $c = 2a$



Long Semiellipse  
 $c \gg a$

Figure 1.1. Schematic diagram of how the shape factor ( $Y$ ) varies at the depth and surface as the shape of a surface-located origin changes from a semicircle to an elongated semiellipse. The shape factor is determined by the Newman-Raju<sup>12</sup> analysis. It is assumed that the cracks are small relative to the specimen thickness. Note that the maximum stress intensity factor is at the surface intersection of the semicircular precrack, but for semiellipses, it shifts to the deepest part of the precrack periphery and becomes larger in magnitude as the semiellipse becomes elongated.

These specimens were machined according to the guidelines given in MIL STD 1942A, ASTM C 1161, and CEN ENV 843-1. The machining guidelines provided in these standards are designed to minimize all forms of machining damage (i.e., chips and deep striations). Nevertheless some machining damage could occur.

The organizers believe that the specimens used for these photograph sets failed from machining damage, in part due to the benefit of examining many specimens from these materials. This enabled the organizers to discern the differences between material related origins and machining-related origins. The participants did not have access to the original three specimens, or to all the other specimens and thus, were handicapped in their fractographic analysis. It should also be noted that machining damage is often typified by several microcracks, any one or combination of which could be the specific origin. In these instances, the organizers make no claim with absolute certainty as to which is the "true" origin and indeed, the organizers were eager to learn how the participants responded in such cases.

### **Topic # 1: Instructions**

The participants were asked to locate the fracture origin on the photograph with the lowest magnification and then mark the fracture origin and associated fracture mirror directly on any of the photographs using some form of permanent markings. They were asked to characterize the origin using the scheme of identity, location and size outlined in MIL HDBK-790 and report the size of the fracture mirror. Complete instructions are given in Appendix 1.

### **Topic #1: Results**

OVERALL COMMENTS - Six of the participants marked both halves of the photograph set while five marked only one half of the photograph set. Five participants marked both halves of the fracture surface, but not for all three sets. One participant did not mark the photographs. Participant 14 failed to report.

Each photograph set will be dealt with individually since there are three different specimens involved. The results section for each set contains copies of the photograph set, the material information that the participants received, the organizers' characterization of each fracture origin and the participants' results.

#### **Photograph Set #1: Zirconia/Alumina Composite (TSZ-14)**

The three pairs of photographs of the zirconia/alumina composite provided to the participants are shown in Figure 1.2. All participants received the material information given in the next paragraph. The participants' results are summarized in Table 1.1.

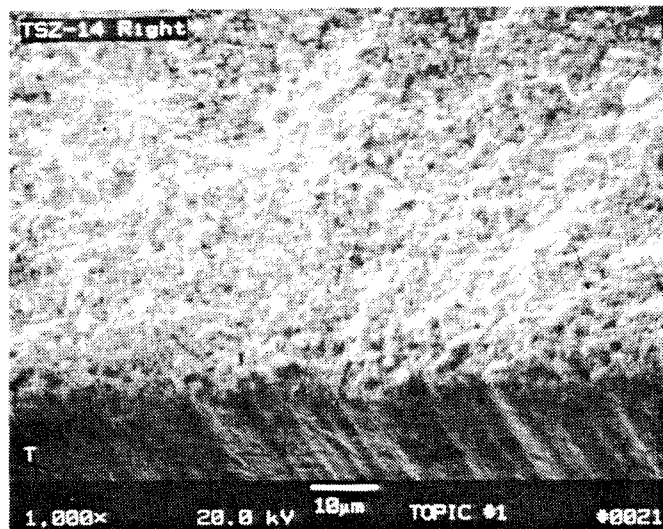
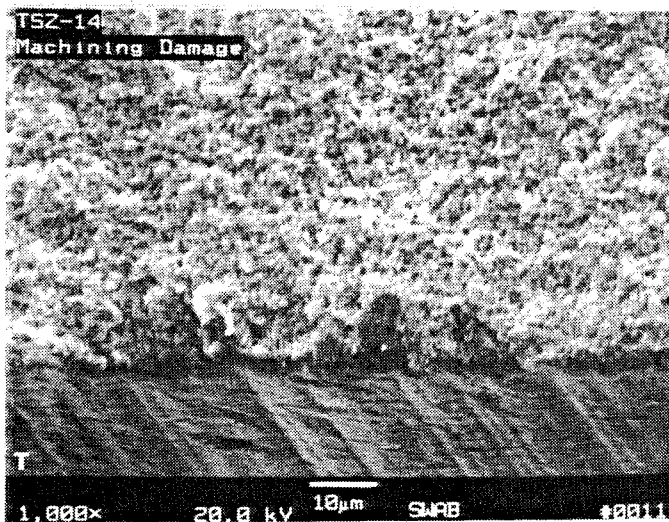
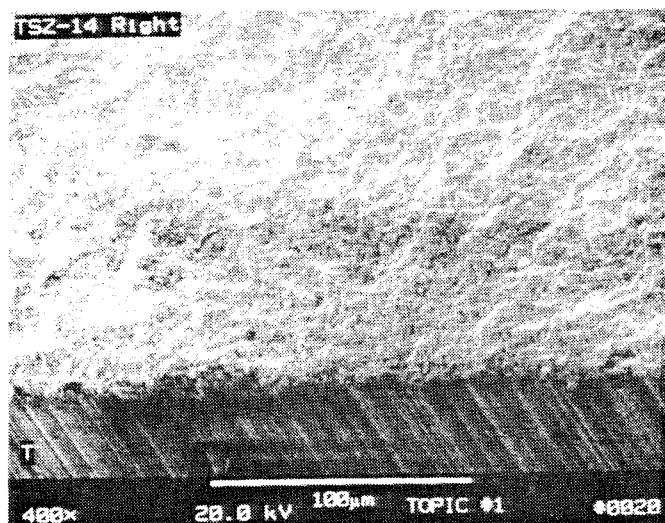
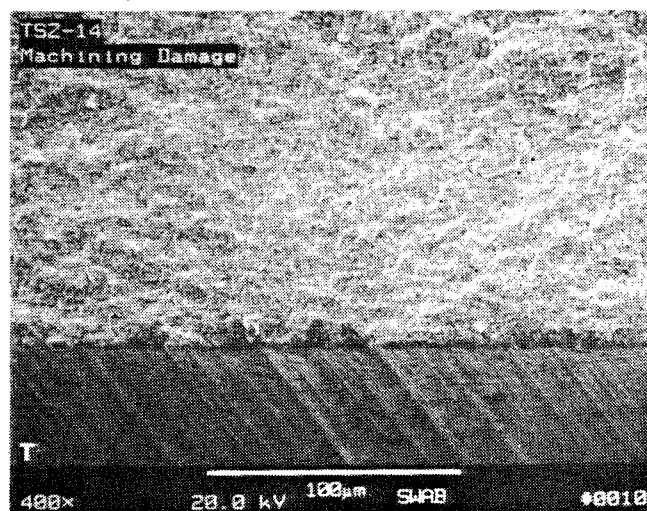
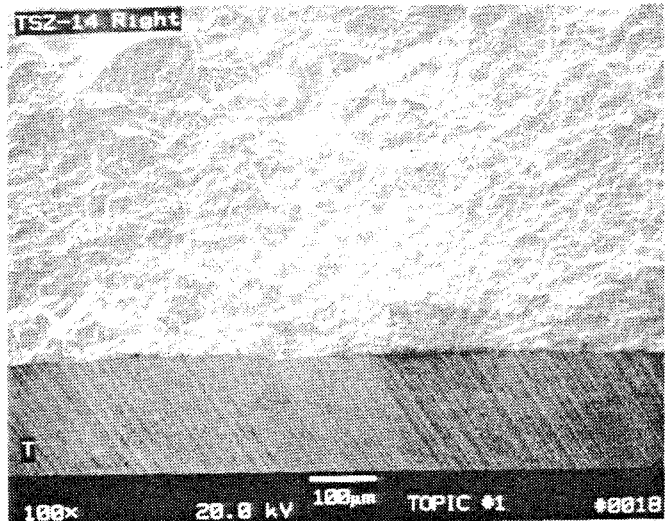
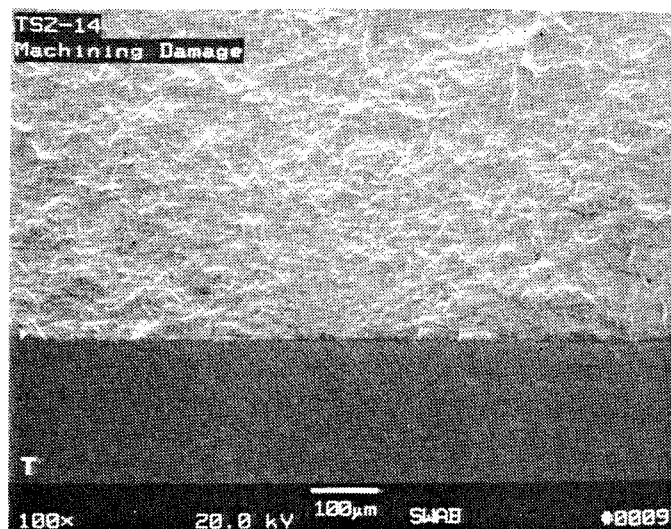


Figure 1.2. The three pairs of photographs for Set #1 (TSZ-14) which were provided to the participants. "T" denotes the tensile surface.

Table 1.1  
PARTICIPANTS' RESULTS FROM PHOTOGRAPH SET #1: ZIRCONIA/ALUMINA (TSZ-14)

No.	Location	Fracture Origin		Mirror		Comments
		Diameter (2c)	Radius (c)	Diameter (2r)	Radius (r)	
ORG SURFACE						
FM		10.6	15*	130 - 160		Used $K_{Ic}$ and Strength to estimate origin size.
			5.3	45 - 192	22.5 - 96	As values used to estimate the mirror size were 7.4 and 15.2
1	SURFACE	5			62.5	Origin is a "deeper groove" - focused on tensile surface damage; "Mirror not obvious"
2	SURFACE	4			50+	Origin is "two grooves which could act alone or jointly" - focused on tensile surface damage
3	NS	20			37.5	Origin is "weakly bonded material"; "No distinct mirror"
4	SURFACE	61		71 - 78		"Shallow 1/2 penny-shaped crack"; Used strength and $2r = 78$ to estimate $K_{Ic}$ (4.9)
5	SURFACE		?		50	Origin "not clearly discernible"; $K_{Ic}$ & strength predict a 7um origin; Mirror easily seen but hard to define
6	SURFACE	62	13*	130	50*	"No direct evidence of machining damage"
7	SURFACE	85.3		102.5		"Linked set of subsurface cracks" - focused on tensile surface damage; "Mirror difficult to discern"
8	SURFACE		15		100	
9	SURFACE	33	11*	140	50*	Calculated $K_{Ic}$ as 7.3 using origin depth; "Heat treatment may have reduced sharpness at crack tip"
10	SURFACE	10 - 15			60+	Not sure if reported size is 2c or c; "Mirror difficult to measure precisely"
11	SURFACE		12*		40	Estimated origin size as 5um but delineated a 12um origin
12	EDGE	40	15*	100	70*	"Difficult to distinguish between flaw and mirror"; Misinterpreted meaning of Edge and Surface
13	SURFACE	63			35	
15	SURFACE	31	12*		46+	Marked photograph holder instead of photographs
16	SURFACE		10*	50 - 80		Provided 2 max/min ranges for mirror size - selected largest
17	SURFACE	66	34*	870	220+	"Interaction between porous seam & machining damage seems to determine the fracture origin"
18	SURFACE		10*		40+	

- ORG: ORGANIZERS' RESULTS

- FM: ORIGIN SIZES ARE DETERMINED FROM EQUATION 1b ( $Y = 1.4$  ASSUMING A SEMICIRCULAR OR SEMIELLIPTICAL SURFACE CRACK) AND MIRROR SIZES ARE DETERMINED FROM EQUATION 2a USING PUBLISHED MIRROR CONSTANTS

- ? NOT MEASURED; \* INDICATES DEPTH RATHER THAN RADIUS

- + INDICATES  $r$  WAS MEASURED AT SOME LOCATION OTHER THAN ALONG THE TENSILE/FRACTURE SURFACE INTERFACE

- ALL DIMENSIONS ARE GIVEN IN MICROMETERS UNLESS STATED OTHERWISE

**MATERIAL INFORMATION** - The ceramic was a zirconia/alumina composite which contained 75 w/o tetragonal zirconia, partially stabilized by 4.2 w/o yttria, with 20 w/o  $\alpha$ -alumina. It was formed into large billets through a sinter/hot isostatic press process. The specimen was a machined flexure bar of the following nominal dimensions: 3mm x 4mm x 50mm. Fracture toughness, as determined by the indentation-strength technique<sup>13</sup>, using a 10kg load, was approximately 5 MPa $\cdot\sqrt{m}$ . Average grain size of the zirconia was  $\approx 0.4 \mu m$  and that of the alumina is  $\approx 0.6 \mu m$ . The specimen was heat treated in air for 100 hours at 1000°C prior to four-point flexure testing, in air, at room temperature. Flexure strength of this particular specimen was 1552 MPa. The strength, toughness and grain size values for this specimen were obtained from Reference 14.

**ORGANIZERS' CHARACTERIZATION** - The organizers identified the fracture origin in this specimen as machining damage. The organizers outlined subsurface cracks which have either a semicircular (Figure 1.3B) or a semielliptical (Figure 1.3C) shape as the possible machining damage. The depth of the crack, in either case, is approximately 15  $\mu m$ . In accordance with the characterization scheme in MIL HDBK-790 the origin in this specimen was labeled as follows:

Machining Damage (MD<sup>s</sup>), Surface, depth  $\approx 15 \mu m$ .

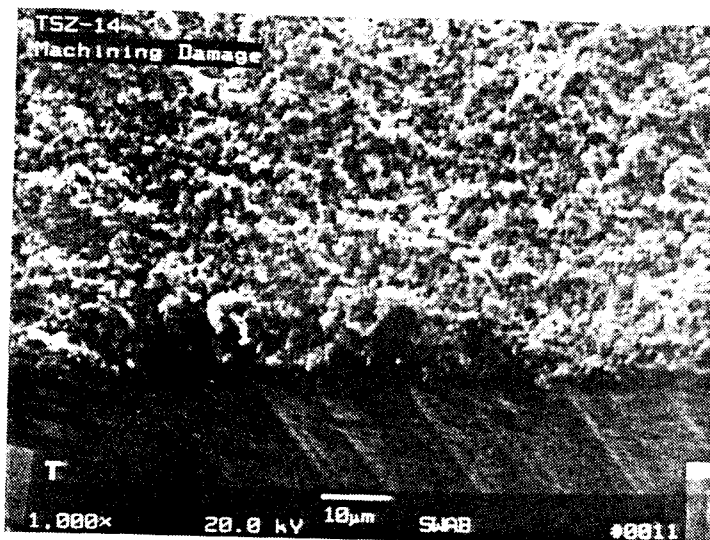
The mirror diameter (2r) was estimated fractographically to be between 130 and 160  $\mu m$ .

**PARTICIPANTS' RESULTS - IDENTITY IN ZIRCONIA/ALUMINA** - Although the participants were told that the fracture origin was machining damage, two did not completely agree. One felt the origin was "weakly-bonded material" and another thought it was the interaction between a porous seam and machining damage. Several participants marked damage on the tensile surface of the specimen such as striations or grooves and one said "No direct evidence of machining damage". Participant 4 stated that it looked like a "shallow half-penny-shaped crack" and participant 7 reported that it was a "linked set of subsurface cracks".

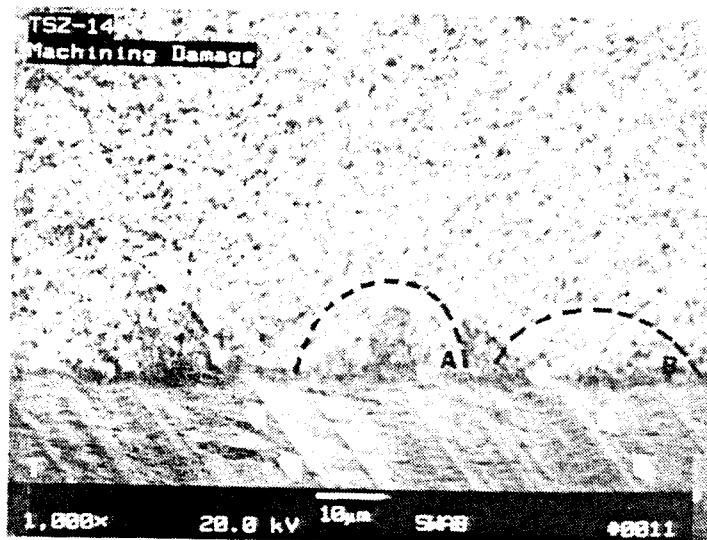
**PARTICIPANTS' RESULTS - LOCATION IN ZIRCONIA/ALUMINA** - The consensus was that the origin was located at the surface. However, one participant believed the origin was close to but not at the surface (thus the near surface label) while another established the origin as being located at an edge.

**PARTICIPANTS' RESULTS - FRACTURE ORIGIN SIZE IN ZIRCONIA/ALUMINA** - The values and methods of reporting the size of the fracture origin widely varied between participants. Some participants reported diameters (2c) while others reported radius (c) values. Still others reported an

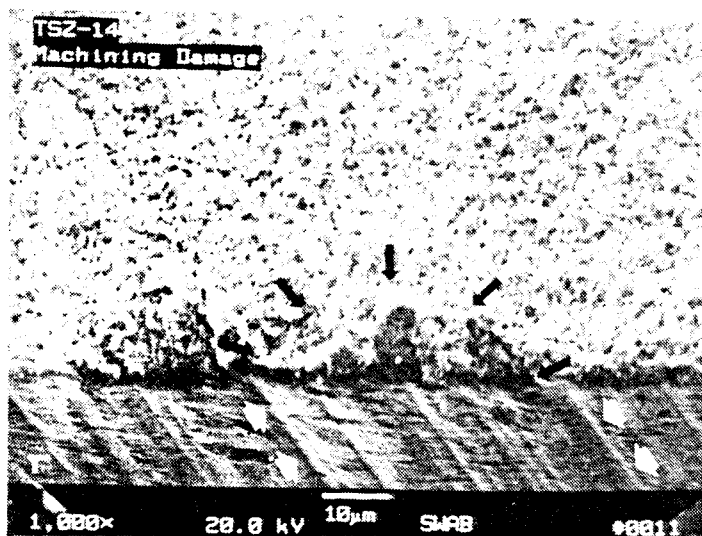




A



B



C

Figure 1.3. High magnification photographs of one half of the fracture surface from Set #1 (TSZ-14). A) Unmarked. B) The organizers outlined two possible semicircular origins. Arrows indicate possible striations on tensile surface. C) The organizers outlined a possible semielliptical origin. "T" denotes the tensile surface.

origin depth or a 2-dimensional value of depth by width. Eleven participants reported a single value, either  $2c$ ,  $c$  or origin depth, while five others listed a 2-dimensional origin size. One did not report a size. It is interesting to note the consistency of the values of the participants who reported an origin depth. Seven of the eight participants who reported depth had a value between 10 and 15  $\mu\text{m}$  which concurs with the organizers assessment.

Equation 1b estimates an origin radius ( $c$ ) of 5.3  $\mu\text{m}$  based on the strength and toughness numbers provided and an assumed shape factor ( $Y$ ), for a semicircular origin located at the surface, of 1.4. Only three of the participants (5, 9 & 11) reported that they used fracture mechanics to assist them in their determination of the origin size. Two (5 & 11) used the provided strength and toughness numbers to predict the size. Participant 5 estimated the origin size but did not report a value because the origin was "not clearly discernible". Participant 9 used the fractographically measured origin size to estimate the fracture toughness and compared this to the value provided. The specimen strength, their measured origin depth and a  $Y$  of 1.43 (determined from Ref. 12) were inserted into Equation 1a which yielded a  $K_{Ic}$  value of 7.3  $\text{MPa}\sqrt{\text{m}}$ .

**PARTICIPANTS' RESULTS - MIRROR SIZE IN ZIRCONIA/ALUMINA** - In general the participants had trouble determining the size of the fracture mirror. First, there was difficulty in ascertaining the boundary. Several said the mirror was not obvious or that they could not discern it. One stated the "mirror is easily seen but hard to define". As a result a wide range of mirror sizes were reported. Second, the participants' measured and reported their mirror sizes differently. The values were reported either as: a diameter ( $2r$ ); a radius ( $r$ ); a depth, or as a 2-dimensional value (depth by width).

It is possible to estimate the radius, or the diameter, of a fracture mirror using Equation 2a. The estimated diameter of the fracture mirror, using the only two mirror constants ( $A_0$ ) found in the literature for zirconia<sup>15</sup> (7.4 and 15.2  $\text{MPa}\sqrt{\text{m}}$ ), is between 45 and 192  $\mu\text{m}$ . Fifteen of the seventeen participants values fell within this estimated range, Table 1.1. Participant 8 reported a value only slightly larger than the estimated number, while participant 17 gave two sets of maximum/minimum values, both of which were significantly larger than the estimated range.

None of the participants apparently used Equation 2a to help them determine the mirror size. However, participant 4 estimated the fracture toughness by calculating a mirror constant. Equation 2b was rearranged to calculate  $A$  from the strength and measured mirror diameter. The participant then divided  $A$  by 2 to yield a  $K_{Ic}$  estimate of 4.9  $\text{MPa}\sqrt{\text{m}}$ . Reference 15 shows that mirror constants ( $A$ ) are typically 2-3 times larger than  $K_{Ic}$ .

## Photograph Set #2 - Silicon Nitride (SN-5)

Figure 1.4 are the photographs provided to the participants. The material information sent to the participants is given below. Table 1.2 summarizes their findings.

MATERIAL INFORMATION - The ceramic was a silicon nitride which was hot-pressed with 8 w/o yttria. The specimen was 2.16mm x 2.16mm x 50mm in size and was machined from a large billet. The fracture toughness was measured as 6.2 MPa $\sqrt{m}$  from double torsion tests<sup>16</sup>. Cross section size of the grains ranged from 1-3  $\mu m$  and the apparent aspect ratio was 6:1 to 8:1. The room temperature four-point flexure strength of this particular specimen, in air, was 910 MPa. All of this information was provided to the participants.

ORGANIZERS' CHARACTERIZATION - Machining damage was identified by the organizers as the fracture origin in this specimen. Several semicircular and semielliptical subsurface cracks are outlined by the organizers in Figures 1.5B and 1.5C, respectively, as the possible machining damage. All are equally plausible interpretations of the fracture origin. The semielliptical crack in Figure 1.5C may be a linked set of semicircular cracks. The depth of the crack of either geometry was  $\approx 25 \mu m$ . Complete characterization of the fracture origin is:

Machining Damage (MD<sup>S</sup>), Surface, depth  $\approx 25 \mu m$ .

The mirror diameter was estimated fractographically to be about 330  $\mu m$ .

PARTICIPANTS' RESULTS - IDENTITY IN SILICON NITRIDE - There was unanimous agreement with the identification of the fracture origin as machining damage. Two participants felt the origin resembled a controlled surface origin i.e., "shallow half-penny-shaped crack". (These were not artificially induced cracks!) The same participants who marked damage on the tensile surface (striations or grooves) of the zirconia/alumina composite (set #1) did the same for this specimen.

PARTICIPANTS' RESULTS - LOCATION IN SILICON NITRIDE - The consensus was that the origin was located at the surface, however, there were three participants who felt the origin was located elsewhere. One felt it was located "at the edge", one thought it was "near-to-the-surface", while the third was not sure if it was surface or near surface.

PARTICIPANTS' RESULTS - FRACTURE ORIGIN SIZE IN SILICON NITRIDE - As was the case with photograph set #1 there was a wide variation in what was measured and how it was reported. Eleven participants reported a 2c,

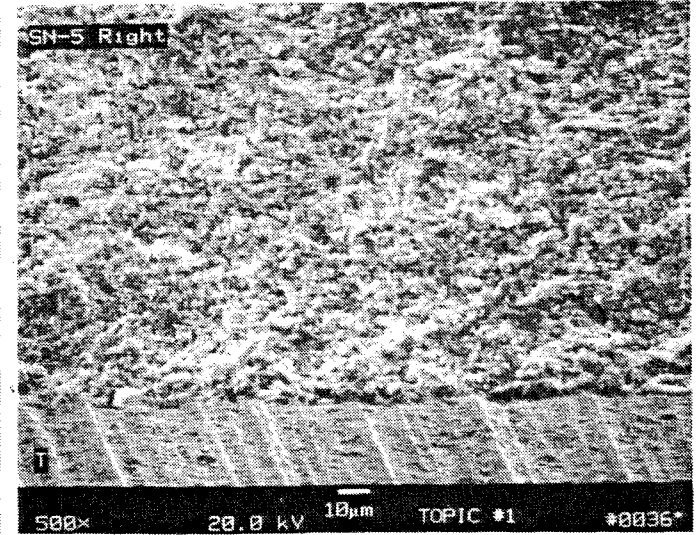
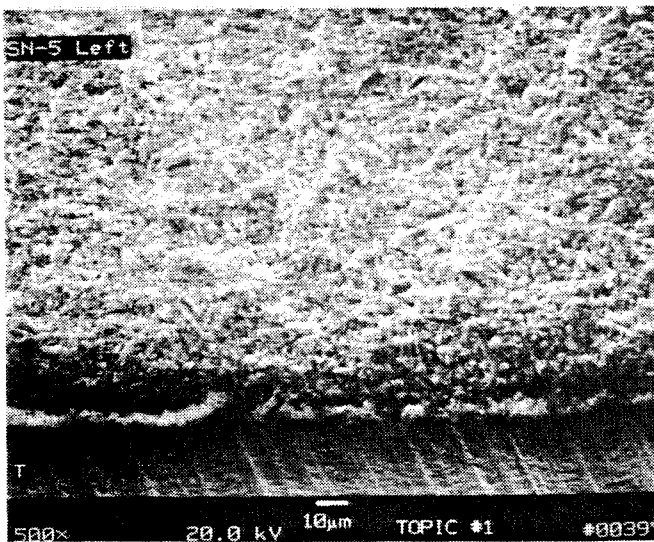
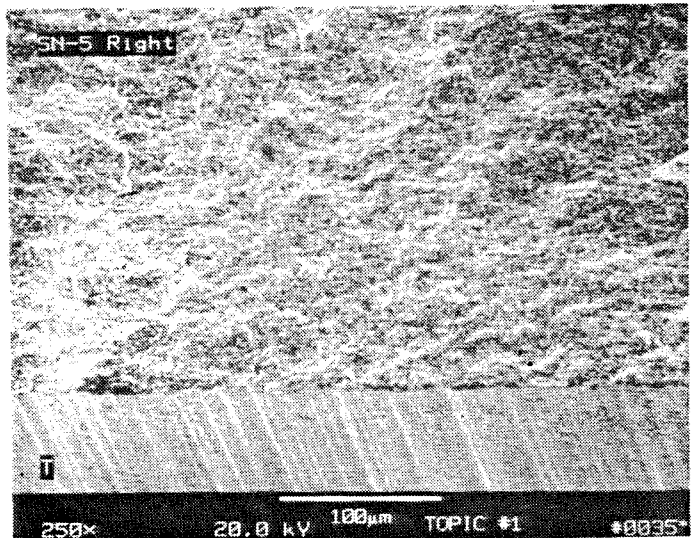
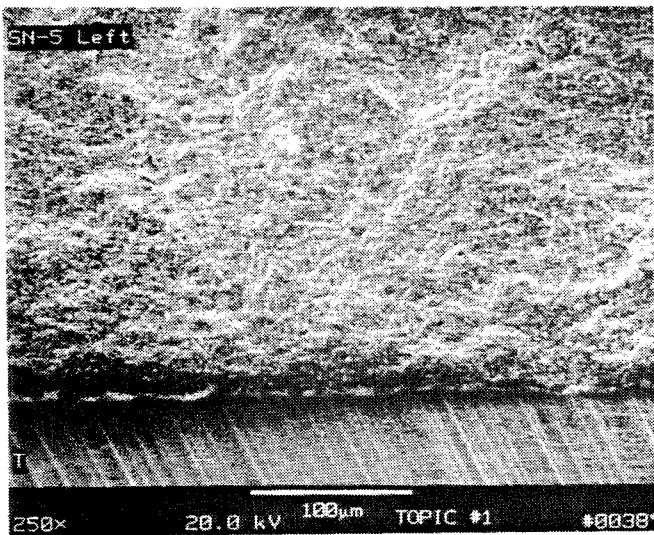
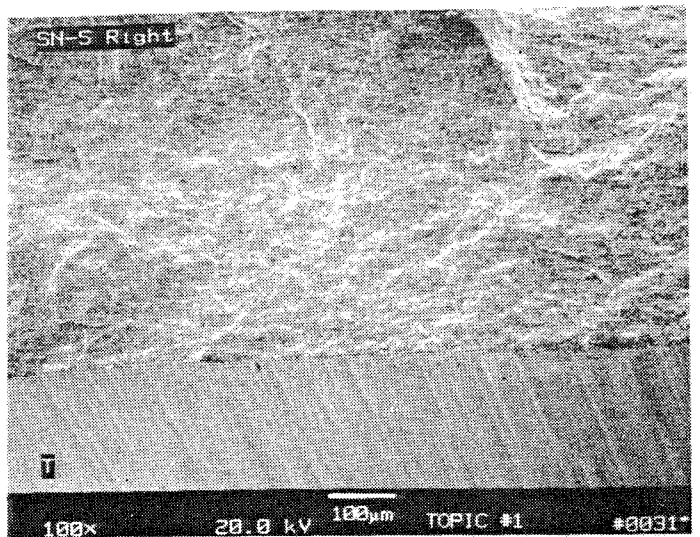
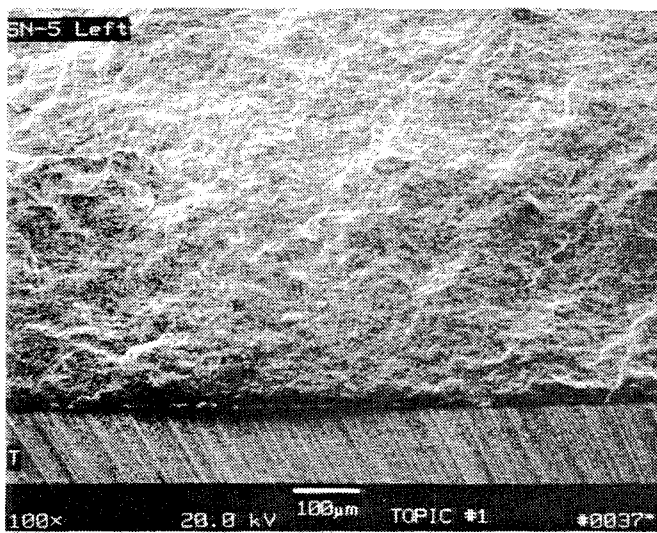


Figure 1.4. The three pairs of photographs for Set #2 (SN-5) which were provided to the participants. "T" denotes the tensile surface.

Table 1.2  
PARTICIPANTS' RESULTS FROM PHOTOGRAPH SET #2: SILICON NITRIDE (SN-5)

No.	Location	Fracture Origin		Mirror		Comments
		Diameter (2c)	Radius (c)	Diameter (2r)	Radius (r)	
ORG SURFACE		47	25*	330		Used $K_t$ & strength to estimate origin size
FM			23.5	192 - 792	96 - 396	As values used to estimate the mirror size were 8.9 and 18.1
1	SURFACE	10			62	Origin is a "deep groove" - focused on tensile surface damage
2	SURFACE	10			200+	Focused on tensile surface damage; "Mirror not obvious"
3	NS	40			80+	"No distinct mirror"
4	SURFACE	74		384		"Shallow 1/2 penny-shaped crack"; strength & 2r to estimate $K_t$ (6.3); "Mirror not distinct"
5	SURFACE		25		150	Used strength & $K_t$ to estimate c; Mirror easily seen but hard to define
6	SURFACE	30	15*	300	125*	
7	SURFACE	112		160		Focused on tensile surface damage
8	SURFACE		40		250	
9	SURFACE	80	28*	420	140*	Calculated $K_t$ as 6.6 using origin depth
10	SURFACE	10			100+	
11	SURFACE		25*		200	Origin looks like a "Controlled Surface Flaw - long but shallow"; Origin size matches estimate
12	EDGE	?	?	80	30*	Misinterpreted the meaning of Edge and Surface
13	SURFACE	?		?	180	"Better photographs could help"
15	SURFACE	32	6*	?		"No mirror found"
16	S/NS	?		?		Detected "contours" at 30, 270, 290 & 670um; Photograph holders marked
17	SURFACE	8 - 18		830	380*	Can not determine how origin size is measured from the markings on photographs
18	SURFACE		20*		200	"Interpretations of several observers did not agree"

- ORG: ORGANIZERS' RESULTS

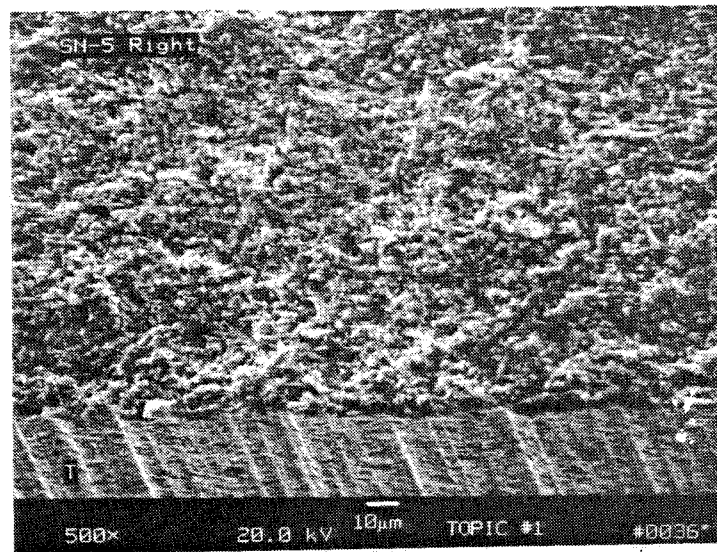
- FM: ORIGIN SIZES ARE DETERMINED FROM EQUATION 1b ( $Y = 1.4$  ASSUMING A SEMICIRCULAR OR SEMIELLIPTICAL SURFACE CRACK) AND MIRROR SIZES ARE DETERMINED FROM EQUATION 2a USING PUBLISHED MIRROR CONSTANTS

- ? NOT MEASURED; \* INDICATES DEPTH RATHER THAN RADIUS

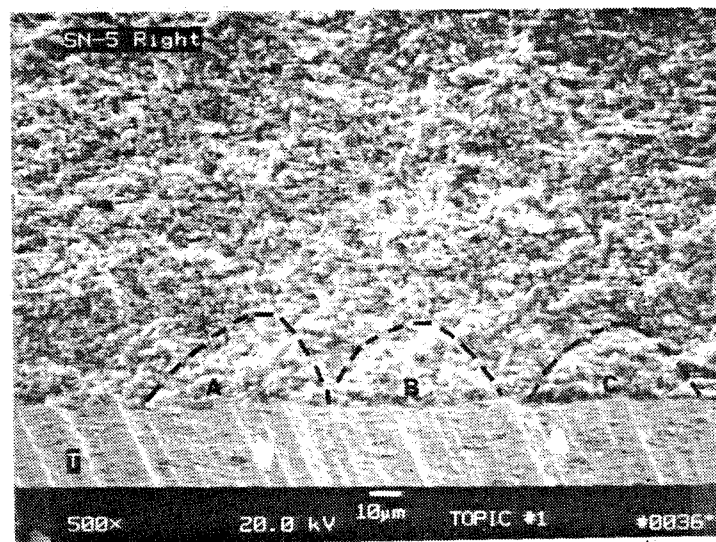
- + INDICATES r WAS MEASURED AT SOME LOCATION OTHER THAN ALONG THE TENSILE/FRACTURE SURFACE INTERFACE

- ALL DIMENSIONS ARE GIVEN IN MICROMETERS UNLESS STATED OTHERWISE

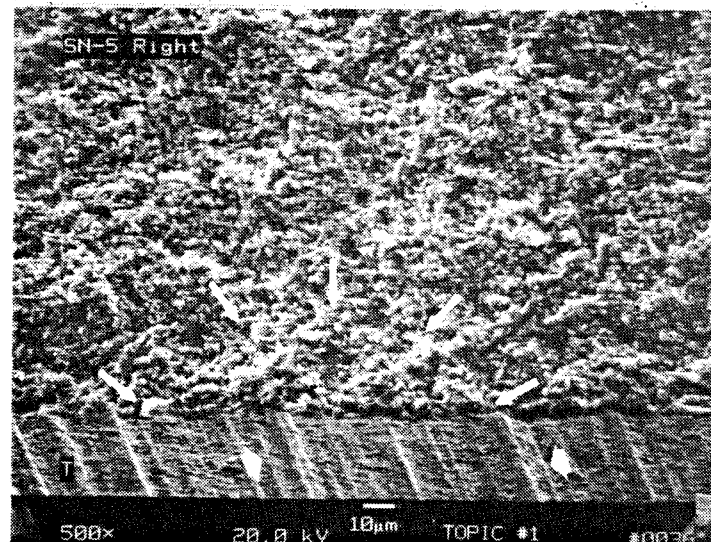




A



B



C

Figure 1.5. High magnification photographs of one half of the fracture surface from Set #2 (SN-5). A) Unmarked. B) The organizers outlined three possible semicircular origins. Arrows indicate possible striations on tensile surface. C) The organizers outlined a possible semielliptical origin. "T" denotes the tensile surface.

c or depth value, three reported a 2-dimensional value and the remaining three did not report a value because they were uncertain as to what was the fracture origin.

Equation 1b predicts a fracture origin radius (c) of 23.5  $\mu\text{m}$  ( $Y = 1.4$ , for a semicircular surface origin located at the surface). The same three participants who used fracture mechanics in set #1 also used it here and in the same manner. Participant 9 again calculated the toughness, from Equation 1a, to be 6.6  $\text{MPa}\sqrt{\text{m}}$  ( $Y = 1.38$  from Reference 12). Six participants were in general agreement with the estimated size of the fracture origin. Three of these reported the origin depth.

#### PARTICIPANTS' RESULTS - MIRROR SIZE IN SILICON NITRIDE -

Again there was a problem in clearly seeing and defining the fracture mirror associated with this fracture origin. The comments given in set #1 are applicable here as well.

A mirror size range ( $2r$ ) was estimated using the lowest (8.9  $\text{MPa}\sqrt{\text{m}}$ )<sup>17</sup> and highest (18.1  $\text{MPa}\sqrt{\text{m}}$ )<sup>15</sup> mirror constant values found in the literature for this class of silicon nitride. The resultant diameter range is 192-792  $\mu\text{m}$ . The results from ten participants fit into this very large range. Four participants (1, 3, 7 & 12) reported values which were below this range while participant 17 again reported a value above the range. Participants 15 & 16 did not report a value. Participant 15 stated "no mirror found" and 16 indicated the presence of "contours" at 30, 270, 290 and 670  $\mu\text{m}$  but did not specify which one might be the mirror. Again none of the participants estimated the mirror size using Equation 2a, but as in set #1 participant 4 estimated the toughness to be 6.3  $\text{MPa}\sqrt{\text{m}}$  from a calculated mirror constant.

#### Photograph Set #3 - Alumina (RR8)

The photographs provided to the participants are shown in Figure 1.6 and the background information for this ceramic material is given below. Table 1.3 summarizes their results.

MATERIAL INFORMATION - The ceramic was a billet (100 mm X 100 mm x 25 mm) of a high purity (99.9%), sintered alumina. The flexure specimen was machined from this billet to the following nominal dimensions: 3mm x 4mm x 50mm. The material fracture toughness is 4  $\text{MPa}\sqrt{\text{m}}$ <sup>18</sup> as determined from surface crack in flexure and double torsion results. The average grain size ranges from 3-6  $\mu\text{m}$ . The room temperature four-point flexure strength of this particular specimen, in air, was 228 MPa.

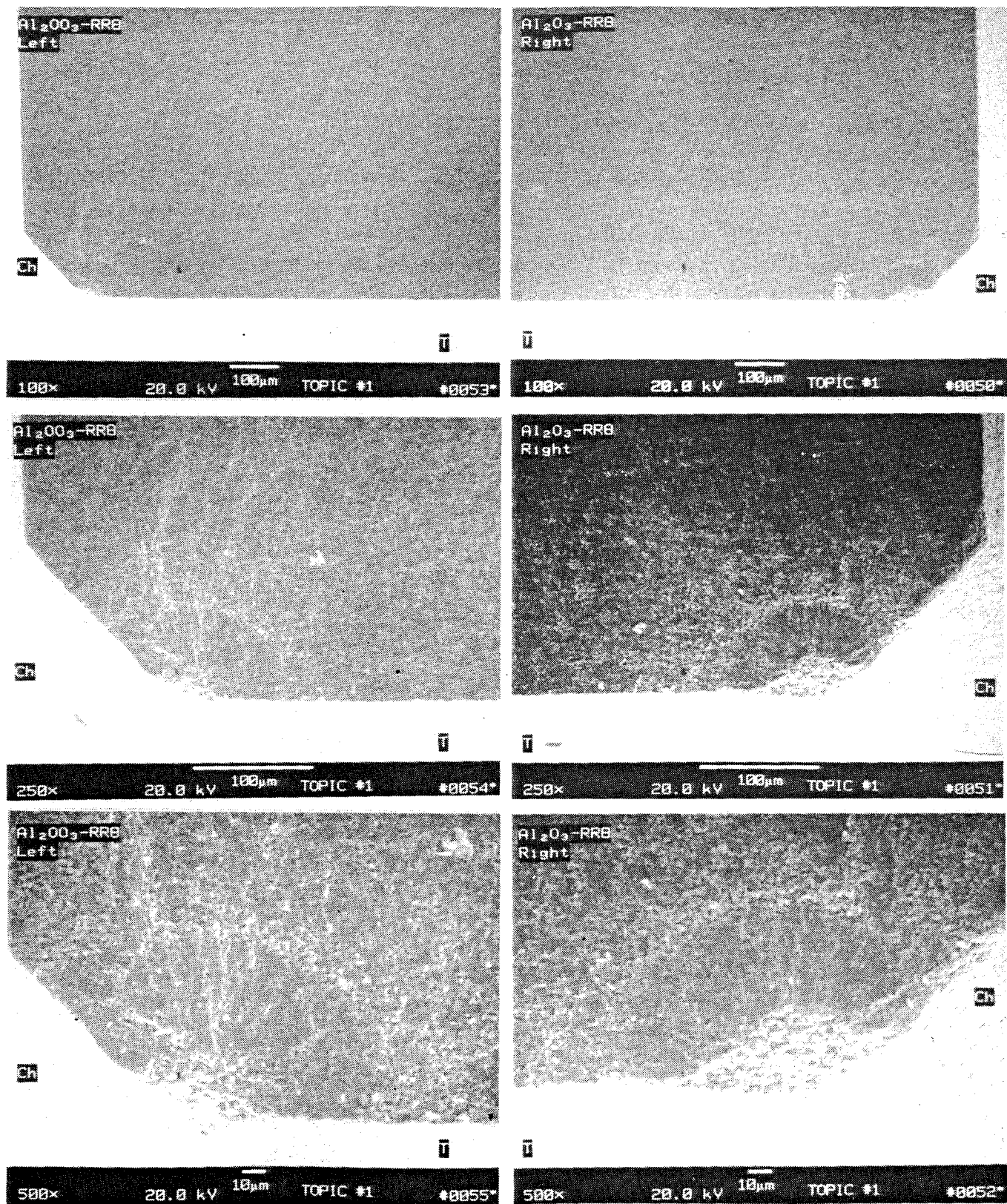


Figure 1.6. The three pairs of photographs for Set #3 ( $\text{Al}_2\text{O}_3\text{-RR8}$ ) which were provided to the participants. "T" denotes the tensile surface and "Ch" the chamfer.



Table 1.3  
PARTICIPANTS' RESULTS FROM PHOTOGRAPH SET #3: ALUMINA (RR8)

No.	Location	Fracture Origin		Mirror		Comments
		Diameter	Radius (c)	Diameter (2r)	Radius (r)	
ORG	EDGE		160	>1mm		
FM		364	182	2650 - 5540	1325 - 2770	Used $K_{IC}$ & strength to estimate origin size; possible subcritical crack growth (SCCG)!! Ao values used to estimate the mirror size were 8.3 and 12
1	S/E	92	40*		80	"Chip missing"; Location: tensile surface at edge of chamber
2	S/E	80	40*		90+	
3	EDGE	80			70+	Origin "Porous Region"
4	EDGE		80	280		Origin "Chip + Crack"; "Mirror distinct"; Possible SCCG
5	EDGE		30-120			Possible PR + MD; possible SCCG
6	S/E	160	80			"Low energy fracture"; Mirror "not evident"
7	S/E	146		159		Origin "looks semicircular - could be Hertzian cone"; Measurements made across corner
8	EDGE		80		140	
9	NE	50		?		Porous region + MD; Origin 50um/Crack 220 x 80; Calculated $K_{IC}$ as 2.7 using $c = 80$
10	EDGE	80			60+	
11	EDGE		80 - 160		?	Chip-30um & Origin-80um, SCCG to 160um; Estimated origin size; Smooth region is too small to be mirror
12	EDGE	80	60*	175	60*	Mean radius of mirror is 80um; Misinterpreted the meaning of Edge and Surface
13	EDGE	50	20*		82	
15	EDGE	80	28*		80+	Better definition needed for determining the size of edge cracks
16	EDGE		25*		80+	"Another contour at 128um"; Photograph holders marked
17	EDGE		36*		134+	Porous region w/crack induced by machining
18	EDGE		80	>1mm"		"Mirror extends over the whole picture because of the small failure stress"

- ORG: ORGANIZERS' RESULTS

- FM: ORIGIN SIZES ARE DETERMINED FROM EQUATION 1b ( $Y = 1.3$  ASSUMING A SEMICIRCULAR OR SEMIELLIPTICAL SURFACE CRACK) AND MIRROR SIZES ARE DETERMINED FROM EQUATION 2a USING PUBLISHED MIRROR CONSTANTS

- ? NOT MEASURED; \* INDICATES DEPTH RATHER THAN RADIUS

- + INDICATES r WAS MEASURED AT SOME LOCATION OTHER THAN ALONG THE TENSILE/FRACTURE SURFACE INTERFACE

- ALL DIMENSIONS ARE GIVEN IN MICROMETERS UNLESS STATED OTHERWISE

ORGANIZERS' CHARACTERIZATION - A machining chip on the chamfer was identified by the organizers as the fracture origin in this specimen. The open appearance of the "chip" may indicate that this was an area that was poorly sintered and thus sensitive to chip formation. The resultant crack is part of a semicircle having a radius of 160  $\mu\text{m}$ . The full characterization of this origin is:

Machining Damage (MD<sup>S</sup>), Edge, radius of approximately 160  $\mu\text{m}$ .

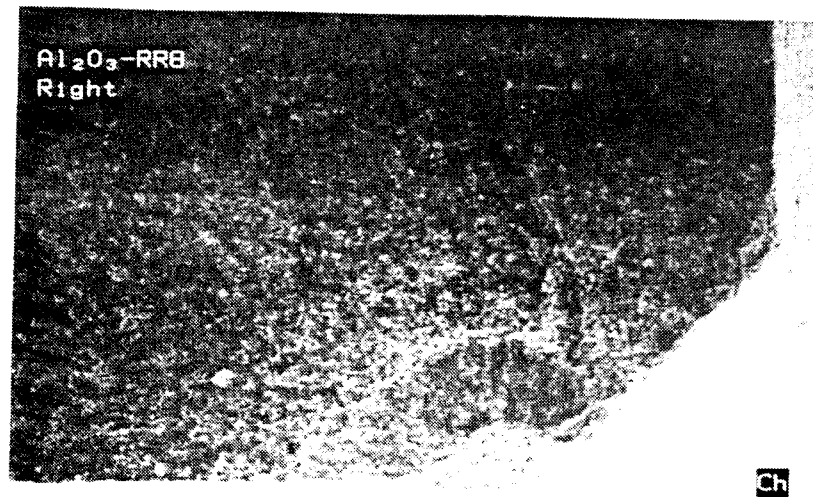
The fracture mirror was estimated fractographically to be in excess of 1 mm in diameter because this was a low strength, low-energy fracture.

PARTICIPANTS' RESULTS - IDENTITY IN ALUMINA - There were four participants who felt the fracture origin was not necessarily machining damage. Participant 3 believed it was a porous region and participants 5, 9 & 17 felt it was a combined origin of a porous region plus machining damage.

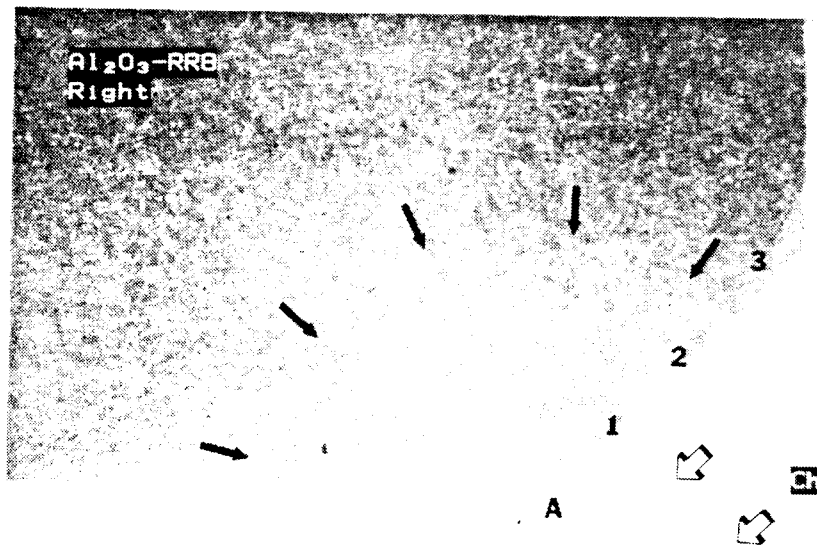
PARTICIPANTS' RESULTS - LOCATION IN ALUMINA - The general consensus was that the origin was located at the edge of the flexure specimen. Four participants felt it could be surface or edge located while one thought it was near the edge.

PARTICIPANTS' RESULTS - FRACTURE ORIGIN SIZE IN ALUMINA - The differences in reporting and measuring the origin size continued with this photograph set. Nonetheless, the overall numbers are fairly consistent between participants. Eleven participants reported a single value of 2c, c or depth with the remainder providing a 2-dimensional value. Because the origin is located at or near the edge some participants were unsure as to how to measure it. Some measurements were made across the corner (chamfer), or on a radius running perpendicular from point A, see Figure 1.7B, into the bulk, still others made their measurements from point A along the tensile/fracture surface interface. One participant felt that special instructions should be provided to measure the origin size in such cases.

Equation 1b estimates a fracture origin having a size of  $c = 182 \mu\text{m}$  ( $Y = 1.3$  assuming a semicircular origin at the surface). Two of the four participants (9 & 11) who used fracture mechanics in the previous two sets did so again. Participant 9 used Equation 1a and estimated the toughness to be  $2.7 \text{ MPa}\sqrt{\text{m}}$  for  $c = 80 \mu\text{m}$  ( $Y = 1.3$  from Reference 12). Participant 11 used Equation 1b and was in agreement with the estimated size of the origin. Participant 5 did not indicate the use of fracture mechanics but the radius reported ( $c = 120 \mu\text{m}$ ) is close to the estimated value. Three participants (4, 5 & 11) indicated that these photographs may also show evidence of subcritical crack growth (SCCG).



A



B

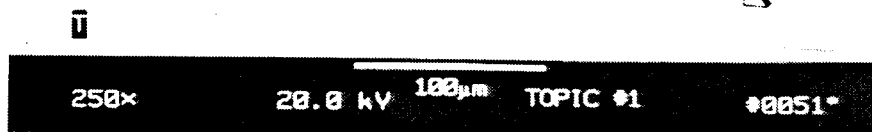


Figure 1.7. High magnification photographs of one half of the fracture surface from Set #3 (Al<sub>2</sub>O<sub>3</sub>-RR8). A) Unmarked. B) Three stages of fracture are outlined by the organizers. Stage 1 is transgranular fracture, Stage 2 is subcritical crack growth and Stage 3 is fast fracture. Open arrows indicate the irregular section of the chamfer. "T" denotes the tensile surface and "Ch" the chamfer.

**PARTICIPANTS' RESULTS** - *MIRROR SIZE IN ALUMINA* - As with the previous photograph sets different measurements of the mirror were reported. Unlike the previous two photograph sets many participants felt the mirror was clearly visible and easily defined, as evident by the relative consistency of the numbers between participants. As discussed below many were misled, however. Four participants did not provide a value for the mirror size.

The estimated mirror diameter from Equation 2a was between 2650 and 5540  $\mu\text{m}$  based on the lowest (8.3 MPa $\sqrt{\text{m}}$ )<sup>17</sup> and highest (12 MPa $\sqrt{\text{m}}$ )<sup>15</sup> mirror constants found in the literature for alumina. This range is as large or larger than the area of the specimen shown in the photograph set or the specimen cross section. In cases where the mirror is so large, in relation to the specimen size, it may not leave markings on the fracture surface. This is especially true in flexure testing where the stress state is not uniform. Only participant 18 who stated "Mirror extends over the whole picture because of the small fracture stress." reported a mirror size that was anywhere near the estimated range. Participant 6 did not report a value but stated that the mirror was not evident because this was a low energy fracture. Additionally participant 11 did not report a value but noted that the "smooth region is too small to be the mirror". None of the participants used either Equation 2a or 2b to assist them in determining the mirror size.

### **Topic #1: Discussion**

**IDENTITY** - The organizers identified the fracture origins in the three specimens used in this topic as machining damage. The subsurface cracks present in sets #1 (Zirconia/Alumina) and #2 (Silicon Nitride) are outlined in Figures 1.3 and 1.5. The identity of the origin in set #3 (Alumina) is different. The open appearance of the "chip" in Figure 1.7B can lead one to conclude that this origin is porosity related. The organizers felt that it was a "machining chip" but it is conceivable that it was an area of poorly bonded material which was sensitive to chip formation. Further examination of the specimen by the organizers did not reveal any additional chips along the chamfers.

The consensus of the participants was that machining damage was the fracture origin in all three sets. There were however, some who believed it was a different form of machining damage or that these origins were something else. These differences may stem from: a lack of familiarity with how machining damage can appear in ceramics; a lack of experience observing this type of origin; or an error on the part of the organizers.

Machining damage can manifest itself in different ways in ceramics. Gross machining damage (e.g. chips, deep striations) can easily be seen, sometimes at very low magnifications, on the machined surface(s) of a specimen, but these features are often too small (from a fracture mechanics perspective) to be the

actual fracture origin. On the other hand, subsurface cracking can be much deeper, but it is extremely difficult to detect, even for fractographers with much fractographic experience, because the subsurface microcracking can blend into the microstructure. This latter type of damage can occur during the typical step-wise machining process. Initial grinding is commonly done with a coarse-grit wheel (coarse in regards to the grit used in subsequent steps). During these initial steps, chips and deep striations can cause subsurface microcracking (10 - 50  $\mu\text{m}$ ) which is not necessarily removed during the subsequently finer grinding steps of the process if insufficient material is removed. The fine grinding may remove deep surface striations, but may not remove enough material to eliminate the subsurface machining damage. Grinding with finer grit wheels can cause its own machining damage but in general it will be smaller and less severe. Many times, multiple microcracks which can overlap and interact result from the diamond grinding process.

In sets #1 (Zirconia/Alumina) and #2 (Silicon Nitride) the subsurface damage is difficult to discern since it blends very well into the normal microstructure of the ceramic. Some of the participants marked striations on the tensile surface as the fracture origin rather than the subsurface cracks. Based on fracture mechanics, Equation 1b, these striations are too small to be the fracture origin. The fact that the SEM photographs show some striations which are deeper than those around them may have misled some participants to think that these were the origin. If the participants had had the chance to analyze all the machined surfaces of the specimen or a group of identically machined specimens, as the organizers had, it would become clear that these few "deep" striations are not unusual.

None of the participant noted the irregular edge along the chamfer in set #3 (Alumina), open arrows in Figure 1.7B. The chamfer is irregular and comprised of several segments at different angles. This feature did not copy well in the photographs sent to the participants and probably accounts for the oversight. This fracture origin may be a case of coincidental origin types, a porous region plus machining damage.

The identity of the fracture origin in photograph sets #1 (Zirconia/Alumina) and #3 (Alumina) as machining damage was questioned by several participants. Both of the participants who disagreed with the identity of the origin in set #1 (Zirconia/Alumina) each had 10 years of combined fractographic experience. Even though this is a significant amount of experience, the combined experience of several individuals is quite different from one individual with 10 years experience. The experience of the participants who disagreed with the identity in set #3 (Alumina) ranged from 1 year to 35 years.

LOCATION - Most participants reported the location of the fracture origins as "surface" in agreement with the organizers and the guidelines of MIL HDBK-

790. Several reported that the origins were "near the surface", however. These respondents may have felt that the subsurface crack was better described by such a characterization, but this may be merely a different of semantics. The organizers feel that machining damage is inherently a surface or edge distributed fracture origin.

For sets #1 (Zirconia/Alumina) and #2 (Silicon Nitride) participant 12 located the origin at the edge contrary to all other participants. Confusion as to the distinction between surface and edge may be cause of this difference. In MIL HDBK-790 the edge location means the junction of two external surfaces (e.g. the chamfer on a flexure bar). This participant may have interpreted the intersection of the fracture and tensile surfaces as an "edge", thus the discrepancy. This issue will have to be clarified for future versions of MIL HDBK-790.

Although a majority of participants located the origin in set #3 (Alumina) at the edge there were some who determined that it could be located at the surface or the edge. An examination of the photographs clearly shows that the origin is in contact with the surface and the edge so either location is correct.

FRACTURE ORIGIN SIZE - The round robin guidelines did not give specific instructions on how to report the origin size, and referred instead to MIL HDBK-790. The handbook states that the diameter shall be reported for equiaxed origins, and the major and minor axes for elongated origins. The organizers intentionally did not specify how the size was to be reported, intending instead to see if the participants would follow the guidelines in the handbook or use some other practice.

The methods of reporting the size of the fracture origin varied widely between participants. Some reported a diameter and others a radius. Still others reported a depth or a 2-dimensional value. The characterization of sizes of fracture origins in ceramics is difficult. In principal, fracture mechanics can be used to relate the size of the fracture origin to the mechanical properties, (strength and toughness), but in practice, there are many complications. The best correlation between size predicted by fracture mechanics and fractographic analysis were in sets #2 (Silicon Nitride) and #3 (Alumina).

Equation 1a would appear to be quite applicable to ceramics since strength and toughness values are readily available for these materials. However, many of the origins observed in ceramic materials tend to have complex geometries (3-dimensional and/or asymmetrical), which does not lend itself to having a single value representing the size or shape of the origin. Additionally the origins' true size and shape may not be revealed on the fracture surface<sup>19</sup>. In such instances, the use of equivalent semicircles or semiellipses is only an approximation.

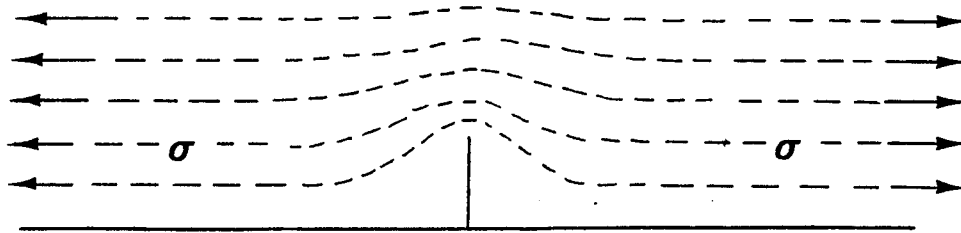
Fortunately, fracture origins created due to machining damage tend to be 2-dimensional and assume a semicircular or semielliptical shape (this is especially true for subsurface damage), and Equations 1a and 1b are applicable when applied to these cases. Evans, et.al.<sup>20</sup> and Rice<sup>21</sup> have shown that for ceramics, machining damage is the origin most amenable to fracture mechanics analysis. Correlations between origin sizes predicted by fracture mechanics and those determined from fractographic analysis are now discussed on a set by set basis.

The origins outlined for set #1 (Zirconia/Alumina), Figure 1.3, and set #2 (Silicon Nitride), Figure 1.5, have essentially a semicircular or a semielliptical shape. The origin in set #3 (Alumina), Figure 1.7, is part of a circle. In Figure 1.3 (set #1) the origin outlined by the organizers can be closely approximated by a semicircle of radius,  $c \approx 15 \mu\text{m}$ . This is approximately three times larger than the value predicted by fracture mechanics ( $K_{Ic} = 5$ ,  $Y = 1.4$ , and  $\sigma = 1552$ ). This calculation assumes the material has a constant toughness. Zirconia-based materials have been shown to exhibit pronounced R-curve behavior for "long-cracks"<sup>22-24</sup> and recent studies indicate that this phenomenon can be present with small cracks, i.e., at the scale of naturally occurring fracture origins, over relatively short crack extensions<sup>25-27</sup>. This "micro" R-curve behavior has shown that the fracture toughness can be as low as 1 to 3  $\text{MPa}\cdot\sqrt{\text{m}}$  for short cracks in a Y-TZP but increases to over 5 once the crack extends more than  $10 \mu\text{m}$ <sup>27</sup>. This effect cannot account for the discrepancy in the present instance, since lower toughness values will lead to smaller crack sizes at criticality. Different toughness testing techniques can also yield different toughness values for the same material<sup>28</sup>.

Several other factors may have affected the measurement of this origin:

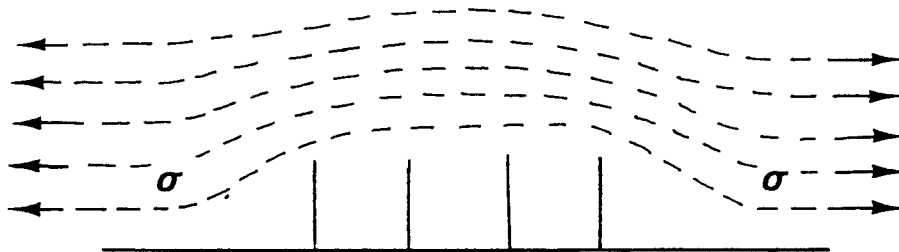
- 1) The specimen was heat treated prior to strength testing. This treatment probably reduced or eliminated any residual stresses created by machining and/or it may have changed the acuity of the associated crack.
- 2) Crack nesting, as illustrated in Figure 1.8, could also have been a factor. It is safe to assume that the machining damage which was strength-limiting in this specimen is not the only machining-induced crack in the specimen. There are probably many similarly sized cracks, where by the cracks can shield each other from experiencing the full stress intensity that is assumed for a single, stand alone crack. The maximum stress intensity diminishes significantly as the distance between cracks diminishes<sup>29</sup>. Errors may also arise from examining a tilted specimen which may foreshorten the depth measurement, or incorrect magnifications, but these are insufficient to explain this difference. Appendix 2 discusses in more detail the complications which can be encountered when comparing the calculated origin size to the fractographically-measured origin size.

## **SURFACE CRACK IN A TENSION STRESS FIELD**



### **Single Crack**

The "flow lines" of stress are distorted or kinked quite a bit,  
causing a large stress concentration  
or a high stress intensity,  $Y$ , at the crack tip.



### **Multiple Nested Cracks**

The flow lines are kinked less.  
The stress intensity on the cracks is much less.

$$K_{Ic} = Y \sigma \sqrt{a}$$

↓

Figure 1.8. Schematic example of the effect of crack nesting on the stress intensity experienced by a crack.



In set #2 (Silicon Nitride) the organizers feel the machining damage also had a semicircular or semielliptical shape. An alternate interpretation is that several small semiellipses merged into one larger one as illustrated by the dashed line in Figure 1.5C. Such linking has been reported previously<sup>30</sup>. Three subsurface cracks can clearly be seen in Figure 1.5B. All three are approximately the same size but the crack labeled B is centered in the fracture mirror. Participants 4 and 11 stated that these origins looked like "controlled surface flaws".

The size of semicircle B is in excellent agreement with the predicted origin radius (25  $\mu\text{m}$  compared to 23.5  $\mu\text{m}$ ). Some of the participants who reported large  $2c$  values may have included more than one of these semicircles into their measurement. The toughness values calculated by participants 4 and 9 were in excellent agreement with the value provided. Recent work by Salem and Choi<sup>31</sup> has shown that the silicon nitride used in this exercise (Norton NCX-34) can exhibit R-curve behavior yielding a toughness between 5.1 and 6.9  $\text{MPa}\cdot\sqrt{\text{m}}$ . Using this toughness range and the strength (910 MPa), yields an origin size between 15 and 30  $\mu\text{m}$ . Only six participants reported a size in this range.

Although there were some different interpretations as to the shape of the origins in sets #1 (Zirconia/Alumina) and #2 (Silicon Nitride) (semicircle or semiellipse), this is not a critical issue. The stress intensity shape factor for the semicircle or alternative wide semiellipse range only from 1.3 to 1.7 and the characteristic origin dimension used, depth, is the same for both geometries.

The shape of the fracture origin in set #3 (Alumina), Figure 1.7B is clearly part of a circle. Because the origin is located at or near the edge some participants were unsure as to how to measure it. Some measurements were made across the corner (chamfer), or on a radius running perpendicular from point A, see Figure 1.7B, into the bulk, still others made their measurements from point A along the tensile/fracture surface interface. One participant felt that special instructions should be provided to measure the origin size in such cases. The simplest way is to extend the plane of the tensile surface and extrapolate the arc of the semicircle from the edge to this extension, completing the semicircle.

The edge crack in the alumina specimen (set #3) had a number of interesting features. As outlined in Figure 1.7B there appears to be three stages of crack growth. Stage 1 is transgranular fracture which may have occurred due to machining. Stage 2 is more intergranular and may indicate subcritical crack growth. Stage 3 could be fast fracture. The time-to-failure in the strength test was approximately 7 seconds. (The specimen was tested in laboratory ambient conditions in which humidity may have had an affect.) Kirchner, et. al.<sup>19</sup> have seen similar types of fractures in 96%  $\text{Al}_2\text{O}_3$  specimens. Application of

Equation 1a using toughness values of 3.4 to 4.0 MPa $\sqrt{m}$  indicate the semicircular feature should have been 110 - 160  $\mu m$  deep at criticality. We note the extent of possible subcritical crack growth correlates well with the larger of the two estimates. The three regions led to different interpretations by the participants as to what was the precrack in the fracture origin. As discussed, some participants overlooked the low strength ( $\sigma = 228$  MPa) of the specimen and defined the outer most ring as the mirror. Most participants labeled either the chip or the "smooth" region of transgranular fracture as the origin. Many labeled the latter as the fracture mirror. Had Equation 1b been applied it would have become clear that the origin in this specimen was quite large and it may have reduced the number of misinterpretations. Even with the misinterpretations and mislabelings, the sizes reported for the various regions were very consistent from participant-to-participant.

**MIRROR SIZE** - In brittle fracture there is an ordered formation of fracture markings, the mirror, mist and hackle, which radiate from the fracture origin. Conceptually, it should be straight forward to measure fracture mirrors and determine mirror constants. Mirrors are essentially semicircular or circular, and are centered on all (or part of) the fracture origin in uniformly stressed specimens or components, but in practice there are a number of complications.

These fracture markings are easily seen and measured in glasses. In polycrystalline ceramics this is not necessarily so. If the specimen is highly-stressed, and the material is fine-grained and dense then a distinct fracture mirror and hackle will form. On the other hand, in lower-energy fractures and those in coarse-grained or porous ceramics a distinct fracture mirror may not form. In both instances the mist region which separates the mirror from the hackle is almost impossible to detect. Although these features can easily be seen their sizes are difficult to determine because the boundaries are not distinct.

Geometric complications arise from non-uniform stress states and free surface effects. In flexure specimens and other parts with stress gradients, the mirror shape can be distorted. For mirrors associated with origins in the bulk it is suitable to measure the mirror diameter and divide by two. The radius in rectangular specimens which fracture due to surface-located origins can be measured along the tensile surface from the origin to the mirror/mist boundary. Measuring the mirror size associated with surface-located origins is however more complex than it appears.

An initial analysis by Johnson and Holloway<sup>32</sup> predicted that crack-branching occurs when the product of the local stresses at the crack front and the square root of the crack radius reach a critical value. Their analysis does not take into account free surface effects and predicts a simple semicircular mirror shape for surface cracks in tension specimens. The stress model also

underestimates the elongation of the mirror towards the neutral axis in flexure specimens.

Kirchner and Conway, Jr.<sup>33</sup> used a stress intensity criterion to predict the formation of crack branching features in brittle materials which fracture, in tension or flexure, due to origins located at the surface. Mirrors will not be semicircular about the origin because free surface effects will reduce the mirror radius near the surface. This is the case for rectangular or cylindrical specimens tested in tension or flexure. For rectangular specimens tested in tension the radii was about 27% shorter at the surface than that measured perpendicular to the surface. As a consequence, there is a dilemma as to what is the best method to measure the mirror size, especially in flexurally loaded specimens. One way to avoid this effect for tension specimens is to measure the mirror along a perpendicular line from the origin into the fracture surface. There is an additional complication in flexure specimens since mirrors tend to be elongated towards the neutral axis due to the stress gradient in the specimen thickness (unless the mirror is very small).

Mecholsky et. al.<sup>15</sup> established a relationship between the mirror size and the fracture origin size. They found that for single crystals, polycrystalline ceramics, and glasses the outer mirror (mist/hackle) to origin size ratio is generally 13:1 while the inner mirror (mirror/mist) to origin size ratio is about 6:1 for the former two cases and about 10:1 for glasses. These relationships are valuable aids in the fractographic interpretation of either mirror or origin sizes.

All of these variations in the interpretation of the formation of a mirror, different modes of viewing, different procedures to estimate size, have led to large differences in the reported values for mirror constants. A compilation of the mirror constants ( $A_0$ ) found in the literature is presented in Table 1.4 for ceramics similar to the three used in this exercise.

Two mirror size ranges were estimated for each specimen in the present round robin exercise. The first range was determined using the lowest and highest values of  $A_0$  found in the literature (Table 1.4) and the strength of each specimen. The second range was obtained from the ratio method, using the origin size estimated from fracture mechanics and the 6:1 ratio for the inner mirror (mirror/mist). These ranges are listed in Table 1.5.

The values in Table 1.1 reported by the participants for set #1 (Zirconia/Alumina) are in very good agreement with the ranges from both methods. Only two participants were outside either range. One was slightly higher while the other was significantly above either range. In set #2 (Silicon Nitride) five participants' mirror sizes (Table 1.2) were outside the  $A_0$  estimated range, four were slightly below the range while the fifth was significantly higher, the rest fell within the ranges. Six participants values were outside the range

Table 1.4  
MIRROR CONSTANTS FOR THE THREE CERAMICS IN TOPIC #1

MATERIAL	$\sigma$ TECHNIQUE	$A_o$ (MPa $\sqrt{m}$ )	REFERENCE
<u>Zirconia</u>			
Zircar	Flexure	15.2	15
Zyttrite	Flexure	7.4	15
<u>Silicon Nitride</u>			
NC-132	Flexure	9.2	34
NC-132	Flexure (Rods)	8.9	17
"	Delayed Fracture	9.2	17
HS-130	Flexure	18.1	15
HS-130	Flexure (Rods)	9.1	17
Si <sub>3</sub> N <sub>4</sub>	Flexure	12	15
Reaction Bonded	Flexure (Rods)	4.2	17
HP-Si <sub>3</sub> N <sub>4</sub>	Flexure (Rods)	14.3	35
<u>Alumina</u>			
HP - Al <sub>2</sub> O <sub>3</sub> (99+ pure)	Flexure	10.3	34
HP - Al <sub>2</sub> O <sub>3</sub> (99+ pure)	Flexure	$A_i = 5.2$	15
HP - Al <sub>2</sub> O <sub>3</sub>	Flexure (Rods)	10.4	36
HP - Al <sub>2</sub> O <sub>3</sub>	Flexure	9.8	37
HP - Al <sub>2</sub> O <sub>3</sub>	Flexure (Rods)	10.3	17
" "	Delayed Fracture	9.9	17
Sintered Al <sub>2</sub> O <sub>3</sub> (96%)	Flexure	8.5	34
Al <sub>2</sub> O <sub>3</sub> (96%)	Flexure (Rods)	8.3	17
"	Delayed Fracture	8.9	17
Sintered Al <sub>2</sub> O <sub>3</sub>	Flexure	9.0	37, 38
Al <sub>2</sub> O <sub>3</sub> (96%)	Flexure (Rods)	9.1	35

$A_o$  is the outer mirror constant unless otherwise noted.

Table 1.5  
MIRROR SIZE RANGES FOR THE THREE SPECIMENS IN TOPIC #1

Set #	$A_o$ Values	Ratio Method
1: Zirconia/Alumina	45 - 192	64 - 139
2: Silicon Nitride	192 - 792	282 - 611
3: Alumina	2650 - 5540	1884 - 4082

All values are in micrometers

estimated by the ratio method. Five were below the range and one was higher. For set #3 (Alumina) none of the participants reported (Table 1.3) a value in either of these ranges. The mirror is actually larger than the area shown in the photographs. In fact the upper end of these ranges are larger than the width or height of the specimen! One participant did indicate that the mirror was in excess of 1 mm. As stated previously many participants were fooled by the appearance of the fracture origin in set #3 (Alumina) and labeled the "smooth" region of transgranular fracture (stage 1 in Figure 1.7B) as the mirror. Additionally, in each set, but especially in set #3, some of the participants reported a mirror size that was only slightly larger than the size of the fracture origin they reported. This is impossible.

The constants used for sets #1 and #2 may not be appropriate for these materials. The ceramic in set #1 is a zirconia/alumina composite. The available mirror constants are for zirconia only and these constants were determined for materials made in the 1970's before the high strength zirconias of today were available. These mirror constants are most likely for a refractory-grade partially-stabilized zirconia. Even so they appear to fit the data reported by the participants. In set #2 the silicon nitride contains yttria and an elongated microstructure that can be the source of R-curve behavior<sup>31</sup> while the mirror constants in the literature are for a magnesia-doped silicon nitride which has negligible R-curve behavior. The constants used for alumina (set #3) would appear to be suitable since the values reported in the literature do not vary much with purity level or processing technique and are very nearly the same for a variety of investigations.

Using the mirror-to-origin size ratio method relies on accurate measurement of the origin size which is difficult in its own right. As stated previously the true size of the origin may not be shown on the fracture surface. Additionally if the origin has a complex geometry it may be difficult to determine which dimension should be used to estimate the mirror size.

### **Topic #1: Conclusions**

The results Topic #1 have revealed several very important aspects of fractography of machining damage in advanced ceramics.

1) Even though there was a general agreement on this origin type (machining damage) a better understanding of what machining damage is (surface vs subsurface damage) is needed. A fractographer must understand not only the different manifestations of machining damage but how these may vary in advanced ceramics. Proper characterization probably requires the examination of many specimens.

2) There does not appear to be any correlation between the overall experience of the fractographer and the ability to observe and characterize subsurface machining damage in these three ceramics. Specific experience in characterizing machining damage is essential.

3) The definition of surface and edge as a location for fracture origins must be clarified.

4) The variety of dimensions reported for the origin size indicates that some form of a consistent measurement scheme is needed.

5) Fracture mechanics can estimate the size of the fracture origin and thus is a useful tool that should be used routinely to aid fractographic

interpretation of machining damage. However, complications arise from residual stresses, crack blunting, errors in toughness values, uncertainties of the shape factor ( $Y$ ), crack nesting, R-curve behavior, and environmentally-assisted stable (slow) crack growth.

6) Machining damage often can have multiple interpretations, especially if several cracks are present which can link up, or if the crack extends stably prior to fracture.

7) In the instances where multiple semielliptical or semicircular microcracks were present at a fracture origin, it was difficult to arbitrarily pick one as the definitive origin. The depth of the machining damage is the key parameter to measure in such cases, and will be approximately the same for each microcrack irrespective of the exact origin boundary chosen.

8) The interpretation of fracture origins from photographs only is not the ideal manner in which to characterize machining damage (or any fracture origin) and its associated fracture mirror. Actually viewing the specimen is more constructive and insightful and will greatly reduce misinterpretations.

9) Fracture mirrors are easier to see at lower magnifications in polycrystalline ceramics but they are somewhat difficult to delineate and even more difficult to measure with confidence.

10) There is a lack of appropriate mirror constants for many of today's advanced ceramic materials.

## ***Topic #2 - Characterization Of Fracture Origins In Specimens***

### **Topic #2: Objective**

To locate and characterize fracture origins in six (6) specimens and determine the effectiveness of the characterization scheme in MIL HDBK-790.

### **Topic #2: Background**

An important feature of MIL HDBK-790 was the adoption of a consistent and comprehensive manner of fracture origin characterization including nomenclature. Fracture origins will be characterized by three attributes: IDENTITY, LOCATION, and SIZE.

### **Topic #2: Approach**

Each participant received both mating halves of the primary fracture surface of six (6) fractured ceramic specimens. Individual laboratories received different sets of six specimens, but all the specimens were from identical batches and believed to have the same origin type. Together the participating agencies evaluated a total of 102 fracture origins. The six ceramics used in this topic were:

- 1) Alumina w/SiC whiskers
- 2) Alumina
- 3) Zirconia
- 4) Silicon Carbide
- 5) Silicon Nitride
- 6) Titanium Diboride

These ceramics were chosen based on their conduciveness to fractographic analysis. All specimens, with the exception of the silicon nitride (specimen 5), were machined from large billets of material. The silicon nitride was machined from as-fired bars. All of the specimens were fractographically characterized by the U.S. Army Research Laboratory - Materials Directorate prior to inclusion in the round robin. The characterization was done in an uncoated state using an SEM. Due to charging problems the silicon nitride specimen was sputter coated with  $\approx 100 \text{ \AA}$  of Au prior to characterization. This coating was not removed from the specimen by the organizers after their initial characterization. Although an optical analysis can provide information that can not be obtained during SEM analysis the organizers believe that characterization of these origins requires the use of an SEM.

## **Topic #2: Instructions**

The participants were told to treat the specimens as if they had fractured them and to characterize the fracture origin as outlined in Military Handbook 790. They were asked to record the information and answer all the questions on an enclosed data sheet. A complete package of instructions is given in Appendix 1.

## **Topic #2: Results And Discussion**

The six specimens will be dealt with separately. Each section will contain the material information that was provided to the participants, the organizers' characterization, a summary of the participants' results, a discussion of these results, and a summary of the findings. In each table instances where the participants' characterization essentially concurred with the organizers' characterization are marked with a check (✓). Participant 14 failed to report.

### **Specimen 1: Large Grains In Alumina w/SiC Whiskers**

**MATERIAL INFORMATION:** The specimens were a ceramic composite comprised of silicon carbide (SiC) whiskers in an alumina ( $\text{Al}_2\text{O}_3$ ) matrix. It was produced by hot-pressing  $\alpha\text{-Al}_2\text{O}_3$  with 29 v/o SiC whiskers. Fracture toughness was determined by double torsion tests to be  $\approx 7.3 \text{ MPa}\cdot\sqrt{\text{m}}^{18}$ . The room temperature four-point flexure strength of these eighteen specimens, in air, was between 429 and 573 MPa.

**ORGANIZERS' CHARACTERIZATION:** The dominant fracture origin in this ceramic was identified as clusters of large alumina grains ( $\text{LG}^V$ ) which are volume distributed<sup>39</sup>. Eighteen (18) specimen from this material were prepared for this round robin. Each had a different strength and different origin location and size, but the origin type was identical. The specific location of each varied: some were in the volume, others were at the surface, near the surface or at an edge. The characterization should be Large Grain ( $\text{LG}^V$ ) which are volume distributed. The size of these origins was best represented by either a single dimension (radius of a circle) or a 2-dimensional value (minor axis x major axis of an ellipse). Origins which were represented by a circle had a radius that ranged from 15 - 35  $\mu\text{m}$ . The elliptical origins had a minor axis between 10 and 50  $\mu\text{m}$  and a major axis between 30 and 200  $\mu\text{m}$ . An example of large grains in this ceramic is given in Figure 2.1.1.

**PARTICIPANTS' RESULTS:** The participants results are summarized in Table 2.1. Only five (8, 9, 10, 13, and 16) of the 17 participants felt that the origin was a large grain(s). Participants 1 and 3 believed that large grains were part of a combined origin. A variety of other identities were also given. All but six of the participants agreed with the organizers' characterization of the location of the



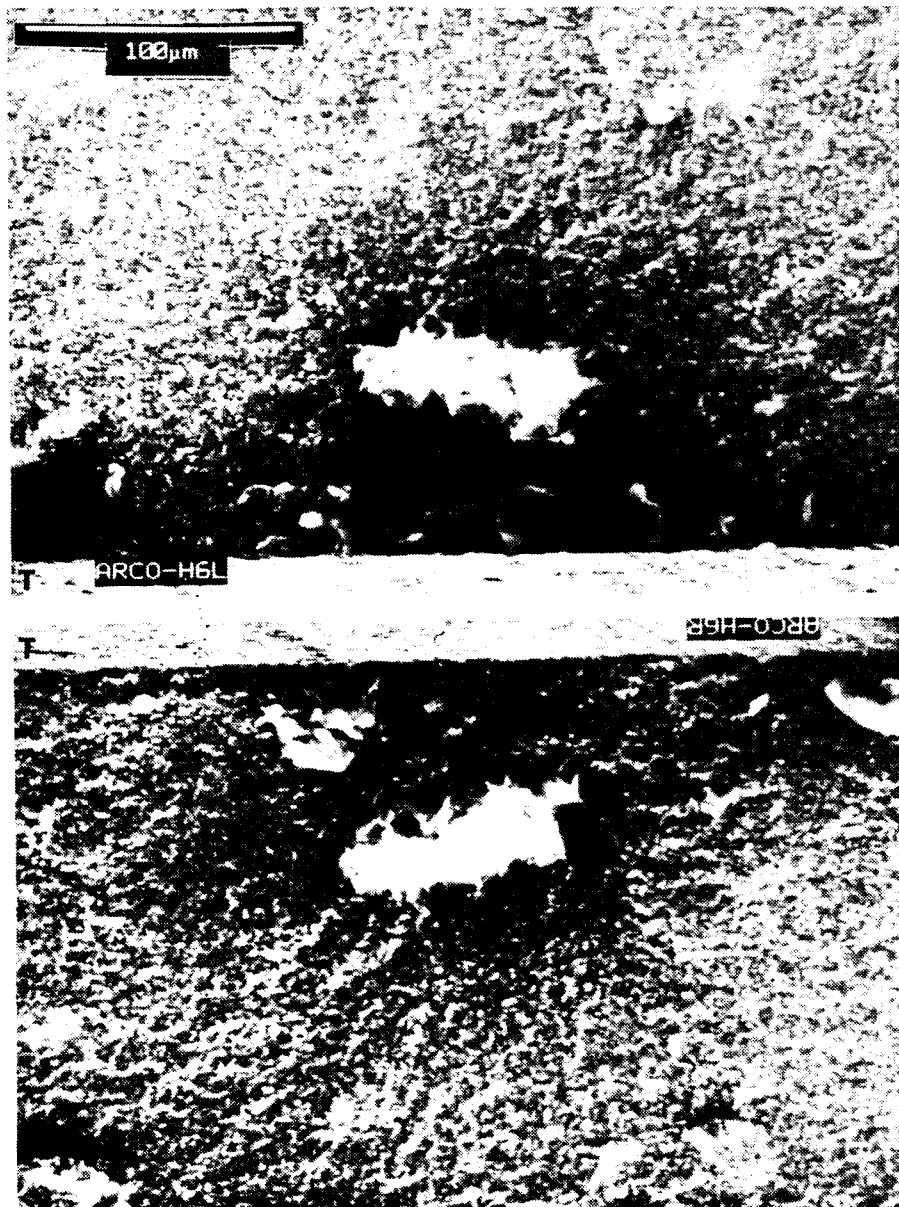


Figure 2.1.1. Example of Large Grains in Specimen 1: Alumina/SiC (whiskers). Mating halves of the primary fracture surface are shown. "T" denotes the tensile surface.

fracture origin while seven agreed with the organizers' size of the origin. Participant 13 was the only one in complete agreement (Identity, Location and Size) with the organizers, but three others (8, 9, and 16) agreed with all but the size attribute. The size values reported were drastically different, as were the methods of reporting the size.

Table 2.1  
**PARTICIPANTS' RESULTS FOR SPECIMEN 1:  
LARGE GRAINS IN ALUMINA w/SiC WHISKERS**

No.	Identity*	Location**	Size (μm)***	Comments
1	PR w/ LG	NS	80 ✓	45 μm below tensile surface; dark spot-optically
2	I	V/NS ✓	60 ✓	40 μm below tensile surface; No EDS
3	LG/P ✓	NS	40 ✓	5 μm below tensile surface
4	MD	S ✓	3+	Photos show LG; No EDS
5	?	S ✓	? ✓	
6	?	S ✓	30 x 70 ✓	Dark spot-optically; Si WDX map no SiC in origin
7	PS	V ✓	190 x 130	Photos show LG; size of LG agrees with estimate
8	LG ✓	V ✓	30, 20	90 μm below tensile surface; EDS shows Al
9	LG ✓	NE ✓	c ≈ 150	K <sub>IC</sub> estimate agrees (Y=1.13)
10	LG ✓	NS	≈ 50	20 μm below tensile surface; Si EDS map no Si
11	I	S ✓	300	"Black area"; No EDS; Size estimated to be 144 μm
12	PR/A	NS	15 x 30	Looked at different area
13	LG ✓	NS ✓	23 - 75 ✓	EDS shows Al
15	MD	E ✓	Depth = 100	Looked at 1/2 of surface; Saw LG-probably not origin
16	LG ✓	NE ✓	40 ✓	75 μm below tensile surface
17	PR	E ✓	No value	Reported a mirror size instead of origin size
18	2P	NS	Depth = 58	"Very large region w/o Si whiskers"

✓ - agreement with the organizers' characterization. ? Not determined. \* PR - Porous Region; LG - Large Grain; MD - Machining Damage; PS - Porous Seam; I - Inclusion; A - Agglomerate; 2P - Second Phase Inhomogeneity. \*\* NS - Near Surface; V - Volume; S - Surface; E - Edge; NE - Near Edge. \*\*\* Single values indicate origin diameter (2c) unless noted. 2-dimensional values are minor axis x major axis unless noted.

**DISCUSSION - Identity** - The main reason many participants had trouble identifying this origin as large grain(s) was they examined only one specimen. Had they had the opportunity to examine the entire group of specimens, as the organizers had, it probably would have become apparent that large grains were the dominant fracture origin in this ceramic. Although this is believed to be the main source of the participant's trouble, there are other possibilities.

One is the failure to use EDS to analyze the chemical composition of the origin. Participants 2 and 11 labeled the origin as an inclusion (IV). Neither participant used EDS. In both cases the organizers' and participants' photographs of the origin are identical. Figure 2.1.2 shows the participants' and the organizers' photographs of the origin in participant 2's specimen. EDS of these origins by the organizers revealed a high Al content with no Si. This indicates that the origin may be large alumina grains. Another reason for the inclusion label could be the appearance of the large Al<sub>2</sub>O<sub>3</sub> grains when viewed



**A**



**B**

Figure 2.1.2. Photographs of large grain fracture origin in specimen 1 from participant 2 specimen set. A) Participants' photograph. B) Organizers' photograph. "T" denotes the tensile surface in B).

in an optical microscope. Three participants (1, 6, and 11) commented that the origin appeared as a "dark spot" or "black area" when viewed optically, see Figure 2.1.3, but this may merely be an optical effect.

Three of the four participants who used EDS properly identified the origin but participant 18 felt the origin was a "microstructural irregularity" because EDS showed a "very large region without SiC whiskers". The origin was identified as a second phase inhomogeneity (2P<sup>V</sup>) instead of large grains. Participant 10 labeled the origin properly but in the attached comments said "the crack initiated at SiC large grains" even though an X-ray map of Si showed the origin region to be devoid of Si. Participant 6 could not identify the origin even though an Si WDX map revealed that there were no SiC whiskers in the origin. Both of these participant did not have a lot of experience with alumina or whisker reinforced ceramics, (see Table Q.2). They only examined one of the mating halves of the primary fracture surface, and as fate would have it, it was the surface on which the origin was not as obvious.

Three other participants (4, 7 and 15) indicated they saw large grains or their photographs showed the presence of large grains, but they did not feel that these were the origins. Participant 4 identified the origin as machining damage (MD<sup>S</sup>) but their photographs clearly show large grains, Figure 2.1.4A and B. The origin was labeled as machining damage because there is a discontinuity in the tensile surface (Figure 2.1.4D). Participant 15 also characterized the origin as machining damage. In this instance the participant only examined one of the mating halves of the primary fracture surface. The presence of large grains was noted but the half that was examined had a chip missing at the chamfer. Had the mating half of the fracture surface been looked at it would have been clear that the origin was a cluster of large grains located at the chamfer and the chip was an artifact of the testing or subsequent handling. Finally the photographs from participant 7 show a cluster of large grains and the participant states that the size of this cluster agrees with a size estimate but the origin was interpreted as a porous seam (PS<sup>V</sup>).

The photographs from participant 17 matched those of the organizers but the participant chose porosity as the dominant origin. The large grains were more obvious on the mating half of the primary fracture surface that was not examined. Participant 5 could not characterize the origin due to limited SEM time while the inexperience of participant 12 led them to examine the incorrect area on the fracture surface.

It is common for porosity to be associated with large grains creating an origin with mixed attributes. For both participant 1 and 3 there is some porosity in and around the cluster of large grains and thus the multiple label they provided for this origin identity is acceptable.

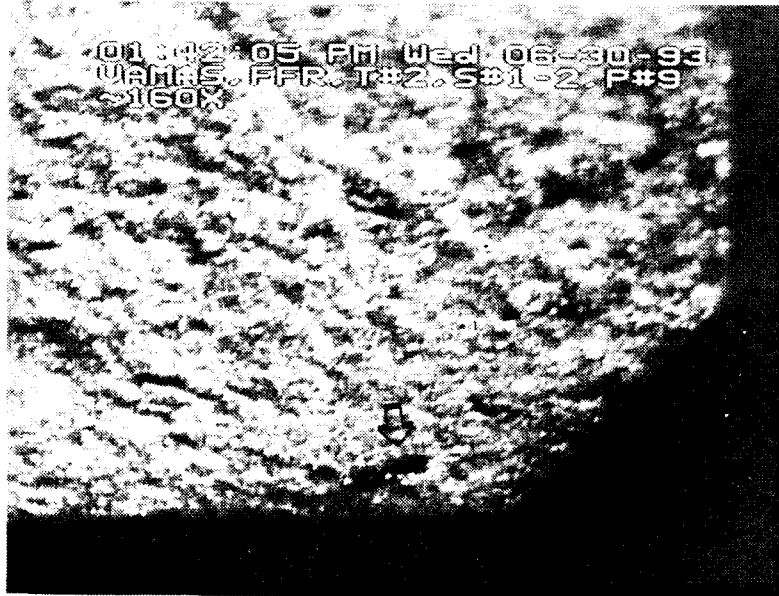


Figure 2.1.3. Optical photograph of alumina grains as the fracture origin in specimen #1. Origin appears as a dark spot when viewed optically. (Arrow added by the organizers.)

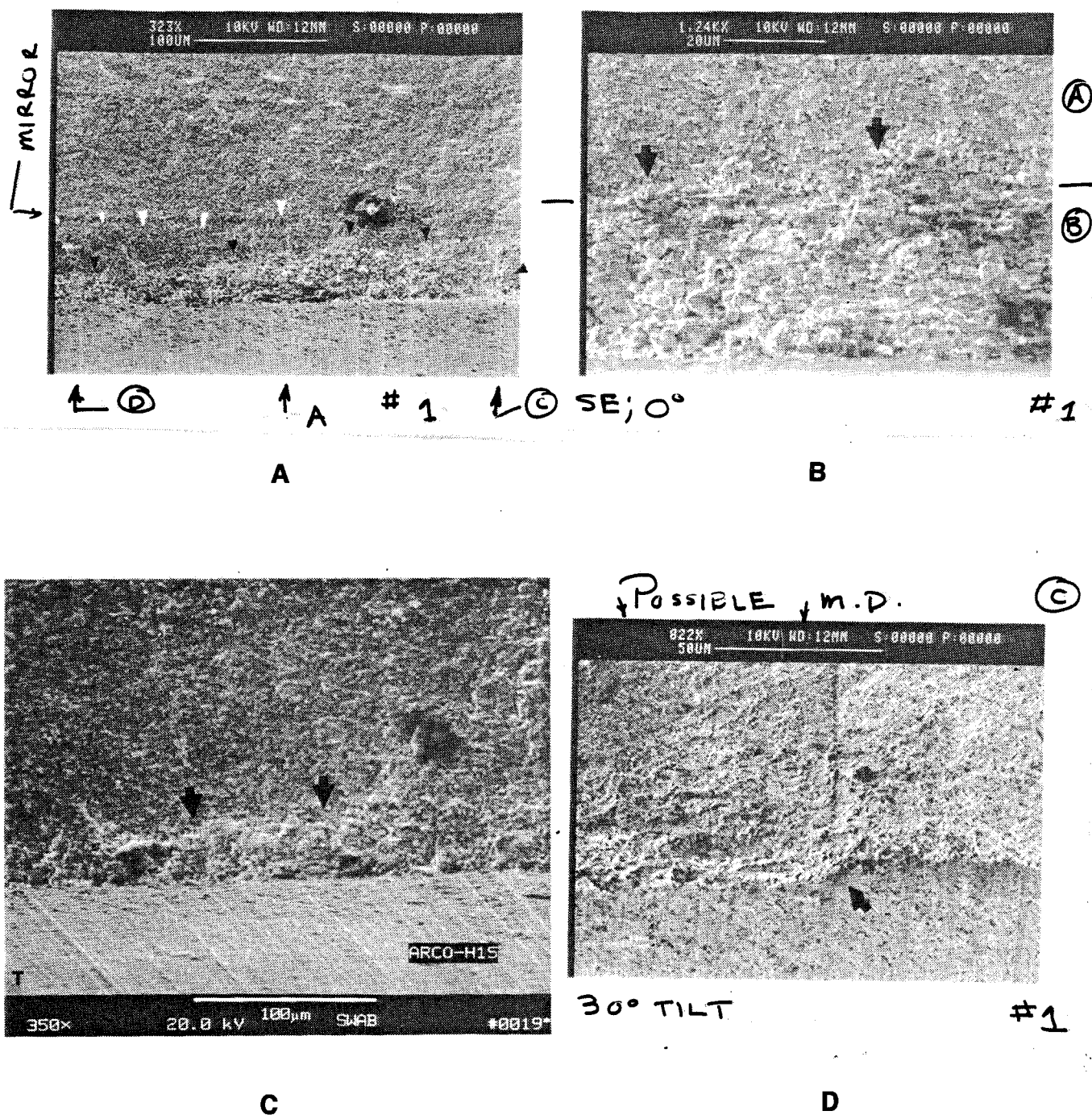


Figure 2.1.4. Photographs of large grain origin in specimen 1 from participant 4. A) and B) are the participants' photographs. Large grains can be seen in B). C) Organizers' photograph. "T" denotes the tensile surface. D) Participants' photograph of the possible machining damage. (Arrows in B and D were added by the organizers. Handwritten notes on A), B) and D) are the participants.)

**Location** - Ten participants agreed with the organizers' location of the fracture origin in their respective specimens. Two others (9 and 16) reported a near edge (NE) location which was a plausible characterization. The origin in both of these cases was located near the edge. However, it is recommended that the location of a subsurface origin be made in relation to its distance from the tensile surface rather than the edge. A comment indicating its relation to the edge can be noted.

There are several reasons for the differences with the remaining participants. Participant 1 characterized the location of the origin based on the porosity rather than the large grains. Participant 12 looked at the wrong area of the fracture surface while participant 18 just located the origin incorrectly, Figure 2.1.5. In the case of participants 3 and 10 there were several clusters of large grains in the central portion of the mirror, Figure 2.1.6, making it difficult to determine which cluster was the primary origin hence their characterization of the location is different from that of the organizers.

**Size** - The origin sizes varied between participants because each was looking at a different specimen, but the variety of ways of reporting size was reminiscent of the variations in Topic #1. The radius ( $c$ ) of the origins in these alumina/silicon carbide specimens should be between  $83\text{ }\mu\text{m}$  ( $\sigma = 573\text{ MPa}$ ) and  $148\text{ }\mu\text{m}$  ( $\sigma = 429\text{ MPa}$ ). (This range was calculated from Eqn. 1b, assuming a semicircular surface crack in a uniform tensile stress field ( $Y = 1.4$ ), with constant toughness.) It can be seen from Table 2.1 that only participants 1, 7, 9 and 15 reported values that were within or near this range. The value reported by participant 4 ( $2c = 3+ \mu\text{m}$ ) is too small from a fracture mechanics perspective.

Similar to the findings of Topic #1 of this exercise, the determination of the size of fracture origins is difficult due to the complex geometries of the origins. This is further complicated if the origin is located near the surface. Did the ligament of material between the surface and origin break prior to catastrophic fracture? If so, should the size of the origin include this ligament? Additionally, these specimens were tested in flexure there is a stress gradient through the specimen cross section and thus the stress at the origin may be less than the calculated value.

**SUMMARY:** In general, there was good agreement between the organizers and the participants of the origin location in these specimens. The main problems were with the origin identity and size characterization. There was no correlation between one's overall fractographic experience or their experience with whisker reinforced alumina and the characterization of this origin identity. Chemical analysis of the origin was not done or the results were misinterpreted. Many participants were misled because they examined only one of the mating halves of the primary fracture surface. Measuring the size was complicated by the complex geometries that were encountered and the lack of a distinct boundary



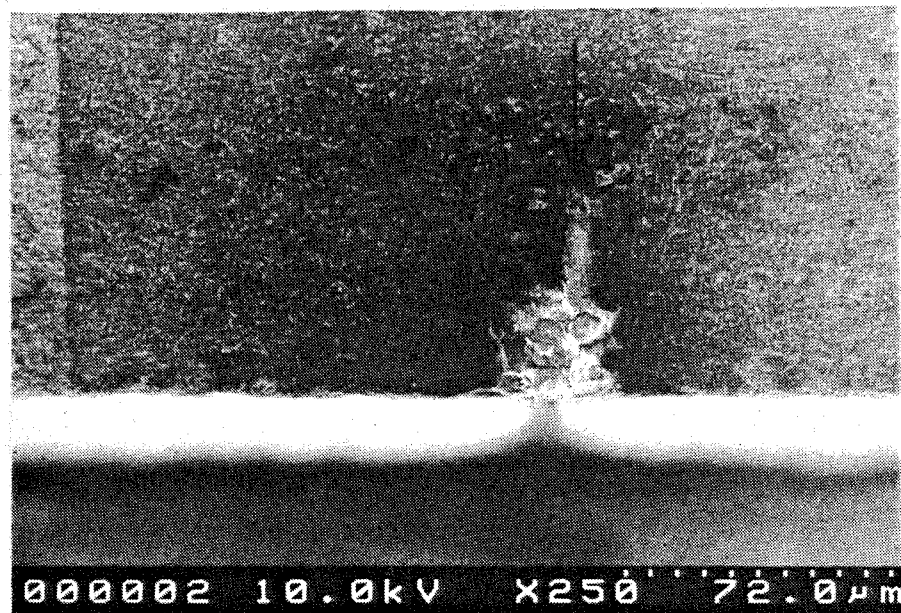


Figure 2.1.5. Two of participant 18's photographs of the origin in specimen 1. The origin is clearly located at the surface.



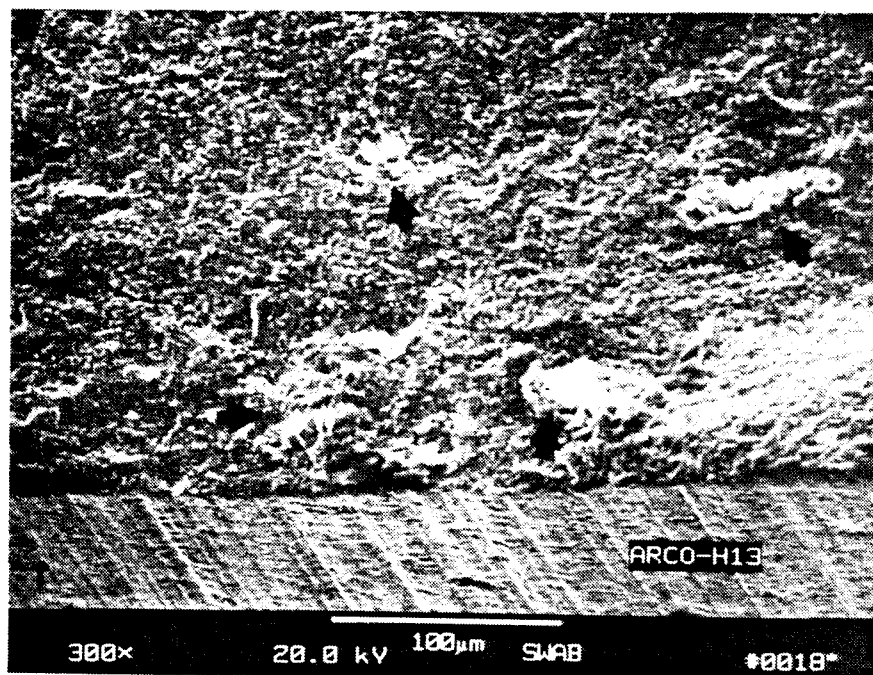


Figure 2.1.6. Organizers' SEM photograph showing several clusters of large alumina grains in specimen 1. "T" denotes the tensile surface.

between the origin and the bulk. Fracture mechanics may have been helpful in determining the size of these origins.

## **Specimen 2: Handling Damage In Alumina**

**MATERIAL INFORMATION:** These specimens were a high purity (99.9%), sintered alumina ( $\text{Al}_2\text{O}_3$ ) with a fracture toughness of  $\approx 4 \text{ MPa}\cdot\sqrt{\text{m}}$ <sup>18</sup>. The room temperature four-point flexure strength of these eighteen specimens, in air, was between 173 and 466 MPa.

**ORGANIZERS' CHARACTERIZATION:** The selected specimens are known to have failed due to handling damage (HDS) because the organizers *intentionally scratched* one of the 4 mm x 50 mm faces. This simulates gross damage due to misuse of the specimen. The scratch was imparted on to the surface with a diamond indenter using only finger pressure. Upon subsequent flexure testing, all specimens fractured from surface or subsurface cracks associated with the scratch. As a result, all of the fracture origins are located at the surface. The size of the subsurface crack was difficult to determine but the width of the scratch was between 10 and 30  $\mu\text{m}$ . The distinction between this fracture origin and machining damage is that the scratch is a gross aberrant feature that can easily be seen on the tensile surface of each specimen with the naked eye as well as the optical microscope or SEM. Figure 2.2.1 is an example of scratch and subsurface cracks as it appears in one of these alumina specimens.

**PARTICIPANTS' RESULTS:** Table 2.2 summarizes the participants' results for specimen 2. Five participants (4, 5, 11, 13 and 15) correctly identified the fracture origin as handling damage (HDS), and one (7) identified it as surface damage. Three others (6, 8 and 9) labeled it as machining damage (MDS), one (3) as a crack (CKV) while the remainder felt the origins were porosity related. All but three participants (3, 12 and 18) characterized the origin at the surface. As with specimen 1 the size values varied greatly as did the method of reporting this size. None of the participants were in complete agreement (Identity, Location and Size) with the organizers, but the same five that properly labeled the origin as handling damage (HDS), also agreed with the organizers' location.

**DISCUSSION - Identity** - The origin in these alumina specimens was handling damage. Although Table 2.2 indicates that only five participants correctly labeled this origin, several others had identities that were similar. Participant 3 identified it as a "preexisting crack" and could see a large longitudinal crack (23 mm long) leading to the fracture origin. Closer examination of the tensile surface would have revealed that this was a gouge and not a crack. Participant 7 noted the presence of "surface damage" which is essentially the same as handling damage, but this participant chose to focus on an area of porosity. Three others (6, 8 and 9) interpreted it as machining damage but the severity of the gouge and its wavy path along the tensile surface is more indicative of

handling damage. The remaining participants incorrectly labeled the origin as something else probably because they did not examine the tensile surface. In one of the photographs provided by participant 16, Figure 2.2.2, the handling damage can be seen on the tensile surface but this is ignored during the characterization.

Table 2.2  
**PARTICIPANTS' RESULTS FOR SPECIMEN 2:  
HANDLING DAMAGE IN ALUMINA**

<u>No.</u>	<u>Identity*</u>	<u>Location**</u>	<u>Size (<math>\mu\text{m}</math>)***</u>	<u>Comments</u>
1	PS	S $\checkmark$	11	Did not look at tensile surface
2	?	NS	?	Did not look at tensile surface
3	CK	S $\checkmark$	180	Called HD a crack
4	HD $\checkmark$	S $\checkmark$	c = 63	
5	HD $\checkmark$	S $\checkmark$	20 - 100	Estimated origin size
6	MD	S $\checkmark$	20 x 800	Interpreted as MD instead of HD
7	SD/PR	S $\checkmark$	120	Saw HD but focused on PR
8	MD	S $\checkmark$	?	Interpreted as MD instead of HD
9	MD	S $\checkmark$	73 x 217	Interpreted as MD instead of HD; $K_{Ic}$ estimate agrees w/size
10	PS	S $\checkmark$	75 - 80	Did not look at tensile surface
11	HD $\checkmark$	S $\checkmark$	?	Optical analysis revealed more details than SEM
12	PR	NS	60 x 40	Did not look at tensile surface
13	HD $\checkmark$	S $\checkmark$	?	
15	HD $\checkmark$	S $\checkmark$	100 x 190	Photos do not show HD but it is noted
16	LG	S $\checkmark$	50 - 70	Did not look at tensile surface; HD obvious in photos
17	A	S $\checkmark$	No value	Did not look at tensile surface; reported mirror size
18	PR/MD(?)	NS/V	65 (29)	Did not look at tensile surface; MD <u>can not</u> be NS or V

$\checkmark$  - agreement with the organizers' characterization. ? could not be determined. \* PR - Porous Region; LG - Large Grain; MD - Machining Damage; PS - Porous Seam; A - Agglomerate; CK - Crack; SD - Surface Damage; HD - Handling Damage. \*\* NS - Near Surface; V - Volume; S - Surface. \*\*\* Single values indicate origin diameter (2c) unless noted. 2-dimensional values are depth x width unless noted.

**Location** - Since handling damage is an inherently surface-distributed fracture origin, like machining damage, it can only be located at the surface or edge of a specimen or component. The three participants which reported an incorrect location also incorrectly identified the origin. Participant 18 felt the origin could be a combination of porosity (PR<sup>V</sup>) and machining damage but provided a location of near surface or volume. Machining damage can not be located in either of these places however, a PR<sup>V</sup> can be surface-located.

**Size** - Based on the given material properties and  $Y = 1.4$ , assuming a semicircular surface crack, the origin size should range from 38  $\mu\text{m}$  ( $\sigma = 466$  MPa) to 273  $\mu\text{m}$  ( $\sigma = 173$  MPa). It should be noted that the width of the gouge was approximately 10-30  $\mu\text{m}$ . The gouge itself is too small to be the origin. Therefore, there must be subsurface cracks, similar to machining damage, associated with the gouge. Over half of the participants reported a value within the origin size range while several others were close to this range and four did

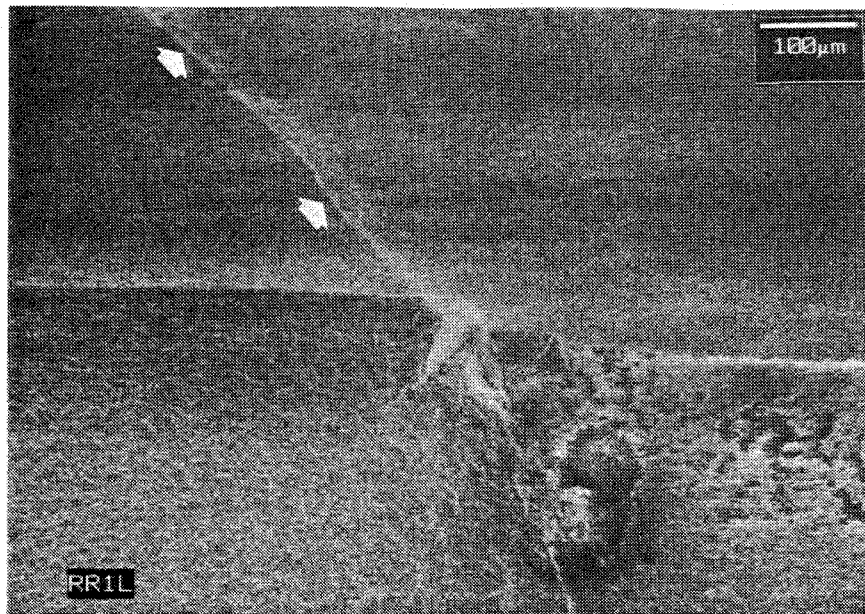


**Figure 2.2.1.** Example of Handling Damage in Specimen 2: Alumina. "T" denotes the tensile surface.

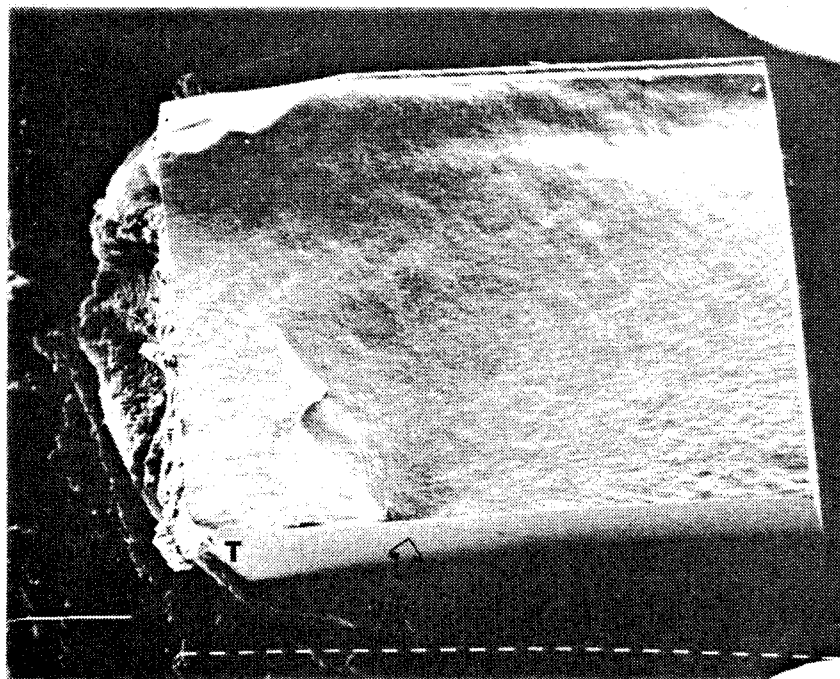


**Figure 2.2.2.** Participant 16's photograph of one of the mating halves of the primary fracture surface in specimen 2. The arrow was added by the organizers and points out the scratch (HD<sup>S</sup>) on the tensile surface (T).

not report a value. The variation in the size values is expected, not only because there were different specimens involved, but because of the low failure stresses. As a result, the markings on the fracture surface are very difficult to discern if they can be seen at all. This makes a size determination extremely difficult.

**SUMMARY:** As with specimen 1 there was excellent agreement on the location of the origin in these specimens. The main problem with characterizing the origin identity was that the tensile surface was not examined by most of the participants. There was no correlation between fractographic experience and proper characterization of the fracture origin, even though a majority of the participants had a lot of experience with alumina. Determining the fracture origin size was also a problem for all participants, the organizers included. This appears to be due to the low fracture stresses of the ceramic.

### **Specimen 3: Pores In Zirconia**

**MATERIAL INFORMATION:** The specimens were a sintered tetragonal zirconia polycrystal ceramic ( $\text{ZrO}_2$ ) containing 3.0 mole % yttria. Fracture toughness, as determined by the indentation-strength technique, was  $\approx 5.5 \text{ MPa}\cdot\sqrt{\text{m}}^{40}$ . The room temperature four-point flexure strength of these eighteen specimens, in air, was 474 to 721  $\text{MPa}^{40}$ .

**ORGANIZERS' CHARACTERIZATION:** The dominant fracture origin in this zirconia is a volume-distributed pore ( $\text{PV}$ )<sup>40</sup>. The characterization should be Pore, which is volume-distributed. Circular or elliptical cracks can be used to model the origin. Circular origins had a radius of 25 - 50  $\mu\text{m}$  and elliptical origins had a minor axis of 10 - 65  $\mu\text{m}$  and a major axis of 40 - 100  $\mu\text{m}$ . An example is given in Figure 2.3.1.

**PARTICIPANTS' RESULTS:** Fourteen of the seventeen participants agreed with the identity of this fracture origin type. Six of these participants (1, 4, 9, 12, 13 and 16) were in complete agreement (Identity, Location and Size) with the organizers' characterization. All but three participants agreed with the origin location. Eleven agreed with the origin size that the organizers determined. One participant did not report a size value. These results are shown in Table 2.3.

**DISCUSSION - Identity** - This was the only specimen in Topic #2 that a consensus was reached on the identity of the origin. Since pores are common features in ceramic materials this may account for the consensus. The possibilities why four participants (3, 5, 11 and 18) did not agree with the majority will be discussed.

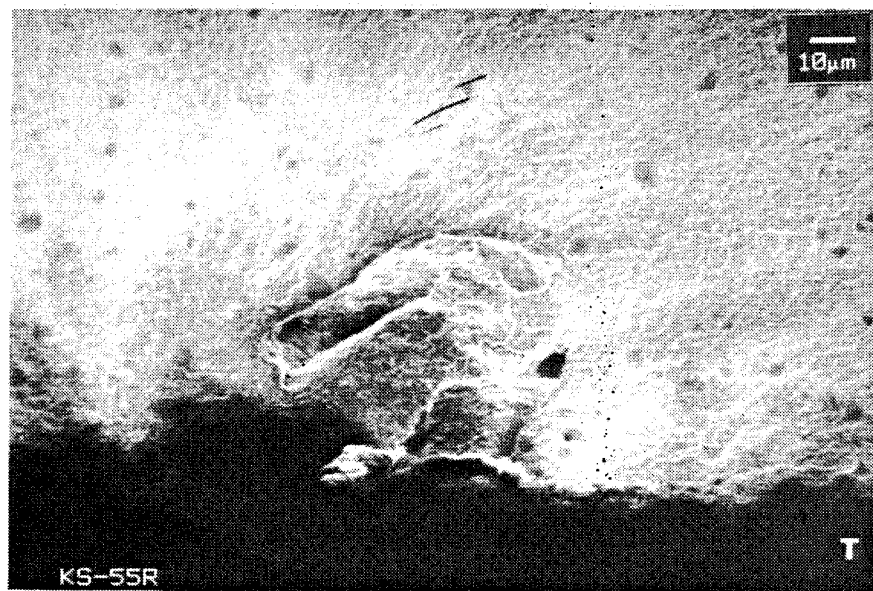


**Figure 2.3.1. Example of a Pore in Specimen 3: Zirconia. "T" denotes the tensile surface.**

Participant 3 was misled by the possible contamination of the specimen. Figure 2.3.2 shows the organizers' initial photograph and participants' photograph of the origin. They are identical except for the globule of material (labeled by +) in the participants' photograph, Figure 2.3.2B. It appears that the globule is a contaminant. EDS by the participant indicates that the globule contains Si, Cl, Na, K, Al and S, thus the inclusion label. The specimen was cleaned only with compressed air prior to examination. Cleaning with compressed air will only remove lightly clinging contaminants such as lint. Removal of this globule would appear to require a stronger cleaning.

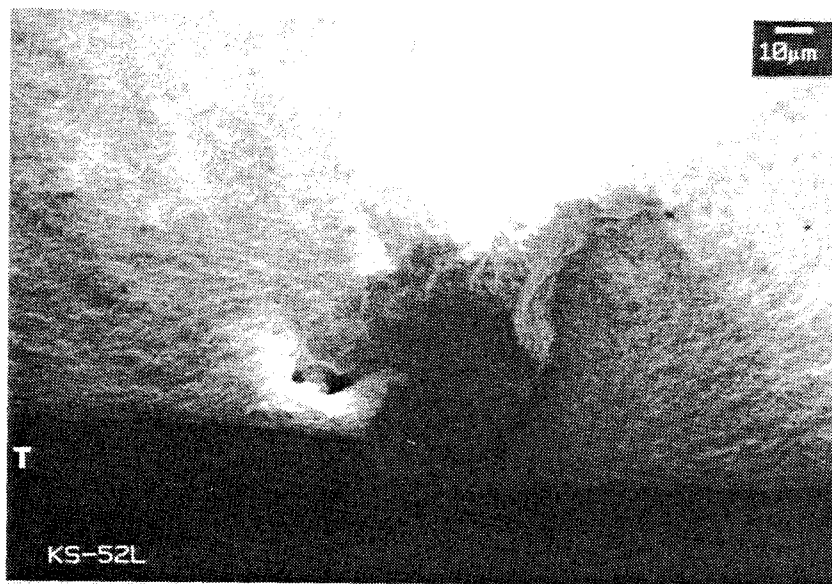
The porous area (PA) identity reported by participant 5 may be appropriate for the particular specimen that participant received. Figure 2.3.3 shows this origin. It has several macroscopic pores close together thus a label of porous region (PR<sup>V</sup>) may be appropriate. (It is believed that PA is equivalent to PR.)

Table 2.3  
**PARTICIPANTS' RESULTS FOR SPECIMEN 3:  
A PORE IN ZIRCONIA**

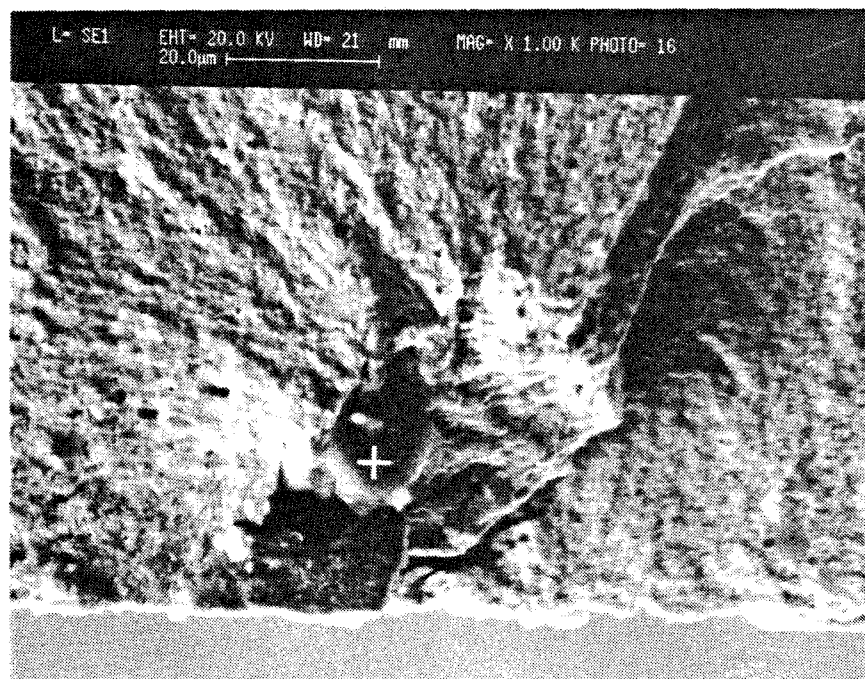
No.	Identity*	Location**	Size (μm)***	Comments
1	P ✓	S ✓	56 x 68 ✓	
2	P ✓	V/NS ✓	90	Origin may be connected to tensile surface
3	I	S ✓	45	Used EDS to identify origin
4	P ✓	S ✓	100 ✓	Origin could be located at S or E
5	PA	S ✓	c = 25 - 30 ✓	Estimated size in agreement with measured size
6	P ✓	V	40 x 125 ✓	Examination of mating half may have changed location
7	P ✓	E	42 x 100 ✓	Location ?
8	P ✓	NS	20 x 80 ✓	Examination of mating half may have changed location
9	P ✓	NS ✓	35 x 80 ✓	Origin may be connected to tensile surface
10	P ✓	NS ✓	60 - 70	
11	P/CK ✓	S ✓	≈ 200	Examined only 1/2 of surface; Size estimated to be ≈ 90 μm
12	P ✓	NS ✓	30 x 80 ✓	
13	P ✓	S ✓	10 - 65 ✓	
15	P ✓	NS ✓	46 x 170	Poor quality of photograph
16	P ✓	S ✓	Depth = 38 ✓	
17	P ✓	S ✓	No value	Reported mirror size
18	MD	E ✓	60	Crack is not present in organizers' photographs

✓ - agreement with the organizers' characterization. ? could not be determined. \* P - Pore; PA - Porous Area; MD - Machining Damage; I - Inclusion; CK - Crack. \*\* NS -Near Surface; V - Volume; S - Surface; E - Edge. \*\*\* Single values indicate origin diameter (2c) unless noted. 2-dimensional values are minor axis x major axis unless noted.

Participant 11 noted the presence of a crack associated with the pore thus the combined label (P/CK), but only one of the primary fracture surfaces was examined with the SEM. Participant 18 also saw a crack in the area of the origin, Figure 2.3.4A, giving rise to the machining damage label, but this crack cannot be seen in any of the organizers' photographs, Figure 2.3.4B, taken prior to the participants' characterization. The organizers reexamined this specimen



**A**



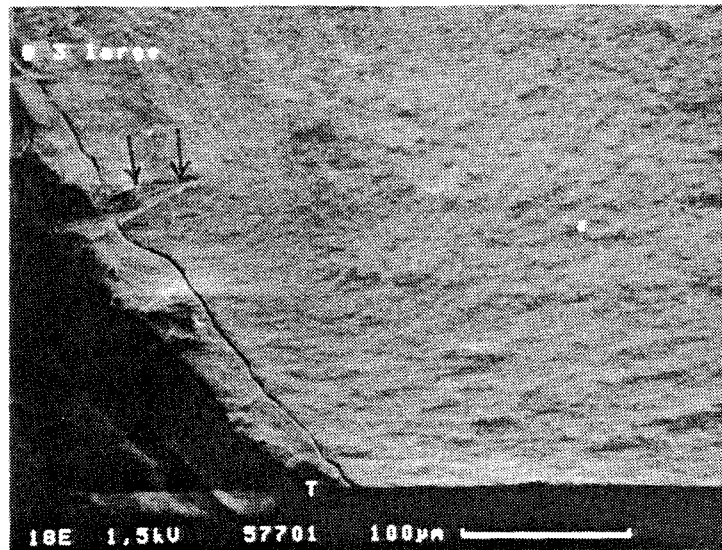
**B**

Figure 2.3.2. SEM photographs of the pore in specimen 3 from the set sent to participant 3. A) Organizers' photograph. "T" denotes the tensile surface. B) Participant 3's photograph. "+" indicates the "globule" where EDS was done.

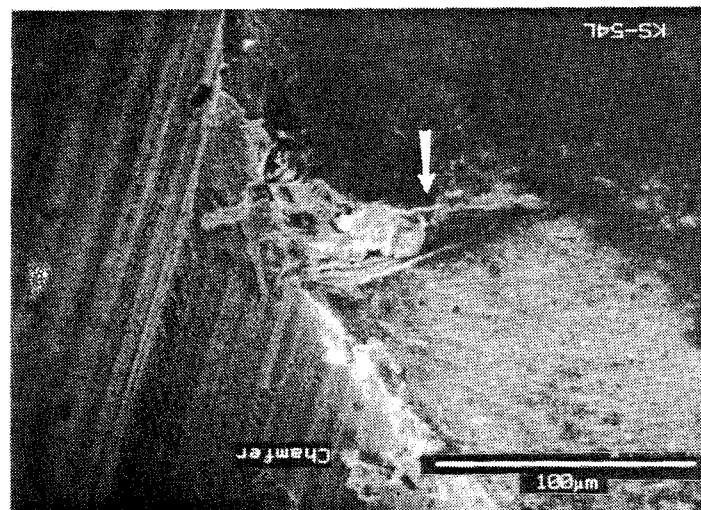




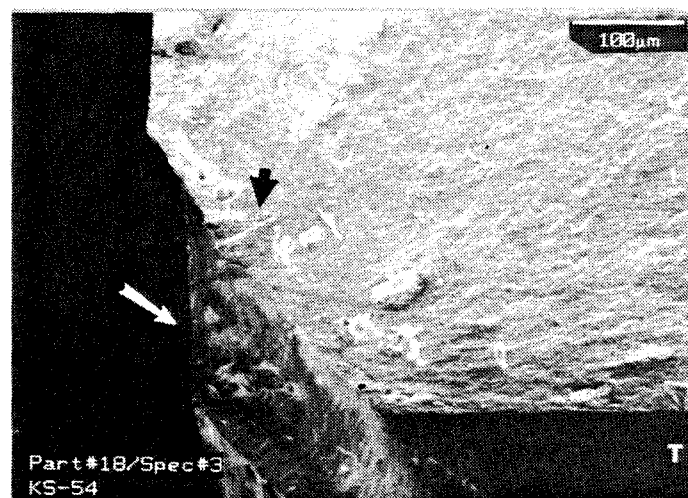
Figure 2.3.3. Participant 5's SEM photograph of the origin in specimen 3. Is this a pore or porous region?



A



B



C

Figure 2.3.4. SEM photographs of specimen 3 from the set sent to participant 18. A) Participant 18's photograph. The participant used hand drawn arrows to show the pore. B) SEM photograph taken by the organizers' prior to sending the specimen to the participant. C) Organizers' SEM photograph of the fracture origin after it was characterized by the participant and returned to the organizers. Black arrow indicates the pore and white arrow shows where the piece was removed. "T" denotes the tensile surface.

and did not find the crack as seen in Figure 2.3.4A, but saw that a piece of the specimen was missing, Figure 2.3.4C. The crack may be an artifact of the testing and/or handling of the specimen. The crack is not seen on the mating half of the primary fracture surface but the pore can clearly be seen. In each case had the participant examined the mating half of their specimen it may have become clear that the pore was the primary origin.

**Location** - Two (6 and 8) of the three participants that did not agree with the location of the origin examined only one of the primary fracture surfaces. Had they examined the mating half the location they reported may have agreed with the organizers. The specimen which participant 7 examined was an unusual case where the origin is located at the side of the specimen above the chamfer, Figure 2.3.5.

**Size** - Unlike the first two specimens in this topic there are many participants who agreed with origin size determined by the organizers even though some of the origins had unusual shapes. The boundary between the pore and the matrix is quite distinct in most instances making a size determination much easier. Those which did not agree with organizers' size tended to have an origin with a very complex shape or that contained a number of macroscopic pores, as seen in Figure 2.3.3.

The mechanical property data and  $Y = 1.4$  (assuming a semicircular crack at the surface) were inserted in to Equation 1b to estimate the size of the origins in these eighteen specimens. The radius of the origins ranged from 30 to 69  $\mu$  m. All but participant 11 reported a size value within or very near this range. The size reported by this participant was much larger than the upper end of the estimated range. This value was a combination of the pore and the crack the participant saw in the specimen.

**SUMMARY:** A general consensus was reached on the characterization of this origin, irrespective of one's experience level. Pores are common anomalies in most ceramics thus it may be safe to assume that most of the participants had seen pores before. Also the pore was quite obvious in most specimens making identification and size determination much easier. The characterization of the origin location was not a problem.

#### **Specimen 4: Pits In Silicon Carbide**

**MATERIAL INFORMATION:** Specimens were a reaction-bonded polycrystalline silicon carbide (SiC). Fracture toughness was unknown but was estimated to be  $\approx 3 \text{ MPa}\cdot\sqrt{\text{m}}$ . Room temperature flexure strength was obtained from four-point flexure testing in air. Prior to strength testing the specimens were thermally shocked between 1,000 and 10,000 times from  $\approx 1350^\circ\text{C}$  to room temperature.

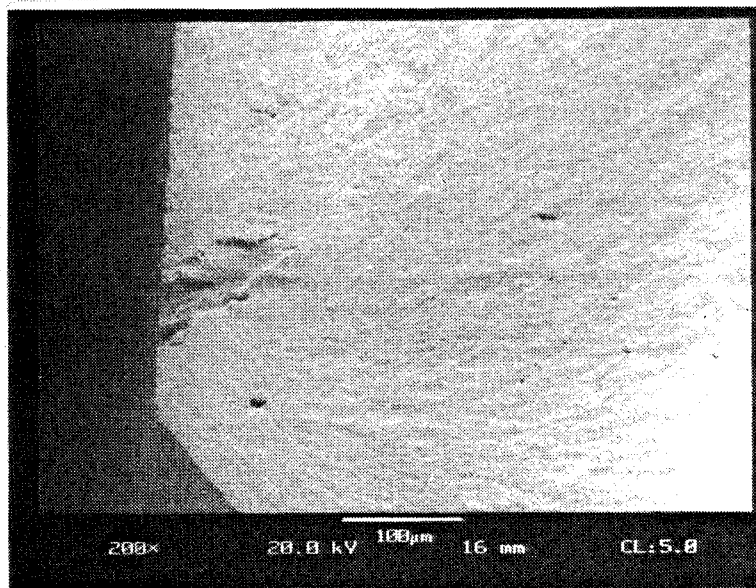


Figure 2.3.5. SEM photograph, from participant 7, of a pore located at the side of the flexure specimen. Appropriate location: Volume (V)\*. \* located at the side of the specimen approximately 175  $\mu\text{m}$  beneath the tensile surface.

Quenching was done during each cycle with a jet of compressed air and took  $\approx$  15 seconds. The strength of these specimens was between 213 and 361 MPa.

**ORGANIZERS' CHARACTERIZATION:** These specimens were subjected to repeated thermal shocks as discussed in References 41 and 42. The external surfaces of each specimen were degraded during this exposure. Fractographic analysis after room temperature flexure testing indicated that the strength was limited by pits (PT<sup>s</sup>) which were created during the exposure. All of these pits are located at the surface and are best represented by an semiellipse with a depth between 10 and 100  $\mu$ m and a width between 25 and 275  $\mu$ m. The pits are obvious on the specimen surfaces as seen in Figure 2.4.1.

**PARTICIPANTS' RESULTS:** Only five participants (6, 7, 9, 15 and 18) agreed with the organizers that this origin type was a pit (PT<sup>s</sup>). Many other identities were given. There was general agreement on the location characterization. Only three participants reported an origin location different from the organizers. The size of the origin varied as did the technique of reporting this size. Participants 2, 10, 11 and 12 were in agreement with the size value of the organizers. None of the participants were in complete agreement (Identity, Location and Size) with the organizers. Table 2.4 summarizes the participants' results for this specimen.

Table 2.4  
**PARTICIPANTS' RESULTS FOR SPECIMEN 4:  
A PIT IN SILICON CARBIDE**

No.	Identity*	Location**	Size ( $\mu$ m)***	Comments
1	P	S $\checkmark$	12 x 45	Did not take thermal history into account
2	SV	S $\checkmark$	125 $\checkmark$	Did not take thermal history into account
3	MD	E $\checkmark$	20 ?	Did not take thermal history into account
4	I(?)	S $\checkmark$	115	
5	CHIP	E $\checkmark$	c = 30 - 35	Did not take thermal history into account
6	PT $\checkmark$	S $\checkmark$	40 x 300+	
7	PT $\checkmark$	S $\checkmark$	128	
8	I	S $\checkmark$	60 x 70	Did not take thermal history into account
9	PT $\checkmark$	S $\checkmark$	57 x 170	
10	MD	S $\checkmark$	90 $\checkmark$	Did not take thermal history into account
11	P/MD	S $\checkmark$	Depth = 68 $\checkmark$	Mentioned thermal history but did not tie together w/origin
12	?	E	50 x 25 $\checkmark$	Inexperience shows; confused meaning of S and E location
13	SV	S $\checkmark$	15	Did not take thermal history into account
15	PT $\checkmark$	S $\checkmark$	34 x 113	
16	?	?	?	
17	P	S $\checkmark$	46 x 251	Did not take thermal history into account
18	PT $\checkmark$	S $\checkmark$	50	

$\checkmark$  - agreement with the organizers' characterization. ? could not be determined. \* P - Pore; PT - Pit; MD - Machining Damage; I - Inclusion; SV - Surface Void. \*\* S - Surface; E - Edge. \*\*\* Single values indicate origin diameter (2c) unless noted. 2-dimensional values are depth x width unless noted.

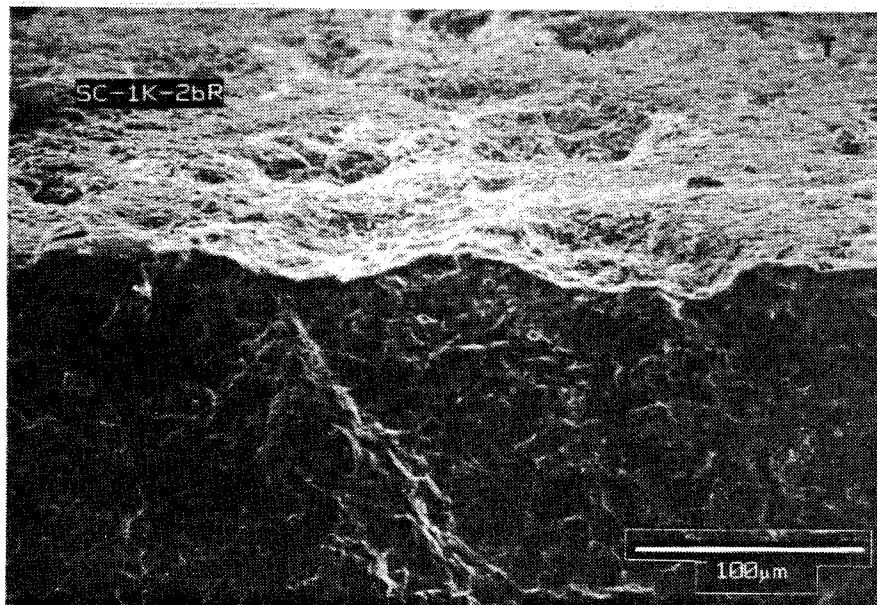
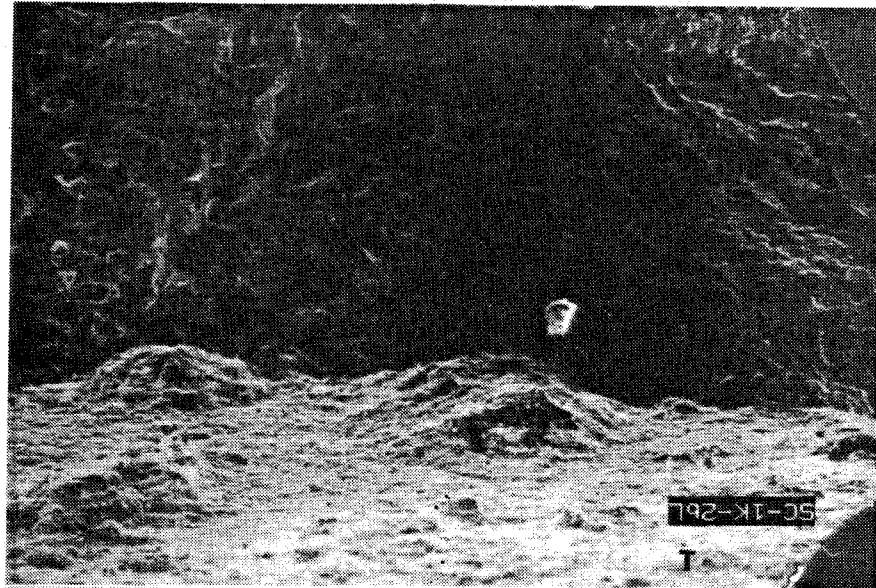


Figure 2.4.1. Example of Pits in Specimen 4: Silicon Carbide. Mating halves of the primary fracture surface are shown. "T" denotes the tensile surface.

**DISCUSSION - Identity** - Eight of the twelve participants who labeled the origin as something other than a pit (PT<sup>s</sup>) did not take the thermal history of the specimen into account. For example, participants 2 and 13 identified the origin as a surface void (SV<sup>s</sup>). These pits appear similar to the examples of surface voids given in MIL HDBK-790, (see Figure 2.4.2), but surface voids are only present on the surface of specimens which are tested in an as-processed state (i.e., no machining of the bar). The bars used for specimen 4 were all machined from a large billet therefore surface voids can not be the origin type.

Participant 4 was uncertain of the inclusion identity that they reported. Although the thermal history was taken into account during characterization, EDS indicated the presence of Si and O at the deepest portion of the pit. The participant believed that the growth of the oxide inclusion initiated fracture at the tip of the cavity. Participant 11 mentioned that the thermal history may have had an effect on the origin but did not tie this together in the characterization. Participants 12 and 16 did not identify the fracture origin.

**Location** - A pit can only be located at the surface or edge of the specimen/component because it is an inherently-surface distributed fracture origin. With the exception of participant 16 every other participant located the origin at the surface or the edge. Participant 12 examined the incorrect area and also confused the meaning of surface and edge.

**Size** - A size range of 35  $\mu\text{m}$  ( $\sigma = 361 \text{ MPa}$ ) to 101  $\mu\text{m}$  ( $\sigma = 213 \text{ MPa}$ ) was obtained from Equation 1b. Since these origins were located at the surface and tended to be semicircular or semielliptical in shape a Y of 1.4 was used in the calculation. As with machining damage the depth of the pit is the critical size measurement. Nine participants reported single values. Four (5, 10, 11 and 18) were within the calculated range while participants 3 and 13 were below and participants 2, 4, and 7 were above this range. Of the seven participants who provided 2-dimensional values six reported a depth value within the size range.

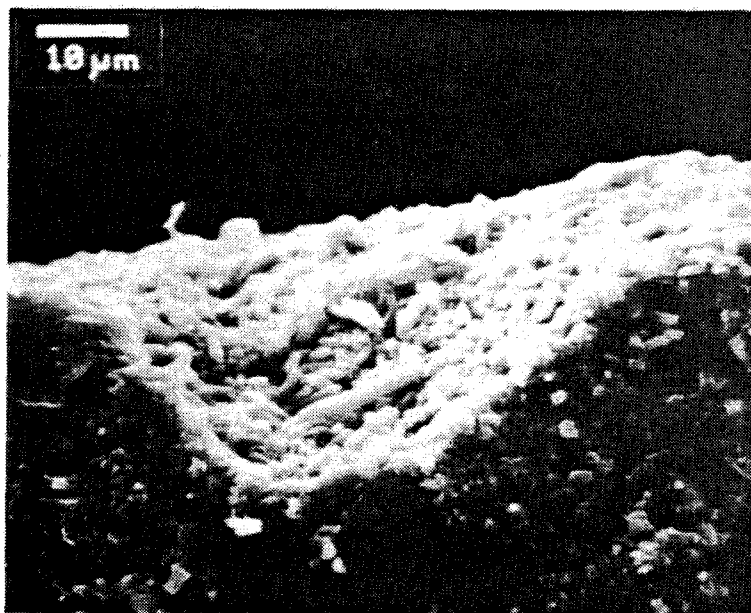
**SUMMARY:** Many participants overlooked or ignored a valuable piece of information: the thermal history of the specimen. Some also did not understand how pits are formed. There was no problem in determining the location of the origin, but size characterization was a problem. There was no correlation between experience and the proper characterization of this origin type.

### **Specimen 5: Machining Damage In Silicon Nitride**

**MATERIAL INFORMATION:** The ceramic specimens were an injection-molded then hot-isostatically pressed silicon nitride ( $\text{Si}_3\text{N}_4$ ) containing 6 w/o yttria. Material fracture toughness was estimated to be between 4.5 - 5.5  $\text{MPa}\cdot\sqrt{\text{m}}$ . The room temperature four-point flexure strength of these specimens, in air, was between 527 and 837  $\text{MPa}$ <sup>43</sup>.



**A**



**B**

Figure 2.4.2. A) Participant 2's SEM photograph of the pit in specimen 4. Arrows added by the organizers. B) SEM photograph of a surface void from Military Handbook 790, Figure 33, page 40. Note the similarity.



**ORGANIZERS' CHARACTERIZATION:** The specimens failed due to gross machining damage (MDS). This damage was typically at the chamfer where it was so severe that sections of the chamfer spalled off prior to or during strength testing. The size of the origin was difficult to characterize but the few that could be determined had depths between 20 and 60  $\mu\text{m}$ . Figure 2.5.1 provides an example of the typical machining damage seen in these specimens.

**PARTICIPANTS' RESULTS:** Eleven participants (1, 2, 3, 5, 6, 7, 8, 9, 12, 15 and 17) were clearly able to identify this as machining damage while three others were very close to this label. Two participants (13 and 16) could not identify the origin and a third (11) believed the origin was related to a microstructural irregularity. In regards to the origin location, eleven participants agreed with the organizers. The participants had difficulty determining the size of the origin with over a third of them not reporting any value. Two participants (3 and 6) were in complete agreement (Identity, Location and Size) with the organizers and seven others (1, 2, 5, 8, 9, 15, and 17) agreed with the identity and location but not the size. These results are generalized in Table 2.5.

**DISCUSSION - Identity** - Unlike the specimens used in Topic #1 of this exercise these specimens exhibited a form of gross machining damage. The cracking due to grinding was so severe that sections of the chamfers spalled off. The organizers had a distinct advantage over the participants because they were able to examine the entire specimen set.

Five of the participants identified the origin as something akin to machining damage. Participant 4 provided a photograph, Figure 2.5.2, which showed the chipping along the chamfer but the origin was labeled as handling damage (HDS). Although handling damage can be in the form of chips the nature of the chips along the chamfer indicates that this is related to machining. The origin was identified as a "chip" by participant 5. This could be interpreted as machining damage. Participant 10 and 12 believed that the fracture origin was a crack (CKV). The photographs provided by participant 10 do not indicate that the external surfaces had been examined, Figure 2.5.3A. Examination of these surfaces would have revealed the extent of machining damage see Figure 2.5.3B. Again this may be a case where examination of only one specimen was inadequate for proper and complete characterization of the origin. Participant 12 while close to the identity of the origin examined the incorrect area.

Participants 11 and 18 examined only one of the primary fracture surfaces. An examination of the mating half may have lead to a different identity since in both cases the mating half showed the machining damage more clearly. Participant 13 did not characterize the fracture origin because "no fracture origin could be identified."

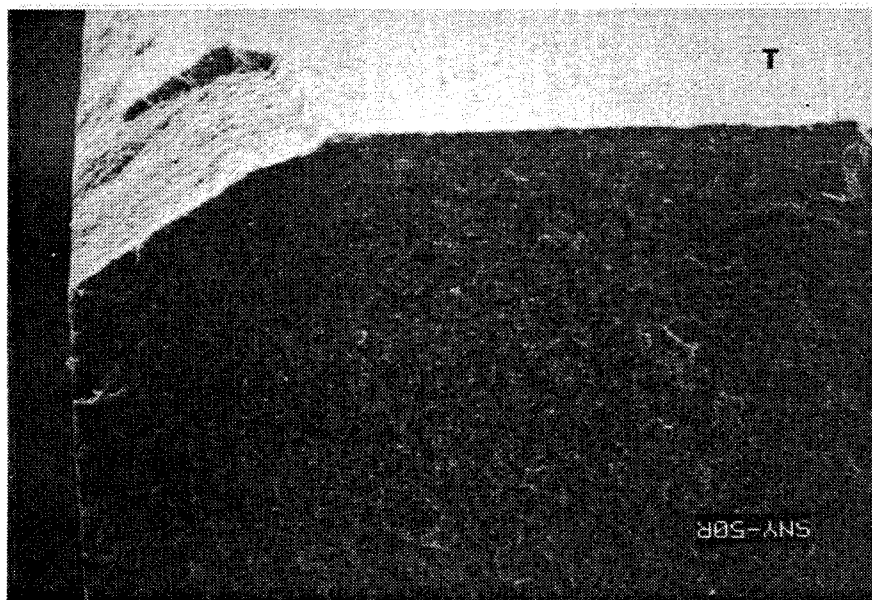
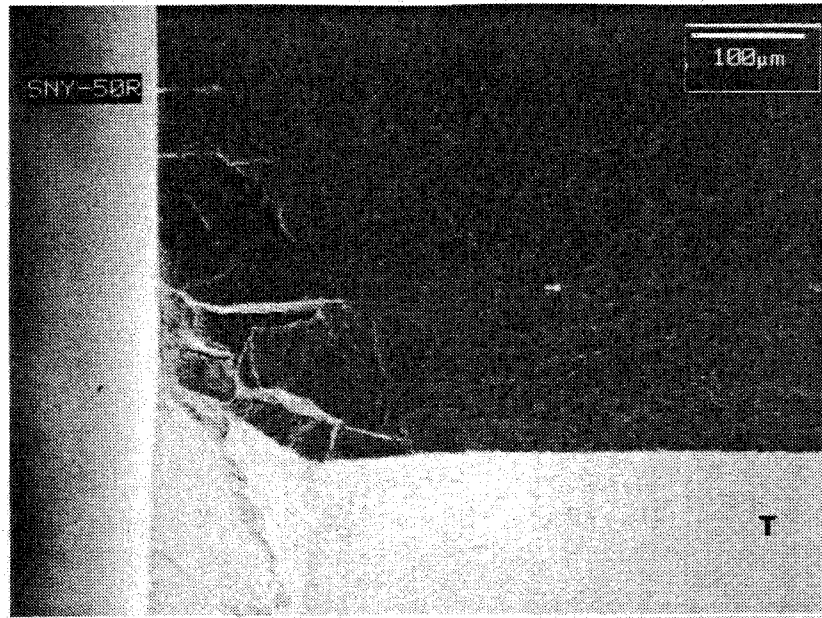


Figure 2.5.1. Example of Machining Damage in Specimen 5: Silicon Nitride. Mating halves of the primary fracture surface are shown. "T" denotes the tensile surface.

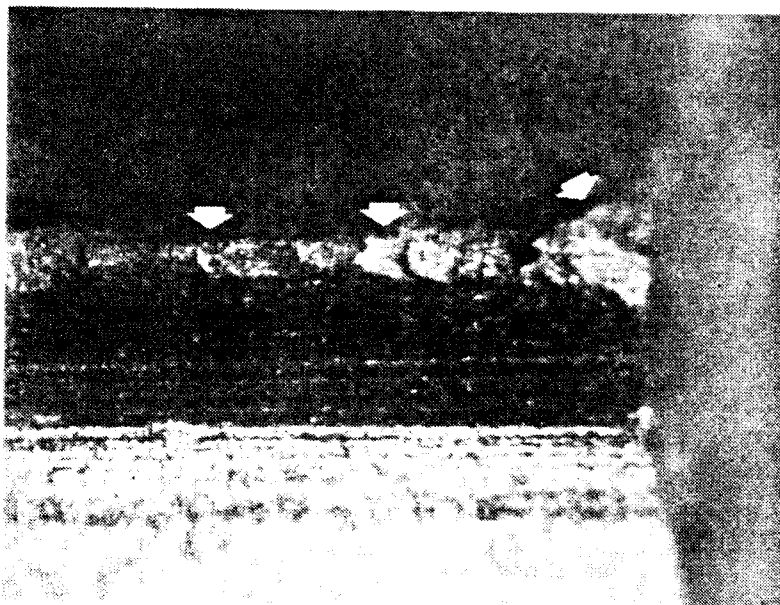


Figure 2.5.2. Optical photograph from participant 4, of machining related chipping on the chamfer of specimen 5. Arrows were added by the organizers.

Table 2.5  
**PARTICIPANTS' RESULTS FOR SPECIMEN 5:  
MACHINING DAMAGE IN SILICON NITRIDE**

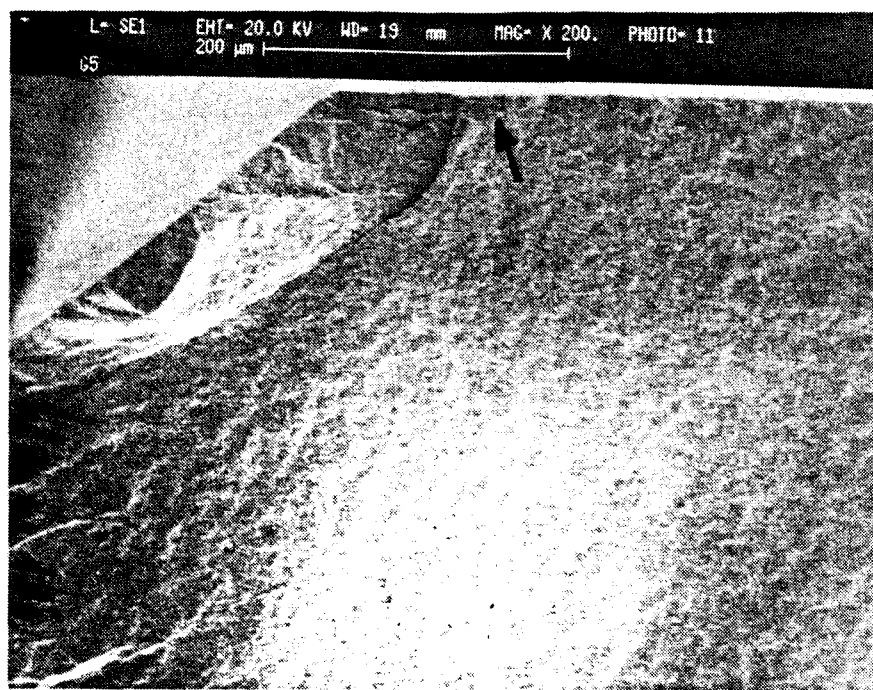
<u>No.</u>	<u>Identity*</u>	<u>Location**</u>	<u>Size (μm)***</u>	<u>Comments</u>
1	MD ✓	E ✓	530	
2	MD ✓	S/E ✓	?	
3	MD ✓	S ✓	50 - 75 ✓	
4	HD	S ✓	c = 91	Noted chipping on chamfer but did not equate to machining
5	CHIP ✓	E ✓	c = 20 ✓	Noted irregularity on chamfer but photos do not show this
6	MD ✓	E ✓	20 x 65 ✓	
7	MD ✓	S	30 x 190 ✓	Markings on photos indicate E location
8	MD ✓	E ✓	?	
9	MD ✓	E ✓	25 x 65	
10	CK	NS	5 - 10	Did not examine mating half of chamfer in detail
11	M	V?	?	M denotes microstructural irregularity
12	CK/MD ✓	E	10 x 50	Confused E and S
13	?	?	?	
15	MD ✓	E ✓	?	
16	?	?	?	No origin detected
17	MD ✓	E ✓	No value	Mirror size reported
18	PR/MD	NS/E	15	

✓ - agreement with the organizers' characterization. ? could not be determined. \* MD - Machining Damage; PR - Porous Region; HD - Handling Damage; CK - Crack. \*\* NS - Near Surface; V - Volume; S - Surface; E - Edge; NE - Near Edge. \*\*\* Single values indicate origin diameter unless noted. 2-dimensional values are depth x width unless noted.

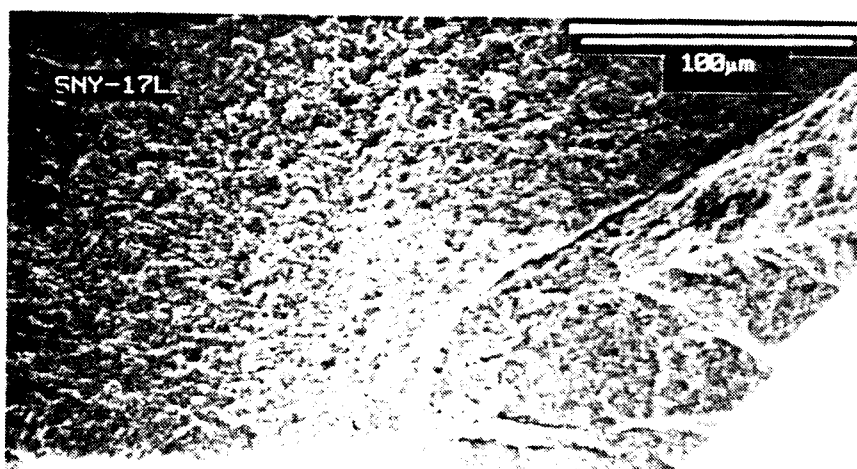
**Location** - Due to its inherent nature machining damage can only be found at the surface or edge of a ceramic piece. Participants 10, 11 and 18 reported other locations. Participant 10 located it near-to-the-surface but it is clearly located at the surface, Figure 2.5.3. The volume location reported by participant 11 is possible for a "microstructural irregularity", as the origin was labeled. Participant 18 characterized the origin as a coincidental origin of porosity (PR<sup>V</sup>) and machining damage with a location of near surface or edge. The near surface label appears to be incorrect for this coincidental origin.

**Size** - Since the toughness of this ceramic was estimated to be 4.5 - 5.5 MPa<sup>1/2</sup>/m an origin size range for each toughness was calculated using Equation 1b. (Y = 1.4 assuming a semicircular crack located at the surface.) These two ranges are: 15 to 37 μm for a toughness of 4.5 MPa<sup>1/2</sup>/m and 22 to 56 μm for 5.5 MPa<sup>1/2</sup>/m. Both ranges appear to be quite small considering the severity of the machining damage. The size values listed in Table 2.5 vary significantly and only seven participants reported a value or a dimension within either of these ranges.

**SUMMARY:** At least half of the participants concurred with the organizers' characterization of the identity and location. This was clearly a case where examination of the entire specimen set would have improved the participants' characterization. In some instances, even when entire sections of the chamfer were removed, there was little evidence of machining damage (striations,



**A**



**B**

**T**



Figure 2.5.3. SEM photographs of specimen 5. A) Participant 10's photograph. B) Organizers' photograph. Arrows point out the machining damage on the tensile surface. "T" denotes the tensile surface.

grooves, etc.). The severity and three-dimensionality of the damage also complicated the size measurement.

### **Specimen 6: Porous Seam Or Porous Region In Titanium Diboride**

**MATERIAL INFORMATION:** The specimens were a high-purity, sintered titanium diboride ( $\text{TiB}_2$ ). Material fracture toughness, as determined by the indentation-strength technique, was  $\approx 4.5 \text{ MPa}\sqrt{\text{m}}$ . The room temperature four-point flexure strength of these specimens, in air, was between 234 and 337 MPa.

**ORGANIZERS' CHARACTERIZATION:** The organizers characterized the fracture origins in these  $\text{TiB}_2$  specimens as a porous seam ( $\text{PS}^V$ ) or a porous region ( $\text{PR}^V$ ) which tended to be located at or very near to the tensile surface. The origin size was best represented by an ellipse having a minor axis of 50 - 270  $\mu\text{m}$  and a major axis of 60 - 380  $\mu\text{m}$ . An example of this origin is shown in Figure 2.6.1.

**PARTICIPANTS' RESULTS:** Four participants (3, 6, 9, and 12) were in complete agreement (Identity, Location and Size) with the organizers' characterization, and three others (1, 16 and 18) agreed with the identity and location only. Most of the participants indicated that the origin was porosity related ( $\text{PV}$  or  $\text{PR}^V$ ). Origin location was not a problem but there was a wide array of sizes reported and methods of reporting these values. Table 2.6 summarizes the participants' results.

**DISCUSSION - Identity** - Most participants labeled the origin as porosity related ( $\text{PV}$  or  $\text{PR}^V$ ) but other labels such as agglomerate ( $\text{AV}$ ), inclusion ( $\text{IV}$ ) and surface void ( $\text{SV}^S$ ) were also given. Five participants (4, 7, 10, 15 and 17) gave the origin an agglomerate label. Their photographs show regions of porosity. This does not fit the definition of agglomerate given in MIL HDBK-790 which states that an agglomerate is a "... solid mass.". Additionally, the organizers believe that if participants 15 and 17 had examined the mating half of the primary fracture surface their identity might have been different. Failure to examine the mating halves of the primary fracture surface can lead to an errant identification of the origin. This is especially true for an agglomerate. Many times one half of the fracture surface will have a depression which is matched on the mating half of the surface by a protrusion of the same size. Figure 2.6.2 shows the mating halves of the fracture surface from participant 15's specimen set.

The organizers do not understand why participant 8 labeled the origin as an inclusion ( $\text{IV}$ ). EDS shows only Ti which is not surprising since this is a  $\text{TiB}_2$  material and unless the detection system has a thin window, which allows for the detection of light elements (below Na), B would not be detected. Thus we can not determine why this label was chosen. Participant 13 reported an identity of surface void ( $\text{SV}^S$ ). The origin in the participants' photograph looks similar to

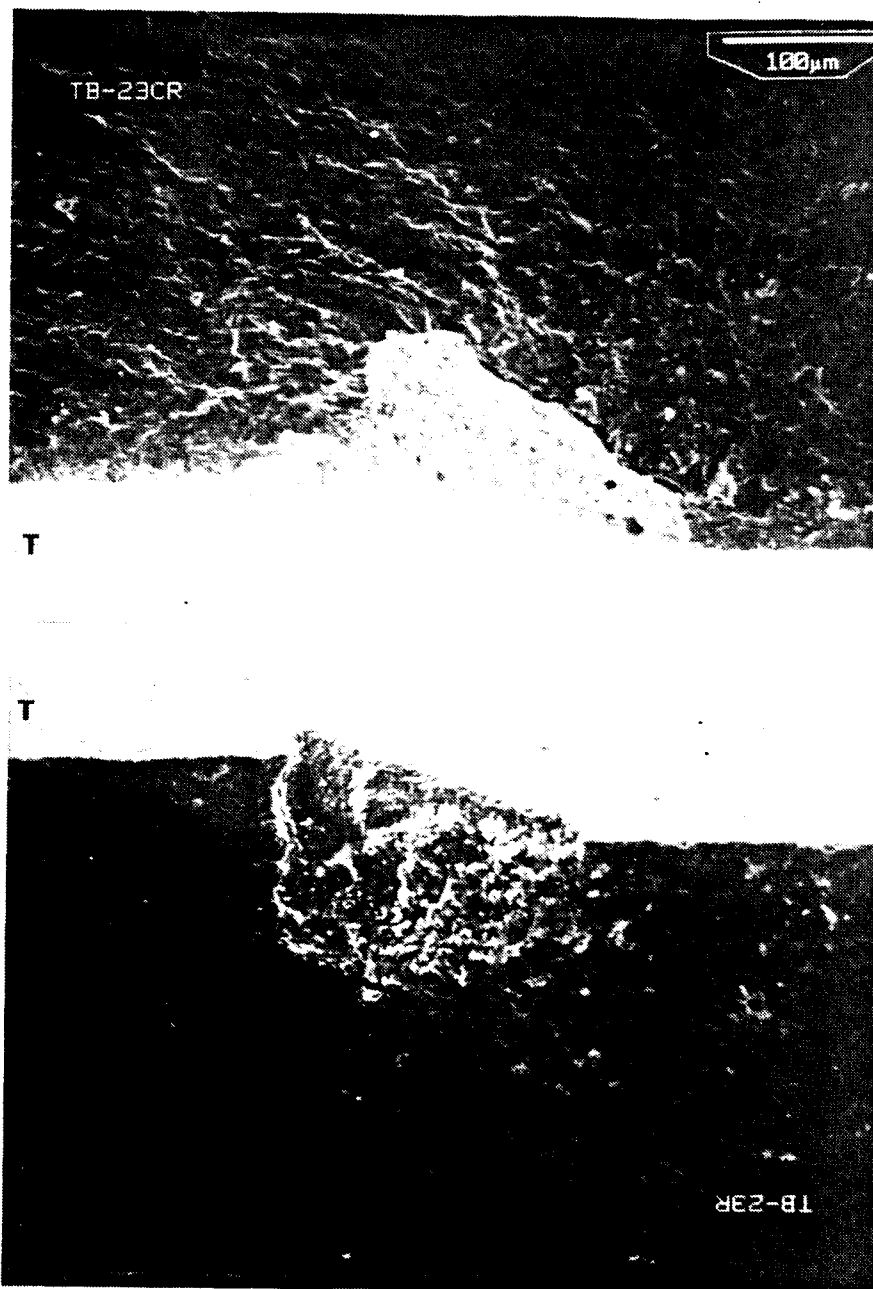
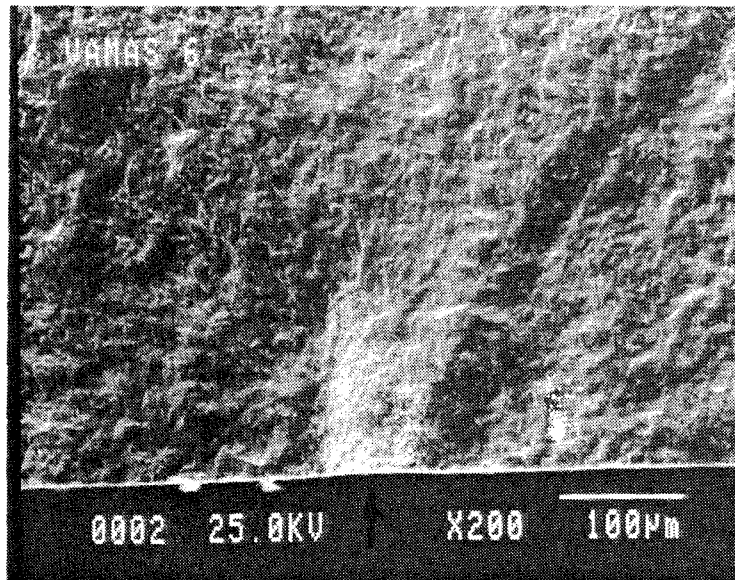
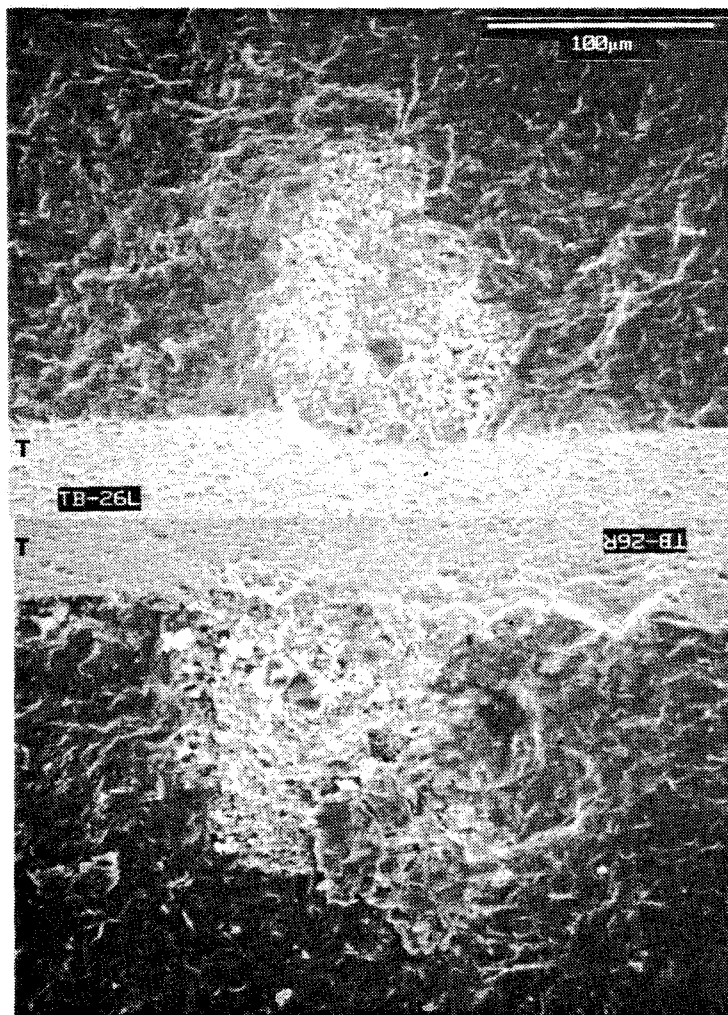


Figure 2.6.1. Example of Porous Seam/Porous Region in Specimen 6: Titanium Diboride. Mating halves of the primary fracture surface are shown. "T" denotes the tensile surface.

Short piece surface



A



B

Figure 2.6.2. SEM photographs of specimen 6. A) Participant 15's photograph. B) Organizers' photographs of the mating halves of the primary fracture surface. The photographs in B) indicate that this origin is a porous region (PR<sup>V</sup>) and not an agglomerate (A<sup>V</sup>). "T" denotes the tensile surface.



the examples of surface void given in MIL HDBK-790, however, this is incorrect because surface voids are located on the surface of the material as a direct consequence of processing. Since this specimen was machined from a large billet, surface voids can not be a type of fracture origin in this instance.

Table 2.6  
**PARTICIPANTS' RESULTS FOR SPECIMEN 6:  
A POROUS SEAM OR POROUS REGION IN TITANIUM DIBORIDE**

No.	Identity*	Location**	Size (μm)***	Comments
1	P/PR ✓	V ✓	230	≈ 211 μm below tensile surface-agreement with organizers'
2	P	V/NS	170 ✓	≈ 20 μm below tensile surface
3	PR ✓	E ✓	230 ✓	
4	A	NS ✓	450	"A" tends to denser
5	PA	V	c = 50	Examined incorrect area
6	PR ✓	S ✓	100 x 145 ✓	
7	PR/A	S ✓	80 x 120 ✓	"A" tends to denser
8	I	S ✓	230 x 400 ✓	EDS shows only Ti thus can not account for I label
9	PR ✓	S ✓	50 x 100 ✓	
10	A	S ✓	≈ 150	"PR from uncrushed A particles"; examined incorrect area
11	PR ✓	NS	150 x 400	≈ 150 μm below tensile surface
12	PR ✓	NS ✓	120 x 160 ✓	
13	SV	S ✓	50 - 250	
15	A	S ✓	160 x 80	Identity might be different if mating half was examined
16	PR ✓	S ✓	Depth = 125	
17	P/A(?)	S ✓	85 x 89 ✓	Identity might be different if mating half was examined
18	PR ✓	S ✓	81	"Easiest material to deal with"

✓ - agreement with the organizers' characterization. ? could not be determined. \* P - Pore; PR - Porous Region; PA - Porous Area; I - Inclusion; A - Agglomerate; SV - Surface Void. \*\* NS -Near Surface; V - Volume; S - Surface; E - Edge. \*\*\* Single values indicate origin diameter (2c) unless noted. 2-dimensional values are minor axis x major axis unless noted.

**Location** - Fourteen of the seventeen participants agreed with the organizer's location of these fracture origins. One of the three who disagreed was participant 5, who identified the wrong feature as the origin. The disagreements with the other two participants were due to the differences in what constitutes volume versus near surface location characterization. Participant 2 labeled the origin as V/NS while the organizers' gave it a NS label. Both agreed that the origin was about 20 μm beneath the tensile surface. In the other instance, participant 11 characterized the origin as near surface even though it was about 150 μm below the tensile surface. The organizers agree with the distance below the surface but because it is a rather large distance, feel that a volume location is more appropriate. A better definition of the near surface location is needed in MIL HDBK-790.

**Size** - There was a range of origin sizes reported as well as a variety of ways to report the size. For the range of fracture stresses in the 18 specimens the fracture origin size for this ceramic is 91 μm ( $\sigma = 337$  MPa) to 189 μm ( $\sigma = 234$  MPa) as determined using Equation 1b and the strength and toughness values

provided. (A shape factor (Y) of 1.4 was used.) Ten participants reported a value within this range and two others were very close. The main problem with accurate measurement of the origin size appears to be the complex geometries which were encountered.

**SUMMARY:** It is important that the mating halves of the primary fracture surface are examined when there is uncertainty in the identify of the fracture origin. Again location of the origin was not a problem but the measurement of the size was complicated by the different geometries that were encountered.

## Topic #2: Summary

The results from this topic of the exercise show that the characterization scheme in Military Handbook 790 contains the necessary attributes for the complete characterization of fracture origins in advanced structural ceramics. The general scheme of identity, location and size worked well, but some clarification and refinements are needed regarding the particulars of each attribute. The exercise also revealed that the guidelines provided can enable an inexperienced fractographer to identify and properly characterize fracture origins.

Table 2.7 lists the ratios of concurrence in interpretation of the participants with the organizers for the six specimens of Topic #2. It is clear that there was mixed success, in some instances there was a good consensus and in other specimens, there was not. One reason for the lack of a consensus appears to be that the participants had only one specimen of each material to analyze while the organizers had eighteen or more specimens available for analysis. Even at that, some participants ignored some of the available information, i.e., the mating half of the primary fracture surface, or the external surfaces of the specimen.

Table 2.7  
CONCURRENCE WITH ORGANIZERS' EVALUATION

<u>Specimen #</u>	<u>Identity</u>	<u>Location</u>	<u>Size</u>
1: LG in Al <sub>2</sub> O <sub>3</sub> /SiC	6/17 = 35%	12/17 = 71%	7/17 = 41%
2: HD in Al <sub>2</sub> O <sub>3</sub>	5/17 = 29%	14/17 = 82%	----
3: P in ZrO <sub>2</sub>	14/17 = 82%	14/17 = 82%	10/17 = 59%
4: PT in SiC	5/17 = 29%	15/17 = 88%	4/17 = 24%
5: MD in Si <sub>3</sub> N <sub>4</sub>	11/17 = 65%	10/17 = 59%	4/17 = 24%
6: PS or PR in TiB <sub>2</sub>	8/17 = 47%	14/17 = 82%	8/17 = 47%
— Size values not determined by organizers.			

In regards to the origin identity, the fractographer must be aware of the material or specimens' past history (processing, exposures, testing conditions,

etc.) and understand how this can affect the type of origin seen on the fracture surface. Several participants mislabeled the pit created due to thermal cycling in specimen 4 as a surface void or a pore. Although these origin types look similar they are different because they were created differently. This is reflected in their respective definitions. Many participants ignored the information about the thermal cycling that these specimens experienced or did not examine the external surfaces. The appropriate identity may have been reported had one or both of these been taken in account.

Location also plays an important role in making the identification characterization. For example, if the origin is clearly located in the volume of the specimen, then all the inherently-surface distributed origin types can be eliminated from consideration. On the other hand if the origin is clearly located at the surface then none of the origin types can be eliminated, but this should be a clue that the tensile surface should be examined, (as typified by the results from specimen 2).

As has been shown by this exercise the determination of the size of a fracture origin is complicated for a variety of reasons. Even so, the use of fracture mechanics can provide valuable information about the size. If the origin is located near the surface and the measured size is smaller than that estimated by fracture mechanics it may indicate that the ligament of material between the surface and the origin should be considered part of the origin size. If the size of the origin can be measured with confidence then fracture mechanics can be used to obtain an estimate of the toughness of the material. This calculated toughness value can then be compared to independently measured toughness values and possibly corroborate the identity of the origin.

Performing fractographic analysis on a ceramic specimen or a group of specimens is much like assembling a jigsaw puzzle or being a detective trying to solve a crime. The analogy of a jigsaw puzzle is apt: if a few key pieces of the puzzle are missing, then the picture cannot be understood, as illustrated in Figure 2.7. As a detective the fractographer must look beyond the fracture surface and investigate all clues and combine them to properly characterize fracture origins.

## **Topic #2: Conclusions**

1) The characterization scheme in MIL HDBK-790 is adequate to characterize fracture origins in advanced structural ceramics, but confusion exists in some details of the three attributes.

2) The guidelines enable an inexperienced fractographer to locate and characterize fracture origins.

## ***FRACTOGRAPHERS ARE DETECTIVES***

They must use all available information ("clues") to find and characterize a fracture.

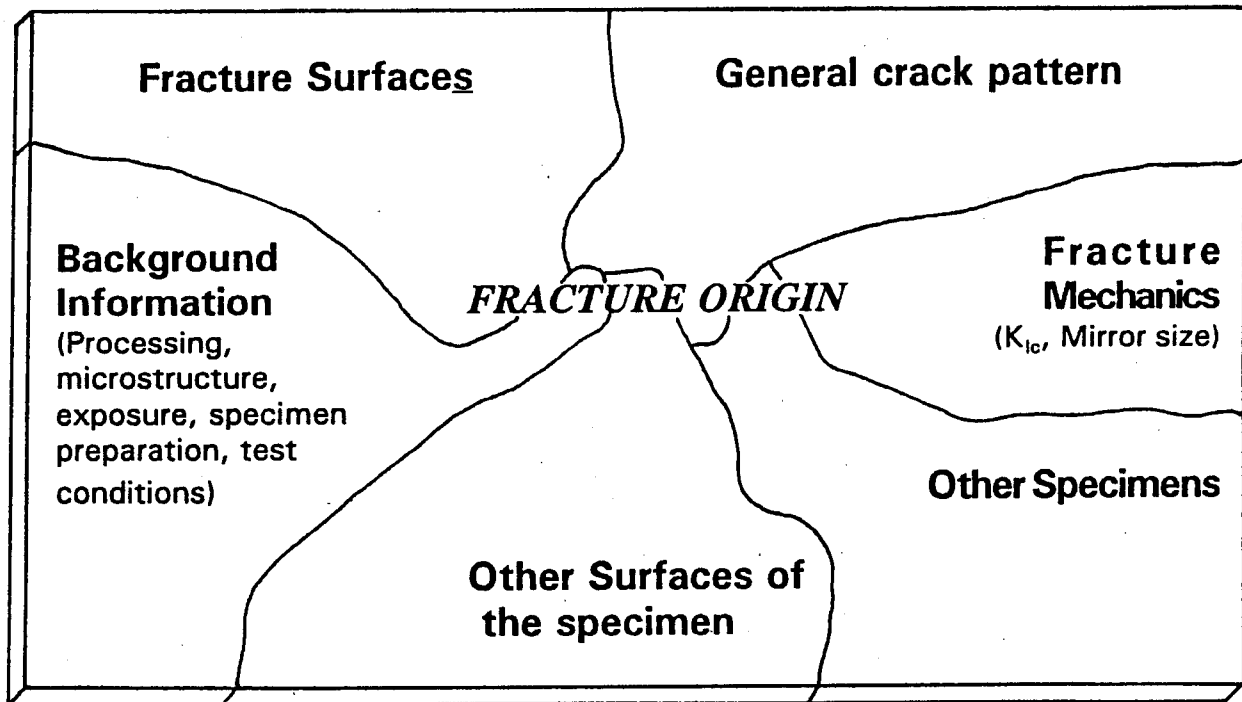


Figure 2.7. Fractography is like assembling a jigsaw puzzle, if a few key pieces are missing then the picture cannot be understood.

3) Fractography of a "single" specimen of a material can be misleading. The "single" specimen may not clearly represent the dominant fracture origin in the material or it may not be possible to completely characterize the origin in that specimen. The identity of the dominant origin may not become clear until many specimens of the same material with the same origin type are examined.

4) Limiting the fractographic examination to only one of the primary fracture surface halves can lead to the misinterpretation of any or all of the characterization attributes.

5) The external surfaces of the specimen or component must be examined, especially if the origin is located at the surface.

6) Fractographers must use all available information to properly characterize fracture origins in advanced structural ceramics. This includes, but is not limited to, fracture mechanics size analysis and the past history of the material.

7) Characterization of the fracture origin size is difficult because of complex geometries and in some instances, the lack of distinct boundaries between the origin and the bulk material.

### ***Topic #3 - Participants' Evaluation Of Their Own Material***

#### **Topic #3: Objective**

To determine the overall effectiveness and applicability of Military Handbook 790 to a variety of ceramic materials.

#### **Topic #3: Approach**

This was an optional topic which asked the participants to fractographically analyze a ceramic material of their choice.

#### **Topic #3: Instructions**

Complete instructions for this topic are given in Appendix 1. The participants were asked to fractographically analyze a ceramic material of their choice. They were to summarize their findings with Weibull plots of the data and photographs of the typical fracture origins and make recommendations on ways to improve future versions of the handbook.

#### **Topic #3: Discussion**

Only four participants chose to take part in this optional topic. Their individual analysis and findings are discussed below.

**PARTICIPANT 2** - Evaluated a commercially available sintered  $\beta$ -SiC that was produced by Coors Ceramics Company. The bars were machined according to the guidelines in ASTM C1161. They were tested at room temperature in four-point flexure using a high temperature flexure fixture. This was done to facilitate comparison to high temperature data. The fractographic analysis was performed with a stereo optical microscope (Bausch & Lomb, Hitachi video camera and monitor). Uncoated specimens were examined with a Hitachi S 800 scanning electron microscope in the secondary electron mode.

Table 3.1 and a Weibull plot, Figure 3.1, summarize the strength and fractographic information. Fifteen flexure specimens were used to generate these data but the fracture origins in only three of the specimens were characterized. All three specimens failed due to pores ( $P^V$ ), see Figure 3.2. The participant realized that the examination of only three specimens was not a sufficient characterization of the material but this was part of work in progress and complete characterization of the sample set could not be completed in time for this exercise.

**Suggestions/Comments on MIL HDBK-790:** None.

# STRENGTH AND FRACTOGRAPHIC INFORMATION FOR THE $\beta$ -SiC TESTED AND EXAMINED BY PARTICIPANT 2

Table 3.1

## Fractography Report (Incomplete)

Commercial sintered  $\beta$  - SiC manufactured by Coors Ceramics Company.  
 Machined into 4-point flexure bars according to ASTM C1161  
 Tested at room temperature (in a high temperature fixture for future comparisons to high temp. data.)  
 Fractography performed with stereo optical microscope (Bausch & Lomb, Hitachi video camera + monitor,) and Hitachi S 800 SEM in SE mode. Specimens were uncoated.

STRENGTH INFORMATION			FRACTOGRAPHIC INFORMATION			
ID	STRESS [MPa]	RANK	IDENTITY	LOCATION	SIZE VIEWING [ $\mu$ m]	COMMENTS
7	378.74	15				
1	378.23	14				
9	371.38	13				
2	367.92	12				
6	361.72	11	PV	NS	50	SEM Photos #38967, #38968
12	360.97	10				
8	347.45	9				
4	346.21	8				
15	345.71	7				
10	345.62	6				
11	339.67	5				
5	336.84	4	PV	V	140	SEM #38969, 38970, 38971
13	336.22	3				
14	325.36	2	PV	S	55	SEM #38972, 38973, 38974
3	272.84	1				

Average Strength = 348 MPa  
 Weibull Modulus (maximum likelihood) = 18.9  
 Weibull Scale parameter  $S_0$  = 358 MPa

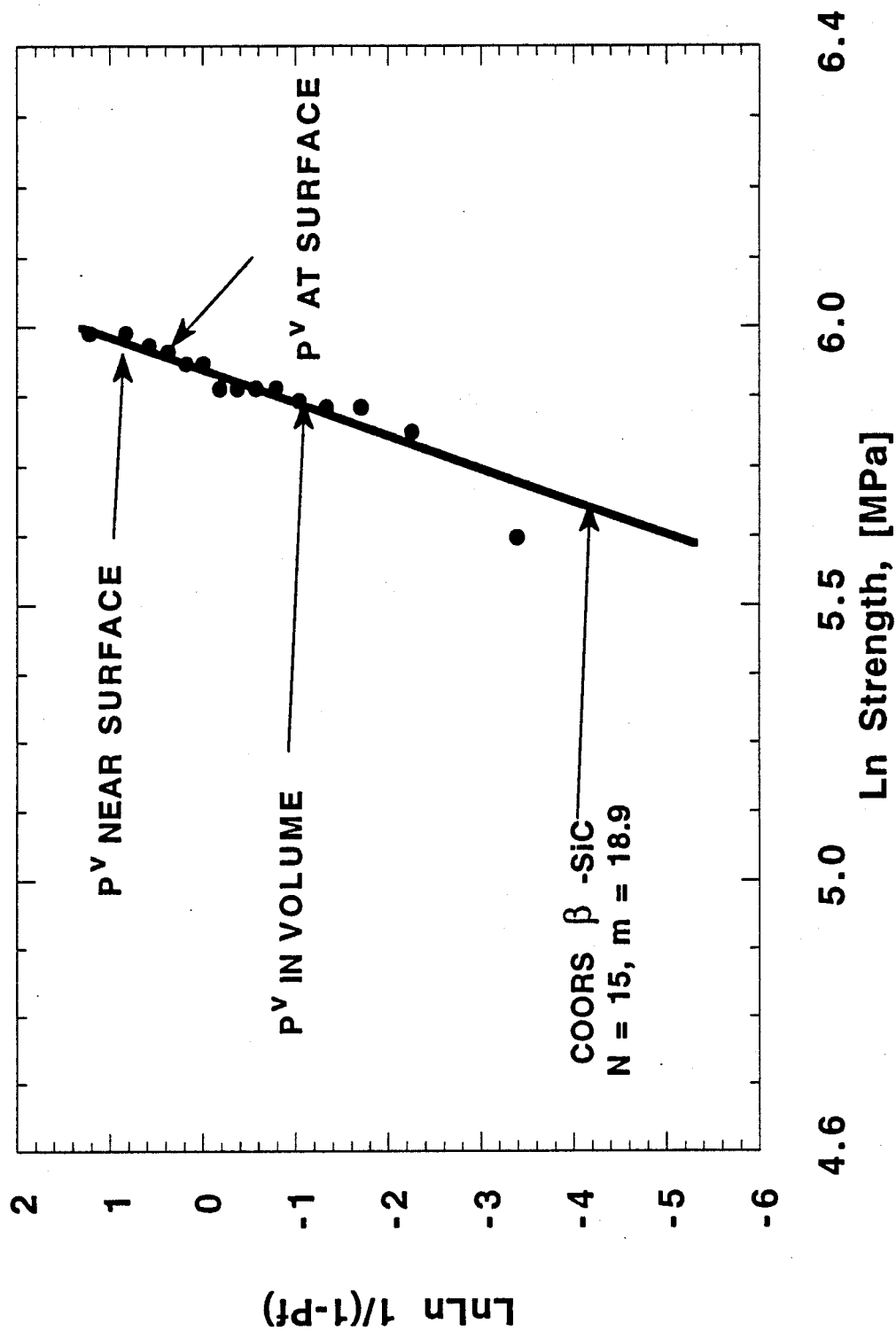
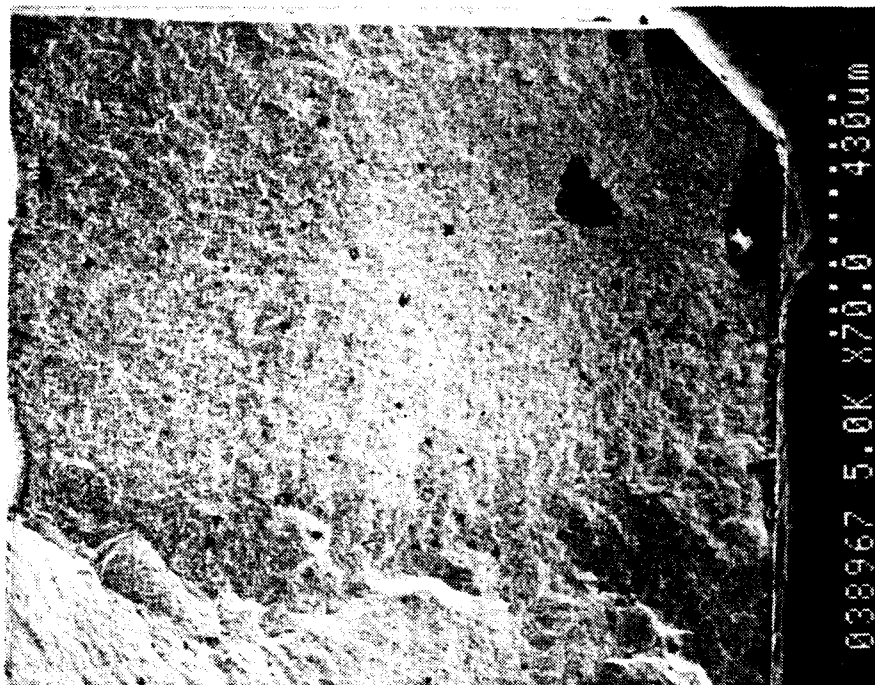
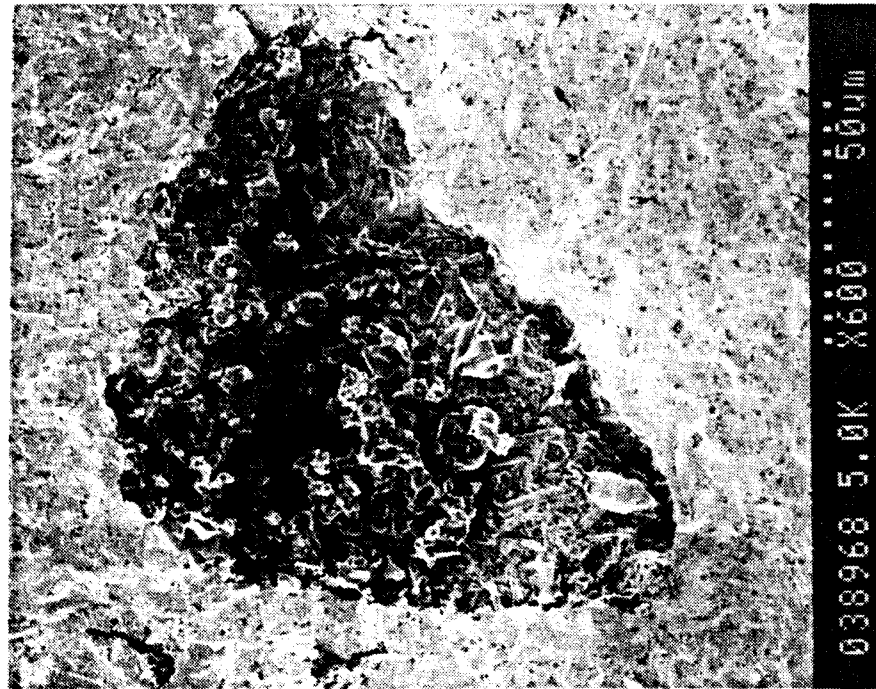


Figure 3.1.1. Participant 2's Weibull plot for a  $\beta$ -SiC. See Table 3.1 for the individual data.





A



B

Figure 3.2. Example of the fracture origin, pore ( $P^V$ ), seen in the  $\beta$ -SiC analyzed by Participant 2. A) 70X. B) 600X.

**PARTICIPANT 6** - This participant chose to evaluate a hot-isostatically pressed  $\text{Si}_3\text{N}_4$  (NT154) produced by Norton Advanced Ceramics. All the specimens were fabricated from a single master lot of powder and additives to ensure chemical consistency. Blending and ball milling were performed as a single batch. The milled powders were cold-isostatically pressed into billets, sintered to full density and HIPed using a glass encapsulation process. After HIPing the material was subjected to a heat treatment to promote crystallization of the grain boundary phase.

Large flexural bars, having a nominal cross section of 18 x 9 mm, were machined from cylindrical billets used for button head tensile and tension/torsion specimens. A post machining heat treatment at 1000°C for 20 hours was done to improve the surface strength. The specimens were tested on edge in a special four-point flexure fixture with inner and outer spans of 63.5 mm and 127 mm, respectively. Rolling pins, 12.7 mm in diameter, were necessary to accommodate the high loads. The specimens were tested on edge to increase the ratio of stressed volume to stressed area.

The fracture surfaces were examined with an optical stereo microscope between 7X and 40X to determine the location of the origin. SEM of the origin on selected specimens of interest was then conducted.

The individual results of the testing are listed in Table 3.2 and a Weibull plot associated with this data are given in Figure 3.3. One hundred specimens were fractured in this analysis and the fracture origins in 26 of these were characterized using the SEM. Figure 3.4 shows some examples of the origins which were encountered. The characterization did not include an origin size measurement nor did it truly identify the origin type. The Weibull plots in Figure 3.3 censor the data based solely on the location. Such an analysis can be misleading. Although the location is an important attribute MIL HDBK-790 states the location "shall not" be used to statistically differentiate the distribution of the origin populations. Since volume-distributed origins, such as pores, can be randomly distributed throughout a material, individual origin locations could be at the edge, surface, near the surface or in the volume. Statistically differentiating based on origin location can imply that there is more than one origin type in the material, when in fact there is only one.

**Suggestions/Comments on MIL HDBK-790: None.**

**PARTICIPANT 10** - Twenty flexure specimens of a silicon nitride ceramic were broken in three-point flexure and fractographically analyzed for this topic. The material was a EDM (Electrical Discharge Machineable) silicon nitride containing titanium nitride particles (trade name KERSIT 601). The material was used to manufacture silicon nitride tools for metal working. It was produced by mixing spray dried granules which are then isostatically pressed. They are then green

**Table 3.2**  
**STRENGTH AND FRACTOGRAPHIC INFORMATION FOR THE HIPed Si<sub>3</sub>N<sub>4</sub> EXAMINED BY PARTICIPANT 6**

FRACTOGRAPHY RESULTS									
FINAL VERSION AFTER SEM PHOTO REVIEW.									
Three batches, LPEL, LPEL2, and LPEL3. Numbers are not continuous.									
Outer span = 127 mm, Inner span = 63.5 mm									
All failures occurred inside the outer span									
Note: Corner = Edge									
Internal = Volume									
Specimen ID	Depth	Width	Stress	Location	Identity	Comment			
	in	in	Ksi						
LPEL- 1	0.7205	0.3500	100.6	Surface	Surface				
LPEL- 4	0.7201	0.3500	97.3	Surface	Surface				
LPEL- 5	0.7205	0.3500	82.0	Surface	Surface				
LPEL- 7	0.7205	0.3500	103.0	Surface	Surface				
LPEL- 8	0.7205	0.3500	107.3	Surface	Surface				
LPEL- 9	0.7209	0.3500	109.3	Surface	Surface				
LPEL- 11	0.7205	0.3500	118.9	Corner	Chip				
LPEL- 12	0.7205	0.3504	101.4	Surface	Surface				
LPEL- 13	0.7209	0.3500	80.1	Internal	Inclusion				
LPEL- 14	0.7205	0.3500	91.9	Surface	Surface				
LPEL- 15	0.7205	0.3504	116.4	Surface	Surface				
LPEL- 16	0.7209	0.3257	116.1	Surface	Surface				
LPEL- 17	0.7205	0.3504	98.8	Surface	Surface				
LPEL- 18	0.7205	0.3504	105.2	Corner	Surface				
LPEL- 19	0.7205	0.3500	76.9	Corner	Surface				
LPEL- 20	0.7205	0.3500	82.8	Corner	Surface				
LPEL- 21	0.7205	0.3500	117.9	Corner	Surface				
LPEL- 22	0.7205	0.3500	87.2	Surface	Surface				
LPEL- 23	0.7205	0.3500	125.4	Surface	Surface				
LPEL- 24	0.7205	0.3500	98.3	Internal	Inclusion				
LPEL- 25	0.7205	0.3500	119.5	Internal	Inclusion				
LPEL- 26	0.7205	0.3500	117.4	Corner	Surface				
LPEL- 29	0.7232	0.3500	77.8	Corner	Chip				
LPEL- 35	0.7205	0.3500	81.0	Corner	Surface				
LPEL- 36	0.7209	0.3496	92.7	Surface	Surface				
LPEL- 37	0.7205	0.3500	107.5	Surface	Surface				
LPEL2- 2	0.7205	0.3504	96.2	Surface	Surface				
LPEL2- 3	0.7205	0.3504	115.5	Surface	Surface				
LPEL2- 5	0.7205	0.3504	109.3	Surface	Surface				
LPEL2- 6	0.7205	0.3504	109.3	Corner	Surface				
LPEL2- 7	0.7244	0.3504	112.0	Corner	Surface				
LPEL2- 8	0.7209	0.3500	91.5	Internal	Inclusion				
LPEL2- 9	0.7205	0.3504	109.6	Surface	Surface				
LPEL2- 10	0.7209	0.3504	110.0	Surface	Crack				
LPEL2- 11	0.7205	0.3504	121.5	Surface	Surface				
LPEL2- 12	0.7205	0.3500	63.4	Corner	Chip				
LPEL2- 13	0.7205	0.3500	131.1	Surface	Surface				
LPEL2- 15	0.7205	0.3504	131.1	Surface	Surface				
LPEL2- 16	0.7205	0.3504	131.1	Surface	Surface				
LPEL2- 17	0.7205	0.3504	131.1	Surface	Surface				
LPEL2- 18	0.7201	0.3500	115.3	Surface	Surface				
LPEL2- 19	0.7205	0.3504	131.4	Corner	Surface				
LPEL2- 20	0.7205	0.3504	131.4	Corner	Surface				
LPEL2- 21	0.7205	0.3504	131.4	Corner	Surface				
LPEL2- 22	0.7205	0.3504	131.4	Corner	Surface				
LPEL2- 23	0.7205	0.3504	131.4	Corner	Surface				
LPEL2- 24	0.7205	0.3504	131.4	Corner	Surface				
LPEL2- 25	0.7205	0.3504	131.4	Corner	Surface				
LPEL2- 26	0.7205	0.3504	131.4	Corner	Surface				
LPEL2- 27	0.7205	0.3504	131.4	Corner	Surface				
LPEL2- 28	0.7205	0.3504	131.4	Corner	Surface				
LPEL2- 29	0.7205	0.3504	131.4	Corner	Surface				
LPEL2- 30	0.7205	0.3504	131.4	Corner	Surface				
LPEL2- 31	0.7205	0.3504	131.4	Corner	Surface				
LPEL2- 32	0.7205	0.3504	131.4	Corner	Surface				
LPEL2- 33	0.7205	0.3504	131.4	Corner	Surface				
LPEL2- 34	0.7205	0.3504	131.4	Corner	Surface				
LPEL2- 35	0.7205	0.3504	131.4	Corner	Surface				
LPEL2- 36	0.7205	0.3504	131.4	Corner	Surface				
LPEL2- 37	0.7205	0.3504	131.4	Corner	Surface				
LPEL2- 38	0.7205	0.3504	131.4	Corner	Surface				
LPEL2- 39	0.7205	0.3504	131.4	Corner	Surface				
LPEL2- 40	0.7205	0.3504	131.4	Corner	Surface				
LPEL2- 41	0.7205	0.3504	131.4	Corner	Surface				
LPEL2- 42	0.7205	0.3504	131.4	Corner	Surface				
LPEL2- 43	0.7205	0.3504	131.4	Corner	Surface				
LPEL2- 44	0.7205	0.3504	131.4	Corner	Surface				
LPEL2- 45	0.7205	0.3504	131.4	Corner	Surface				
LPEL2- 46	0.7205	0.3504	131.4	Corner	Surface				
LPEL2- 47	0.7205	0.3504	131.4	Corner	Surface				
LPEL2- 48	0.7205	0.3504	131.4	Corner	Surface				
LPEL2- 49	0.7205	0.3504	131.4	Corner	Surface				
LPEL2- 50	0.7205	0.3504	131.4	Corner	Surface				
LPEL2- 51	0.7205	0.3504	131.4	Corner	Surface				
LPEL2- 52	0.7205	0.3504	131.4	Corner	Surface				
LPEL2- 53	0.7205	0.3504	131.4	Corner	Surface				
LPEL2- 54	0.7205	0.3504	131.4	Corner	Surface				
LPEL2- 55	0.7205	0.3504	131.4	Corner	Surface				
LPEL2- 56	0.7205	0.3504	131.4	Corner	Surface				
LPEL2- 57	0.7205	0.3504	131.4	Corner	Surface				
LPEL2- 58	0.7205	0.3504	131.4	Corner	Surface				
LPEL2- 59	0.7205	0.3504	131.4	Corner	Surface				
LPEL2- 60	0.7205	0.3504	131.4	Corner	Surface				
LPEL2- 61	0.7205	0.3504	131.4	Corner	Surface				
LPEL2- 62	0.7205	0.3504	131.4	Corner	Surface				
LPEL2- 63	0.7205	0.3504	131.4	Corner	Surface				
LPEL2- 64	0.7205	0.3504	131.4	Corner	Surface				
LPEL2- 65	0.7205	0.3504	131.4	Corner	Surface				
LPEL2- 66	0.7205	0.3504	131.4	Corner	Surface				
LPEL2- 67	0.7205	0.3504	131.4	Corner	Surface				
LPEL2- 68	0.7205	0.3504	131.4	Corner	Surface				
LPEL2- 69	0.7205	0.3504	131.4	Corner	Surface				
LPEL2- 70	0.7205	0.3504	131.4	Corner	Surface				
LPEL2- 71	0.7205	0.3504	131.4	Corner	Surface				
LPEL2- 72	0.7205	0.3504	131.4	Corner	Surface				
LPEL2- 73	0.7205	0.3504	131.4	Corner	Surface				
LPEL2- 74	0.7205	0.3504	131.4	Corner	Surface				
LPEL2- 75	0.7205	0.3504	131.4	Corner	Surface				
LPEL2- 76	0.7205	0.3504	131.4	Corner	Surface				
LPEL2- 77	0.7205	0.3504	131.4	Corner	Surface				
LPEL2- 78	0.7205	0.3504	131.4	Corner	Surface				
LPEL2- 79	0.7205	0.3504	131.4	Corner	Surface				
LPEL2- 80	0.7205	0.3504	131.4	Corner	Surface				
LPEL2- 81	0.7205	0.3504	131.4	Corner	Surface				
LPEL2- 82	0.7205	0.3504	131.4	Corner	Surface				
LPEL2- 83	0.7205	0.3504	131.4	Corner	Surface				
LPEL2- 84	0.7205	0.3504	131.4	Corner	Surface				
LPEL2- 85	0.7205	0.3504	131.4	Corner	Surface				
LPEL2- 86	0.7205	0.3504	131.4	Corner	Surface				
LPEL2- 87	0.7205	0.3504	131.4	Corner	Surface				
LPEL2- 88	0.7205	0.3504	131.4	Corner	Surface				
LPEL2- 89	0.7205	0.3504	131.4	Corner	Surface				
LPEL2- 90	0.7205	0.3504	131.4	Corner	Surface				
LPEL2- 91	0.7205	0.3504	131.4	Corner	Surface				
LPEL2- 92	0.7205	0.3504	131.4	Corner	Surface				
LPEL2- 93	0.7205	0.3504	131.4	Corner	Surface				
LPEL2- 94	0.7205	0.3504	131.4	Corner	Surface				
LPEL2- 95	0.7205	0.3504	131.4	Corner	Surface				
LPEL2- 96	0.7205	0.3504	131.4	Corner	Surface				
LPEL2- 97	0.7205	0.3504	131.4	Corner	Surface				
LPEL2- 98	0.7205	0.3504	131.4	Corner	Surface				
LPEL2- 99	0.7205	0.3504	131.4	Corner	Surface				
LPEL2- 100	0.7205	0.3504	131.4	Corner	Surface				

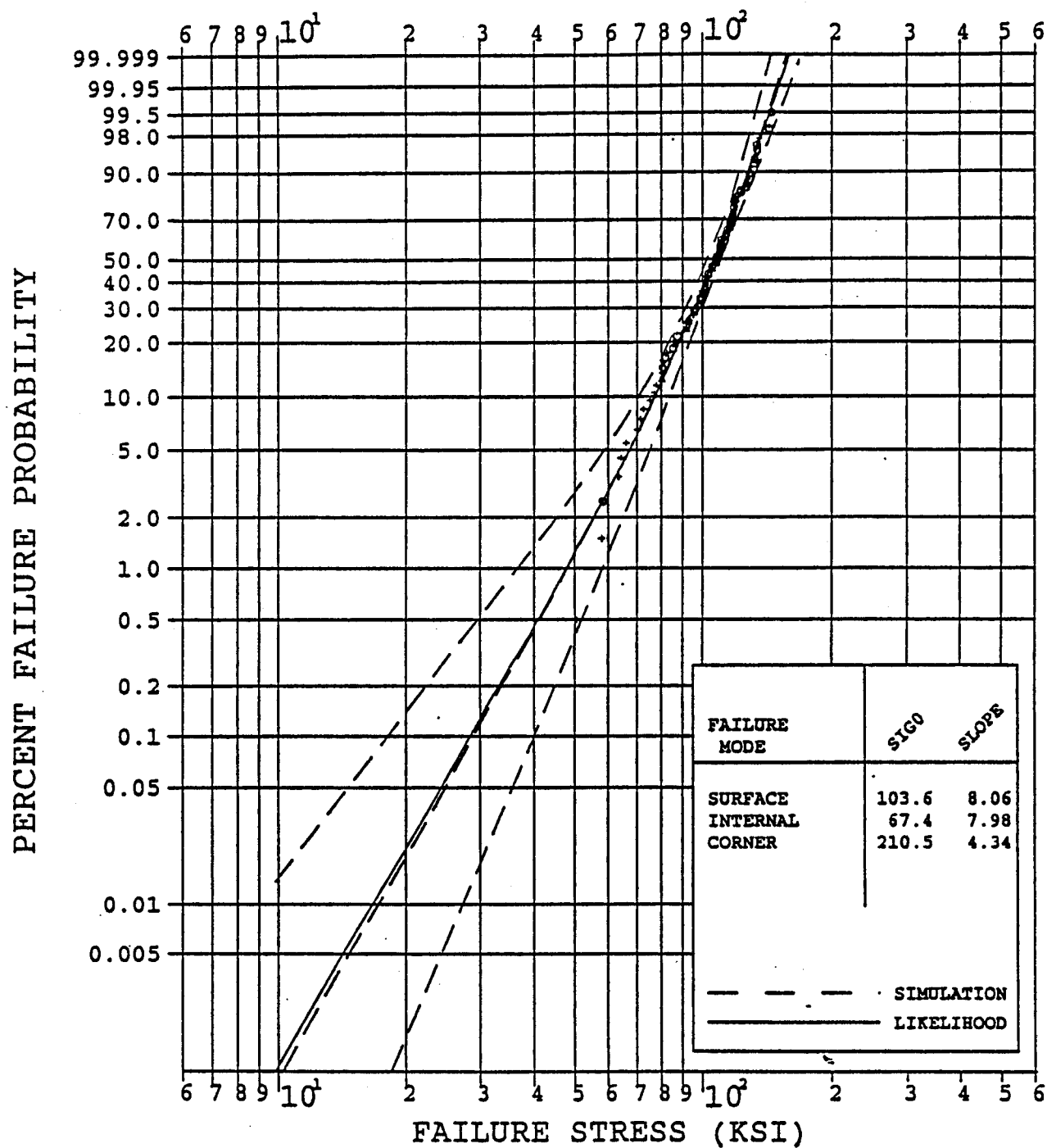
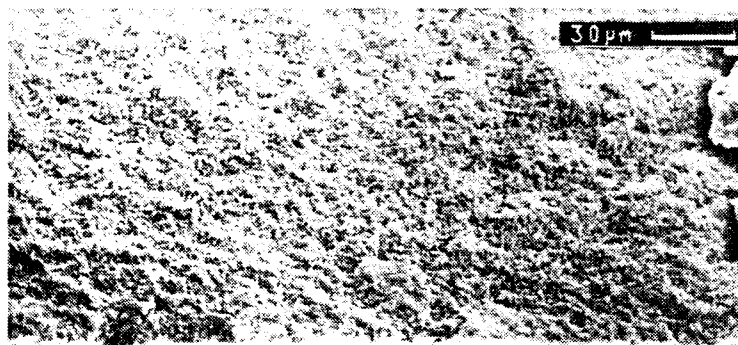
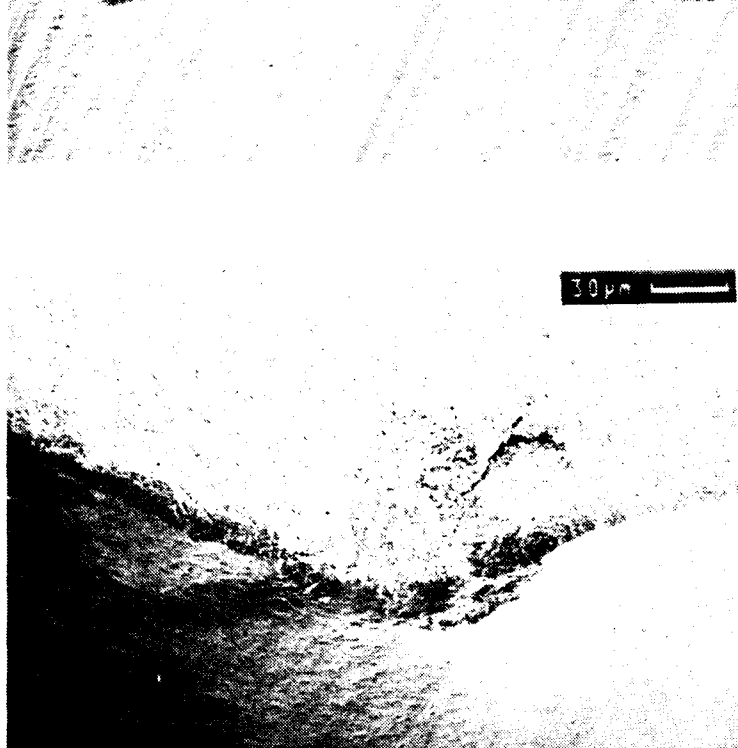


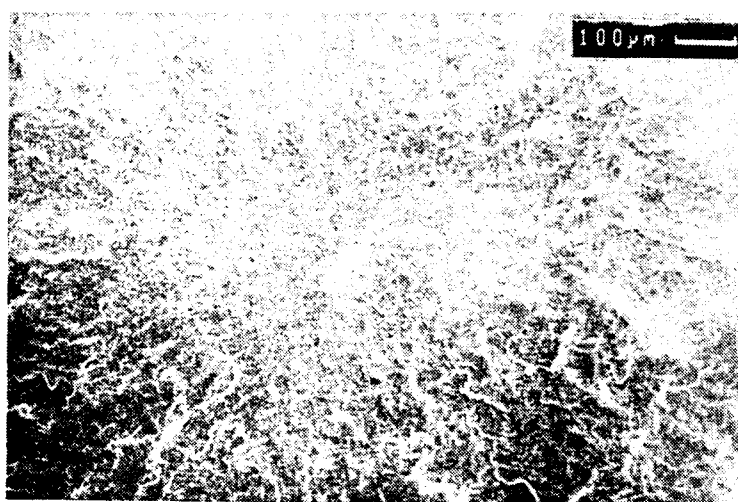
Figure 3.3. Combined Weibull plot of surface, internal and chamfer failures from the room temperature flexure of the HIPed  $\text{Si}_3\text{N}_4$  examined by Participant 6. See Table 3.2 for the individual data.



**A**



**B**



**C**

Figure 3.4. Examples of the fracture origins seen in the HIPed  $\text{Si}_3\text{N}_4$  analyzed by Participant 6. A) Specimen LP-37, Surface at surface? B) Specimen LP-29, Chip located at the edge. C) Specimen LP2-26, Inclusion located in the volume.

machined and the binder is removed under nitrogen, followed by gas pressure sintering in a nitrogen environment. Flexure bars were machined from sintered parts using resin-bonded diamond tools according to internal specifications. The nominal dimensions were 3.5 mm x 2 mm x 24 mm. Three-point flexure testing was done with a 20 mm span at a displacement rate of 0.5 mm/min. A compilation of the data is given in Table 3. 3. and is graphically illustrated by a Weibull plot in Figure 3.5.

Table 3.3  
**STRENGTH AND FRACTOGRAPHIC INFORMATION FOR A  $\text{Si}_3\text{N}_4/\text{TiN}$   
MATERIAL TESTED AND EXAMINED BY PARTICIPANT 10**

**EDM SILICON NITRIDE : KERSIT 601**  
Batch Ref. : T 302-5

3 Points Flexural test on 3.5x2x24 mm bars  
Calibrating load = 1000 N  
Span = 20 mm  
Span displacement rate = 0.5 mm/mn

**MEAN VALUE = 762.8 MPa**  
**STD = 198.85 MPa**

N°	MODULUS OF RUPTURE (MPa)	LN (MOR)	FLAW	LOCATION	SIZE
1	808,42	6,70	I	NS (10 $\mu\text{m}$ )	= 7 $\mu\text{m}$
2	850,38	6,75	MD	S	
3	163,31	5,10	CK	V	very large
4	844,98	6,74	FR	E	
5	857,03	6,75	@	NS (7 $\mu\text{m}$ )	= 20 $\mu\text{m}$
6	886,47	6,79	?		
7	799,68	6,68	FR	E	5 $\mu\text{m}$
8	906,93	6,81	MD	S	
9	901,81	6,80	?		
10	680,21	6,52	FR	NS (20 $\mu\text{m}$ )	20-30 $\mu\text{m}$
11	814,95	6,70	FR	NS	10 $\mu\text{m}$
12	879,93	6,78	?		
13	905,22	6,81	?		
14	863,88	6,76	P	E	5 $\mu\text{m}$
15	561,97	6,33	CK	V	very large
16	871,40	6,77	?		
17	730,23	6,59	non considered		
18	751,06	6,62	P	E	5 $\mu\text{m}$
19	324,27	5,78	CK	NS (5 $\mu\text{m}$ )	20-30 $\mu\text{m}$
20	844,01	6,74	?		

@ : Glassy phase

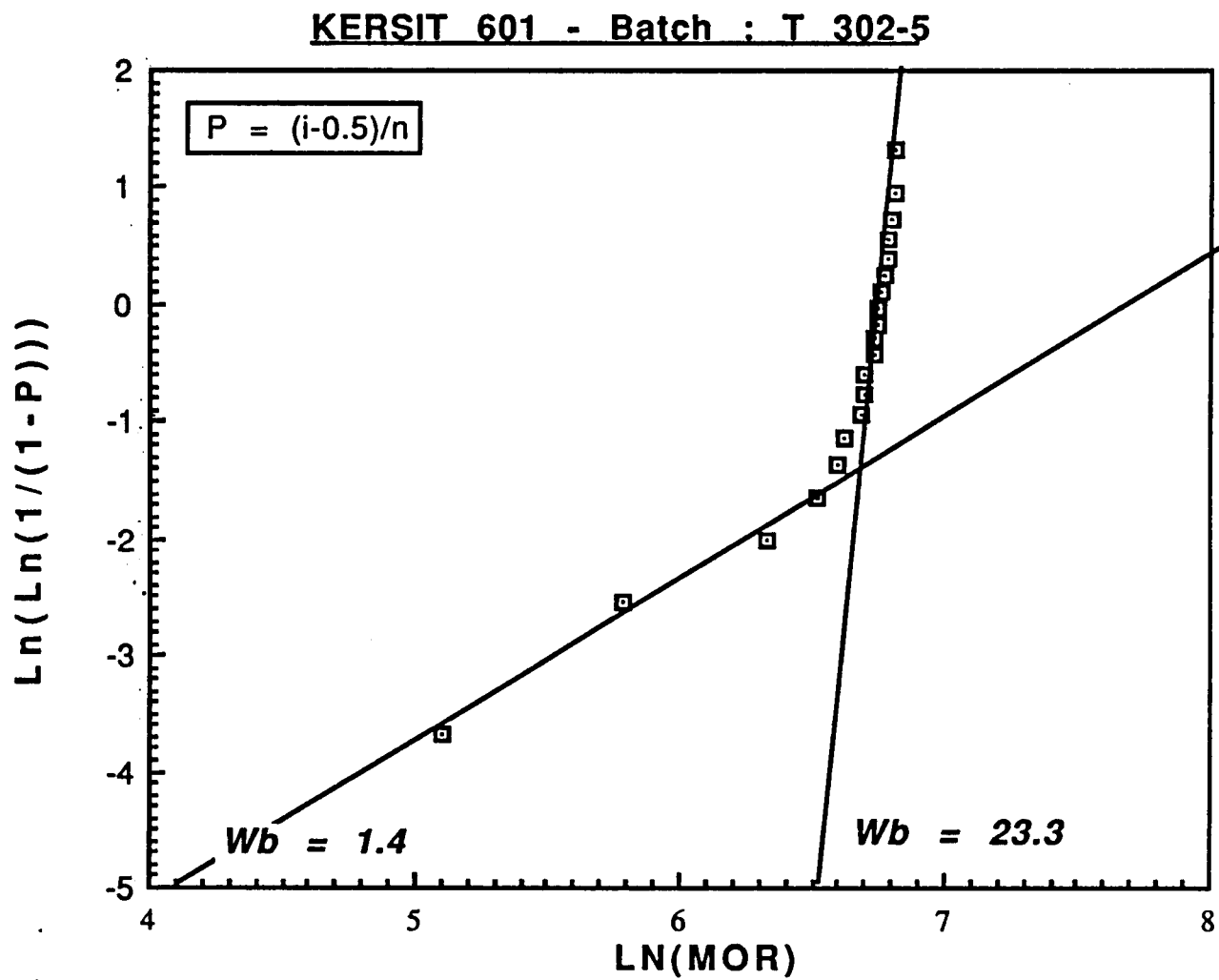


Figure 3.5. Weibull plot of room temperature strength data generated by participant 10 on a  $\text{Si}_3\text{N}_4/\text{TiN}$  material. Plot shows two possible origin populations. See Table 3.3 for the individual data.

All twenty of the specimens were fractographically examined but only one of the fracture surface halves of each was examined. The Weibull plot, Figure 3.5, shows two possible origin populations. The participant identified the origin for specimens at the low end of the strength distribution ( $m = 1.4$ ) as cracks, (Figure 3.6) while the origin at the high strength end of the distribution ( $m = 23.3$ ) tended to be porous regions (Figure 3.7), or machining damage (Figure 3.8).

**Suggestions/Comments on MIL HDBK-790:** The participant stated that MIL HDBK-790 provides a "very accurate and easy way to identify and analyze fracture images". The participants' agency has decided to adopt MIL HDBK-790. The participant suggested that two additional origin types be included under the category of inherently volume-distributed origins. These are:

**HARD AGGLOMERATE:** These origins are observed in die pressed or isostatically pressed samples when hard spray dried granulates, uncrushed during pressing, are present. This origin type is easily recognized according to the participant.

**GLASSY PHASE:** Large glassy phases can be observed in ceramics produced by liquid phase sintering. They can not be considered as inclusions since they have the correct chemical composition.

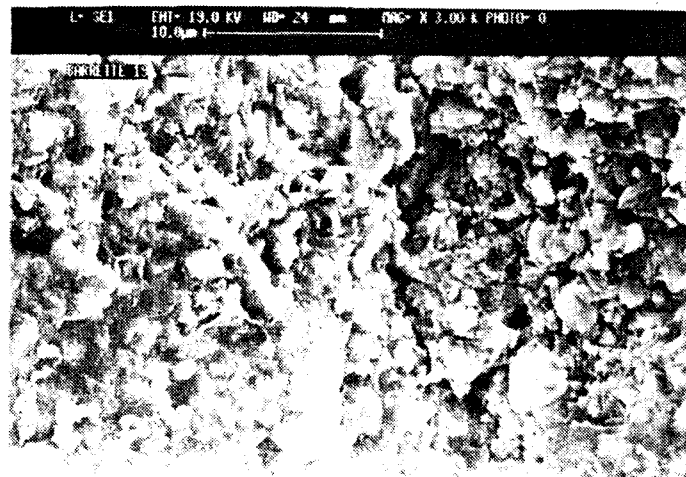
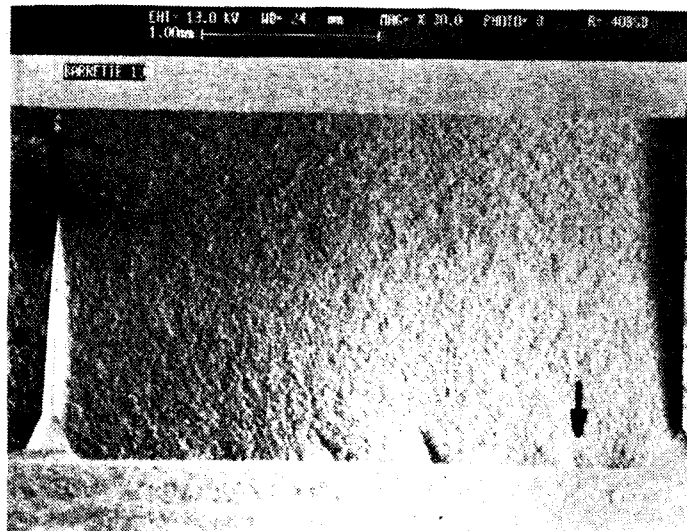
**Organizers' Reply:** These new origin types will be considered.

**PARTICIPANT 11** - Instead of examining a group of specimens from the same ceramic this participant examined a single specimen from two different materials.

The first specimen was a sintered SiC. No processing details were available. The specimen had a fracture stress of 314 MPa. Optical examination of the fracture surface at 25X using grazing incidence illumination revealed that the origin was located near one of the corners, Figure 3.9A. At an optical magnification of 100X using mixed lighting the origin appears to be an agglomerate or an inclusion, Figure 3.9B and C, because there is a raised sphere on one half and a corresponding depression on the mating half. It was noted that even though there are large grains very close to this agglomerate these can not be the origin because river lines pointing to the sphere can clearly be seen in these grains. The origin size was estimated assuming an internal penny-shaped crack,  $Y = 1.13$ , a fracture toughness of  $3 \text{ MPa}\sqrt{\text{m}}$  and a local stress of 180 MPa (This stress took into account the distance the origin was from the tensile surface.). The estimated size ( $c$ ) is about  $218 \mu\text{m}$  which is about twice the reported diameter of the origin.

The second specimen was a commercial alumina which contained 4% MnO and TiO<sub>2</sub> as low-temperature sintering aids. It has a trade name of Hilox

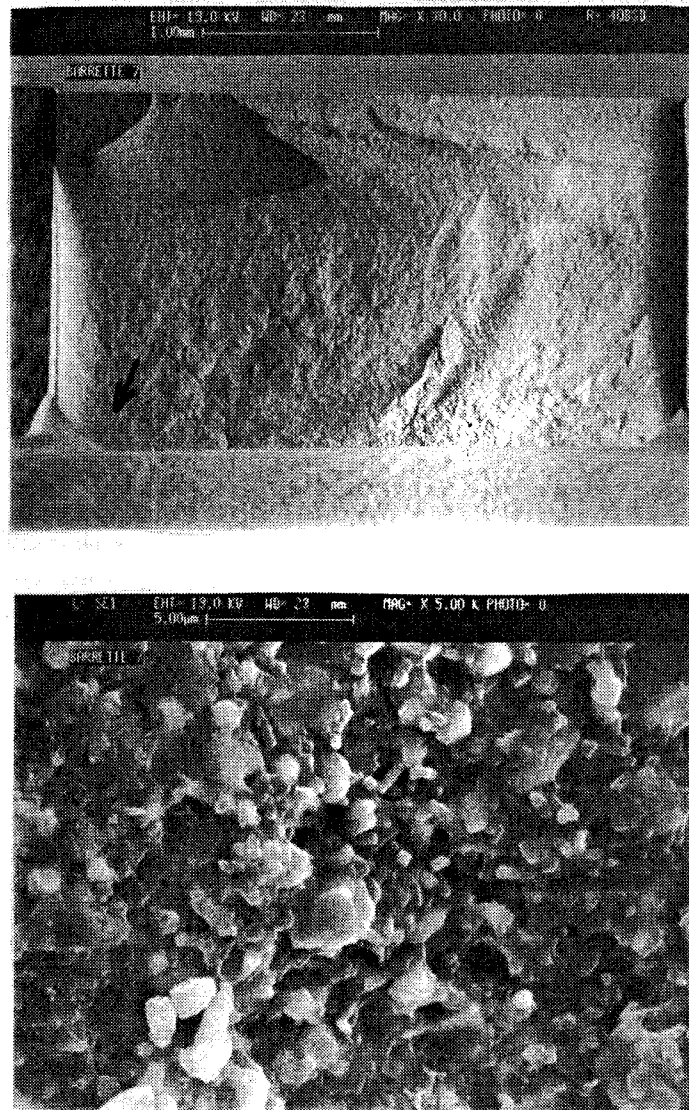




SAMPLE N° 19

MOR = 324.27 MPa

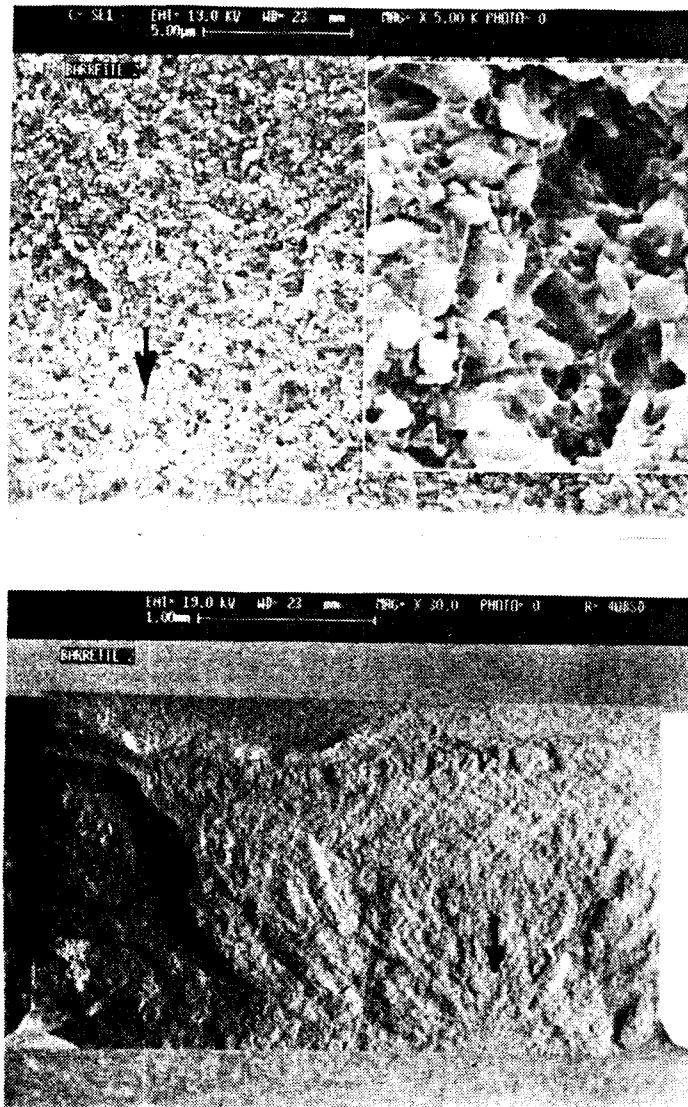
Figure 3.6. Example of an origin in a  $\text{Si}_3\text{N}_4/\text{TiN}$  specimen. Labeled by participant 10 as a crack.



**SAMPLE N° 7**

**MOR = 799.68 MPa**

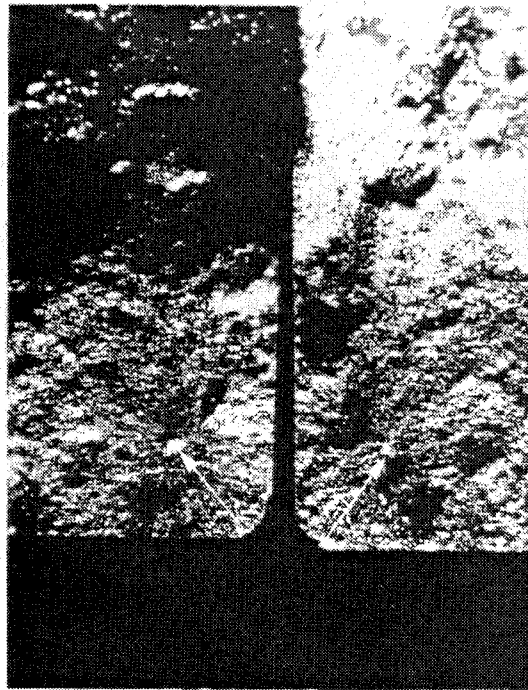
**Figure 3.7. Example of an origin in a  $\text{Si}_3\text{N}_4/\text{TiN}$  specimen. Labeled by participant 10 as a porous region.**



### SAMPLE N° 2

MOR = 850.38 MPa

Figure 3.8. Fracture origin in specimen 2 for a  $\text{Si}_3\text{N}_4/\text{TiN}$  specimen. Labeled by participant 10 as machining damage.



**A**



**B**



**C**

**Figure 3.9. Origins in a sintered-SiC from participant 11. A) Optical photograph taken at 25X using grazing incident illumination. B) and C) Optical photographs of the mating halves of the fracture surface showing the origin. Taken at 100X under mixed lighting. Note large grains with river lines.**

961 and was produced by Morgan Matroc, UK. The alumina grains are typically 3-4  $\mu\text{m}$  with the manganese and titanate phases appearing as sub-micron grains at the alumina grain boundaries. This specimen was machined from die-pressed, fired bars and tested in three-point flexure with a very fast crosshead speed of 5 mm/min. The fracture strength was 366 MPa and the toughness was about 4 MPa $\sqrt{\text{m}}$ . The origin is clearly at or close to the surface, Figure 3.10, thus Y was assumed to be 1.4 and the origin size estimated to be about 61  $\mu\text{m}$ . The participant states that there is a "crack-like defect" visible having approximately the right size. The participant further states "It is known that this material is prepared from spray-dried powder, and it is likely that the crack-like defects are elongated pores left by remnants of particles insufficiently crushed in pressing."

Although optical examination of these specimens was quite revealing it does not allow for complete characterization of the fracture origin. SEM analysis may have enabled the participant to reach a definitive characterization of the origin.

**Suggestions/Comments on MIL HDBK-790:** MIL HDBK-790 was found to be very helpful but only for high-strength ceramics which have "localised defects". There were four suggestions made to improve the handbook.

1) The addition of more optical photomicrographs at approximately 25X. These would be more helpful than a sketch in interpreting the fracture markings on some of the more difficult materials, especially in coarse-grained materials.

2) More guidance, such as a logical sequence, for the detection and measurement of machining induced origins.

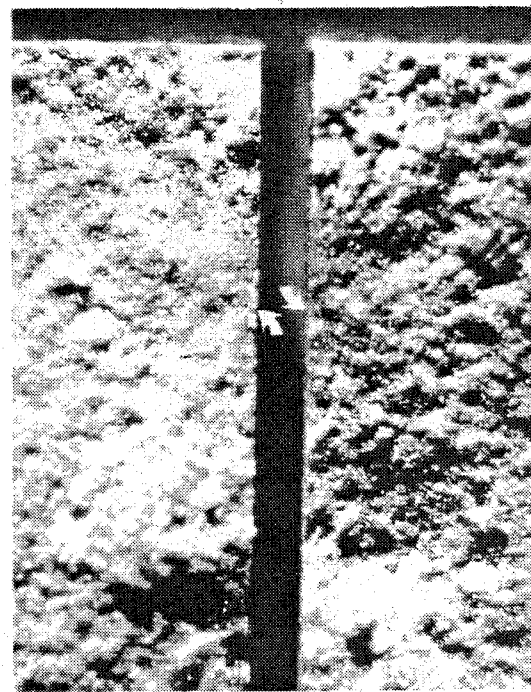
3) MIL HDBK-790 implies that failures due to the normal microstructure, i.e., fractures resulting from large grains which are at the upper end of the grains size distribution, are "unidentified" or "other". These should be treated as a separate class of origins.

4) Address the issue of subcritical crack growth and how it affects the determination of the origin size.

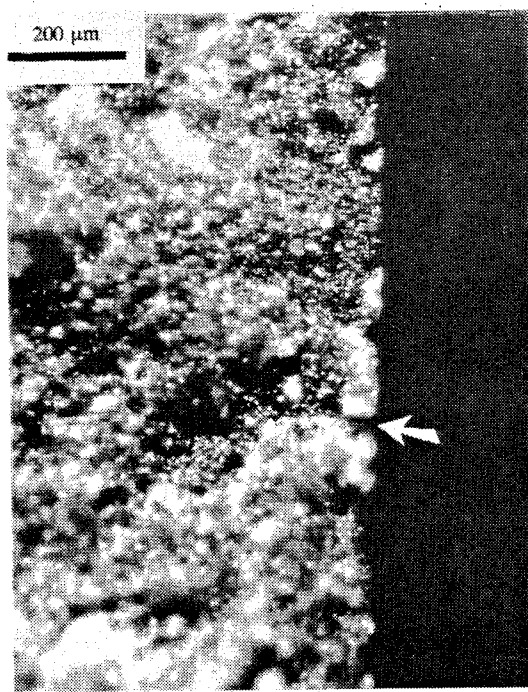
#### **Organizers' Reply:**

1) Several optical photomicrograph will be incorporated into the handbook to provide further guidance for interpreting fracture features in coarse-grained ceramics.

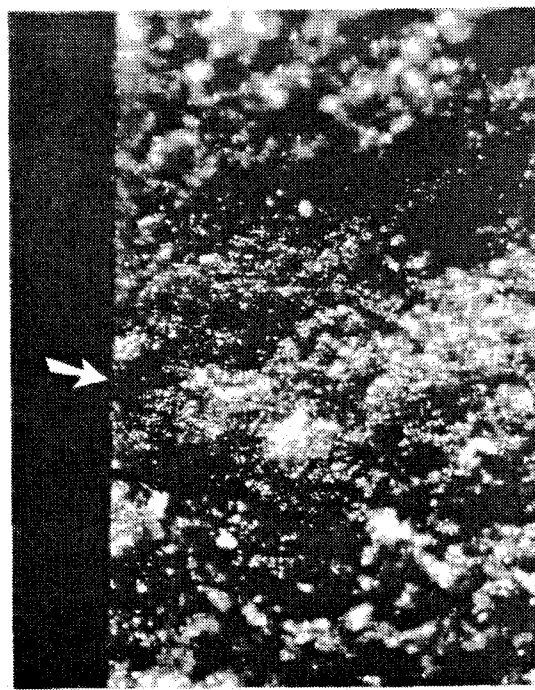
2) The organizers will consider this.



**A**



**B**



**C**

**Figure 3.10:** Origins in an alumina from participant 11. A) Optical photograph of the mating halves of the primary fracture surface, taken at 25X using grazing incident illumination. B) and C) Optical photographs of the mating halves of the fracture surface showing the origin. Taken at 100X under mixed lighting.

3) The organizers will take this under consideration, but MIL HDBK-790 does discuss this issue.

4) This will be taken under consideration.

## **Synopsis**

### **GENERAL CONCLUSIONS:**

- 1) The guidelines and characterization scheme in MIL HDBK-790 are adequate for the complete characterization of fracture origins in advanced ceramics but some refinements are needed for each attribute in the characterization scheme. These revisions are listed in the next section.
- 2) Fracture mechanics was not used enough by the participants in this exercise to assist in the characterization of fracture origins.
- 3) In many instances fractographers failed to use all available information about the material and its history during the characterization.
- 4) Characterization of the fracture origin size is difficult in many instances.
- 5) Characterization of origins from photographs or a single specimen can be misleading. The participants were handicapped due to this.
- 6) Fractographers must examine the mating halves of the primary fracture surface.
- 7) Fractographers must examine the external surfaces of the specimen or component.
- 8) Few participants were familiar with fracture mirror size analysis. There is a need for new mirror constants for today's advanced ceramic materials.

### **AMENDMENTS TO MIL HDBK-790:**

This section lists amendments that will be made to MIL HDBK-790 based on the results and comments from this exercise.

#### ***General:***

- 1) Actual photographs of fracture features (mirror and hackle lines) on the fracture surfaces of advanced ceramics will be added to complement the schematics.
- 2) Use of fracture mechanics will be explained more clearly and illustrated. It shall also be required as a step in the characterization of fracture origins.



3) Examination of both halves of the primary fracture surface will be mandated.

4) Examination of the external surfaces as well as the fracture surface will be mandated.

5) Additional information, (e.g., a list of mirror constants) will be added to MIL HDBK-790. The Bibliography in the handbook was initially intended as a source of such information, but the users may be reluctant to search out these references.

***Characterization Scheme:***

6) The definition of surface and edge as possible origin locations will be clarified.

7) An example of an origin located near-to-the-surface and a definition of near surface will be included.

8) The method to characterize the origin size will be defined better. For machining damage and other origins located at the surface which have a semielliptical shape the characteristic dimension is the depth.

9) A possible revision may be to include mirror size as an optional, fourth attribute for an origin.

One final point is that fractography is a time-consuming process. A preliminary draft version of this report was sent to the participants for their comments and review. Several participants indicated that their analysis may have been better if they had the opportunity to spend more time on the specimens. The organizers concur. We believe that time-constraints led many participants to examine only one half of the fracture surface, and to neglect the examination of the external specimen surfaces. As noted in the text, this can cause a misidentification of an origin. The detective work entailed in fractographic analysis requires experience, patience, and time on the part of the fractographer.

Successful fractography has a number of ingredients: broken pieces, a material conducive to fracture surface interpretation, background information, skilled fractographer, equipment, adequate time, and a framework or guide for the analysis. This round robin has identified a number of key factors that are necessary for the last item, and revisions to the Military Handbook 790 shall be made.

### PROPOSED FUTURE WORK:

\* Develop mirror constants for the advanced ceramics which are commercially available and those which have potential commercial applications.

### ***Acknowledgment***

The authors wish to acknowledge Michael Slavin at the U.S. Army Research Laboratory - Materials Directorate who was instrumental in the development of MIL HDBK-790 and this round robin exercise. A thank you is also extended to Dr. Kristin Breder of Oak Ridge National Laboratory for supplying the silicon nitride specimens used in Topic #2, and most importantly to the agencies and individuals who kindly took the time to participate in this exercise.

## **References**

1. G.D. Quinn, J.J. Swab and M.J. Slavin, "A Proposed Standard Practice for Fractographic Analysis of Monolithic Advanced Ceramics", Fractography of Glasses and Ceramics, Advances in Ceramics, Vol. 22, eds., J. Varner and V. Frechette, American Ceramic Society, Westerville, OH, 309-362, (1988).
2. G.D. Quinn, J.J. Swab and M.J. Slavin, "A Proposed Standard Practice for Fractographic Analysis of Monolithic Advanced Ceramics", MTL TR 90-57, November 1990, NTIS Access No. ADA-231989.
3. Fractography of Glasses and Ceramics, Advances in Ceramics, Vol. 22, eds., J. Varner and V. Frechette, American Ceramic Society, Westerville, OH, (1988).
4. Fractography of Ceramic and Metal Failures, eds., J. Mecholsky, Jr and S. Powell, Jr., ASTM STP 827, Philadelphia, PA, 1984.
5. Concepts, Flaws and Fractography, Fracture Mechanics of Ceramics, Vol 1., eds., R. Bradt, D. Hasselman and F. Lange, Plenum Press, New York, 1974.
6. Failure Analysis of Brittle Materials, Advances in Ceramics, Vol. 28, V. D. Frechette, American Ceramic Society, Westerville, OH, 1990.
7. J.J. Mecholsky, Jr. and S.W. Freiman, "Determination of Fracture Mechanics Parameters Through Fractographic Analysis of Ceramics," Fracture Mechanics of Ceramics Applied to Brittle Materials, ed. S. Freiman, ASTM STP 678, 136-150, (1979).
8. R.W. Rice, "Ceramic Fracture Features, Observations, Mechanisms and Uses," Fractography of Ceramic and Metal Failures, ASTM STP 827, 5-103 (1984).
9. "Failure Analysis" Engineering Materials Handbook, Vol 4, Ceramics and Glasses, 629-673 (1991).
10. J.J. Mecholsky, Jr., S.W. Freiman, and R.W. Rice, "Effect of Grinding on Origin Geometry and Fracture of Glass," J. Am. Ceram. Soc., 60 [3-4] 114-117 (1977).
11. R.W. Rice, J.J. Mecholsky, Jr. and P.F. Becher, "The Effect of Grinding Direction on Origin Character and Strength of Single Crystal and Polycrystalline Ceramics," J. Mat. Sci., 16, 853-862 (1981).

12. J.C. Newman Jr. and I.S. Raju, "An Experimental Stress-Intensity Factor Equation for the Surface Crack," *Eng. Fract. Mech.*, 15 [1-2] 185-192 (1981).
13. P. Chantikul, G.R. Antis, B.R. Lawn and D.B. Marshall, "A Critical Evaluation of Indentation Techniques for Measuring Fracture Toughness: II, Strength Method," *J. Am. Ceram. Soc.*, 64 [9] 539-543 (1981).
14. J.J. Swab and S.C. Stowell, "Properties of a TZP/ $\text{Al}_2\text{O}_3$  Composite After Long-Term Exposure at 1000°C," U.S. Army Materials Technology Laboratory, MTL TR 91-54, December 1991, NTIS Access No. ADA-246407.
15. J.J. Mecholsky, Jr., S.W. Freiman and R.W. Rice, "Fracture Surface Analysis Of Ceramics," *J. Mat. Sci.*, 11, 1310-1319 (1976).
16. G. Quinn, unpublished data.
17. H.P. Kirchner, R.M. Gruver & W.A. Sotter, "Fracture Stress-Mirror Size Relations for Polycrystalline Ceramics," *Phil. Mag.*, 33 [5] 775-780 (1976).
18. C.A. Tracy and G.D. Quinn, "Fracture Toughness by the Surface Crack in Flexure (SCF) Method," *Ceram. Eng. Sci. Proc.*, 15 [5] 837-845 (1994).
19. H.P. Kirchner, R.M. Gruver and W.A. Sotter, "Characteristics of Flaws at Fracture Origins and Fracture Stress-Flaw Size Relations in Various Ceramics," *Mat. Sci. Eng.*, 22, 147-156 (1976).
20. A.G. Evans, M.E. Meyers, K.W. Fertig, B.I. Davis and H.R. Baumgartner, "Probabilistic Models of Defects Initiated Fracture in Ceramics," *J. Non-Destruct. Eval.*, [1] 111-114 (1980).
21. R.W. Rice, "Fractographic Determination of  $K_{Ic}$  and Effects of Microstructural Stresses on Ceramics," *Fractography of Glasses and Ceramics, Advances in Ceramics*, Vol. 22, eds., J. Varner and V. Frechette, American Ceramic Society, Westerville, OH, 509-545 (1988).
22. D.B. Marshall, "Strength Characteristics of Transformation-Toughening Zirconia," *J. Am. Ceram. Soc.*, 69 [3] 173-180 (1986).
23. J. Wang and R. Stevens, "Review: Zirconia-Toughened Alumina (ZTA) Ceramics," *J. Mat. Sci.*, 24, 3421-3440 (1989).
24. S.J. Bennison and B.R. Lawn, "Origin Tolerance in Ceramics with Rising Crack Resistance Characteristics," *J. Mat. Sci.*, 24, 3169-3175 (1989).

25. R.M. Anderson and L.M. Braun, "Technique for the R-Curve Determination of Y-TZP Using Indentation-Produced Flaws," J. Am. Ceram. Soc., 73 [10] 3059-3062 (1990).
26. S.Y. Liu and I.W. Chen, "Fatigue of Yttria-Stabilized Zirconia: II, Crack Propagation, Fatigue Striations, and Short-Crack Behavior," J. Am. Ceram. Soc., 74 [6] 1206-1216 (1991).
27. A.P. Vicente, F. Guiberteau, A. Dominguez-Rodriguez, G.W. Dransmann and R.W. Steinbrech, "Propagation of Short Surface Cracks in Y-TZP," Euro-Ceramics II, Vol. 2, eds., G. Ziegler and H. Hausner, (1993).
28. G.D. Quinn, J. Salem, I. Bar-on, K. Cho, M. Foley and H. Fang, "Fracture Toughness of Advanced Ceramics at Room Temperature," J. Res. Natl. Inst. Stand. Technol., 97, [5] 579-607 (1992).
29. Stress Intensity Factors Handbook, Vol. 1, eds. Y. Murakami, S. Auki, H. Miyata, K. Tohgo, N. Hasebe, N. Miyazaki, Y. Itoh, H. Teradaund and R. Yuuki, Pergamon Press, New York, 868-870 (1987).
30. R.W. Davidge, Mechanical Behavior of Ceramics, Cambridge University Press, New York, 98-100 (1979).
31. J.A. Salem and S.R. Choi, "Toughened Ceramics Life Prediction," Department of Energy, "Ceramic Heat Engine Technology Program, Oct.-Nov. Bimonthly report, 220-234 (1991).
32. J.W. Johnson and D.G. Holloway, "On Shape and Size of Fracture Zones on Glass Fracture Surfaces," Philos. Mag., [14] 713-743 (1966).
33. H.P. Kirchner and J.C. Conway, Jr., "Fracture Mechanics of Crack Branching in Ceramics," Advances in Ceramics, Vol. 22, eds., J. Varner and V. Frechette, American Ceramic Society, Westerville, OH, 187-213 (1988).
34. H.P. Kirchner, R.M. Gruver and W.A. Sotter, "Use of Fracture Mirrors to Interpret Impact Fracture in Brittle Materials," J. Am. Ceram. Soc., 58 [5-6] 188-191 (1975).
35. H.P. Kirchner and R.M. Gruver, "Fracture Mirrors in Polycrystalline Ceramics and Glass," Fracture Mechanics of Ceramics, Vol. 1, 309-321 (1974).
36. H.P. Kirchner and R.M. Gruver, "Fracture Mirrors in Alumina Ceramics," Phil. Mag., 27 [6] 1433-1446 (1973).

37. G.K. Bansal, "On Fracture Mirror Formation in Glass and Polycrystalline Ceramics," *Phil. Mag.*, 35 [4] 935-944 (1977).
38. G.K. Bansal and W.H. Duckworth, "Fracture Stress as Related to Origin and Fracture Mirror Sizes," *J. Am. Ceram. Soc.*, 60 [7-8] 304-310 (1977).
39. C. A. Tracy and M.J. Slavin, unpublished work.
40. J.J. Swab "Properties of Yttria-Tetragonal Zirconia Polycrystal (Y-TZP) Materials After Long-Term Exposure to Elevated Temperatures," MTL TR 89-21, March 1989, NTIS Access No. ADA-207064.
41. G.D. Quinn, R.N. Katz and E.M. Leno, "Thermal Cycling Effects, Stress Rupture and Tensile Creep in Hot Pressed Silicon Nitride," in Proceedings of the DARPA/NAVSEA Ceramic Gas Turbine Demonstration Engine Program Review, MCIC Report 78-36, Battelle, Columbus, OH, 1978.
42. G.D. Quinn, "Characterization of Turbine Ceramics After Long-Term Environmental Exposure," U.S. AMMRC Technical Report, TR 80-15, April 1980.
43. M.K. Ferber and M.G. Jenkins, "Evaluation of the Strength and Creep-Fatigue Behavior of Hot Isostatically Pressed Silicon Nitride," *J. Am. Ceram. Soc.*, 75 [9] 2453-2462 (1992).

## **APPENDIX 1: Instructions For The Round Robin**

### **Topic #1: Machining Damage**

**OBJECTIVE:** To determine the ability to characterize (location, size and shape) machining damage in advanced ceramics.

**GENERAL INFORMATION:** Enclosed are three (3) sets of photographs from ceramic specimens which failed due to machining damage. Each set contains three (3) pairs of photographs, taken at different magnifications, representing each half of the fracture surface. Included is an information sheet describing the ceramic material in each set and the conditions under which it fractured. Also attached is a data sheet.

All the specimens used in TOPIC #1 were machined according to the guidelines given in MIL STD 1942A, ASTM C1161, and CEN EN 843-1. (All grinding shall be done with an ample supply of water-based coolant to keep the work piece and wheel constantly flooded and particles flushed and filtered. Grinding shall be in at least two stages, ranging from coarse to fine rates of materials removal. All machining shall be in the surface grinding mode, parallel to the specimen long axis. No Blanchard or rotary grinding shall be used. The stock removal rate shall not exceed 0.03 mm per pass to the last 0.06 mm per face. Final and intermediate finishing shall be performed with a diamond wheel that is between 320 and 500 grit. No less than 0.06 mm per face shall be removed during the final finishing phase, and at a rate of not more than 0.002 mm per pass. Remove approximately equal stock from opposite faces. The four long edges of each specimen shall be uniformly chamfered at 45°, a distance of 0.12 ± 0.03 mm with the finishing comparable to that applied to the specimen surfaces. Grinding must be parallel to the specimen long axis.)

A "T" on the photograph denotes the tensile surface and "Ch" denotes the chamfer.

### **INSTRUCTIONS:**

- 1) On the lowest magnification photograph indicate the location of the fracture origin.
- 2) Using one or both of the remaining pairs of photographs outline the fracture origin and the shape of the associated fracture mirror. Mark the point at which the mirror radius was measured. Also indicate any tensile surface or chamfer damage which may be present.

**NOTE:** We suggest using permanent makers or rub-off arrows that can be affixed to the photograph.
- 3) On the data sheet provided record the location of the origin as well as the size of the fracture origin and fracture mirror. Please include units.
- 4) Include any comments, such as a description of the origin, which may help characterize the fracture origin. If your comments do not fit in the space provided attach a separate sheet and note such. Please make sure your comments legible.
- 5) Make a photocopy of all information for your records.
- 6) Return all photographs and data sheets.

## **Topic #1: Machining Damage**

### **MATERIAL INFORMATION**

#### **PHOTOGRAPH SET #1**

Labeled TSZ-14

The ceramic is a zirconia/alumina composite. It contains 75 w/o tetragonal zirconia, partially stabilized by 4.2 w/o yttria, with 20 w/o  $\alpha$ -alumina. It was formed into large billets through a sinter/hot isostatic press process. The specimen was machined into a flexure bar of the following nominal dimensions: 3mm x 4mm x 50mm. Material fracture toughness, as determined by the indentation-strength technique, is  $\approx 5 \text{ MPa}\sqrt{\text{m}}$ . Average grain size of the zirconia is  $\approx 0.4 \mu\text{m}$  and that of the alumina is  $\approx 0.6 \mu\text{m}$ . The specimen was heat treated in air for 100 hours at 1000°C prior to room temperature four-point flexure testing in air. Flexure strength of this specimen was 1552 MPa.

#### **PHOTOGRAPH SET #2**

Labeled SN-5

The ceramic is a silicon nitride which was hot-pressed with 8 w/o yttria. The specimen was nominally 2.16mm x 2.16mm x 50mm in size and was machined from a large billet. The material fracture toughness was measured at  $6.2 \text{ MPa}\sqrt{\text{m}}$  from double torsion tests. Cross section of the grains ranged from 1-3  $\mu\text{m}$  with an aspect ratio of 6:1 to 8:1. The room temperature four-point flexure strength of this specimen, in air, was determined to be 910 MPa.

#### **PHOTOGRAPH SET #3**

Labeled  $\text{Al}_2\text{O}_3$ -RR8

Photographs are of a high purity (99.9%), sintered alumina. The specimen was machined into a flexure bar of the following nominal dimensions: 3mm x 4mm x 50mm, from a large billet. Material fracture toughness is  $4 \text{ MPa}\sqrt{\text{m}}$ . The average grain size ranges from 3-6  $\mu\text{m}$ . The room temperature four-point flexure strength of this specimen, in air, was 228 MPa.



VAMAS Fractography Round Robin Exercise

**TOPIC #1: MACHINING DAMAGE**  
**DATA SHEET**

**\*PLEASE INCLUDE UNITS\***

PARTICIPANT # \_\_\_\_\_

-----  
**PHOTOGRAPH SET #1: TSZ-14**

IDENTITY: MD LOCATION: \_\_\_\_\_ SIZE: \_\_\_\_\_

Size of Fracture Mirror: \_\_\_\_\_

Comments:

-----  
**PHOTOGRAPH SET #2: SN-5**

IDENTITY: MD LOCATION: \_\_\_\_\_ SIZE: \_\_\_\_\_

Size of Fracture Mirror: \_\_\_\_\_

Comments:

-----  
**PHOTOGRAPH SET #3:  $\text{Al}_2\text{O}_3$ -RR8**

IDENTITY: MD LOCATION: \_\_\_\_\_ SIZE: \_\_\_\_\_

Size of Fracture Mirror: \_\_\_\_\_

Comments:

## Topic #2: Characterization Of Fracture Origins

**OBJECTIVE:** To locate and characterize fracture origins according to Military Handbook 790 and determine the effectiveness of the characterization scheme.

**GENERAL INFORMATION:** Enclosed are the mating halves of six (6) ceramic specimens which were fractured. Unless otherwise noted the entire specimen is enclosed. Included is a material information sheet describing each specimen, any pre-test treatments, and the conditions under which it was fractured. The ceramic materials selected for this topic were chosen based on their conduciveness to fractographic analysis. In order to complete the round robin in a timely fashion, metallographic analysis is not needed to properly characterize any of these fracture origins. Also attached is a data sheet for recording your results.

All the specimens used in this topic, with the exception of Specimen 5, were machined from large billets of the material. Specimen 5 was machined from an as-fired bar having the nominal dimensions of 4mm x 6mm x 50mm.

These specimens have already been characterized by the U.S. Army Research Laboratory - Materials Directorate. With the exception of Specimen 5, the characterization was done in an uncoated state using an SEM. Due to charging problems Specimen 5 was sputter coated with  $\approx 100 \text{ \AA}$  of Au prior to SEM characterization. The coating was not removed from the specimen.

### INSTRUCTIONS:

- 1) Treat the specimens as if you had fractured them.
- 2) Characterize the fracture origin by IDENTITY, LOCATION and SIZE as outlined in Military Handbook 790. For origins which are located in the volume or near the surface provide the distance from the tensile surface in the comments section of the data sheet. See Section 2.2.3 (b) in Military Handbook 790 for details.
- 3) If EDS (energy dispersive spectroscopy) is used to analyze the specimen attach a copy of the results.
- 4) Answer all the questions listed on the data sheet.
- 5) Mark your photographs as stated in the Topic #1 instructions.
- 6) Include any comments, especially those which may help describe the fracture origin. If your comments do not fit in the space provided attach a separate sheet and note such. Please make sure your comments are legible.
- 7) Make a copy of all information (data sheets & photographs) for your records.
- 8) Return all specimens, photographs and data sheets. Please wrap the specimens in tissue to avoid damaging the coating or fracture surface.

VAMAS Fractography Round Robin Exercise

**TOPIC #2: CHARACTERIZATION OF FRACTURE ORIGINS**

**DATA SHEET**

SPECIMEN SET \_\_\_\_\_ PARTICIPANT # \_\_\_\_\_

-----  
**SPECIMEN #**

IDENTITY: \_\_\_\_\_ LOCATION: \_\_\_\_\_ SIZE: \_\_\_\_\_

1) Was the specimen cleaned prior to examination? Y or N. If yes, how was it cleaned? \_\_\_\_\_

2) Was the specimen coated prior to examination? Y or N. If yes, what is the coating and approximately how thick is it? \_\_\_\_\_

3) Circle the microscopic technique(s) used to characterize the origin?  
Optical SEM Other: \_\_\_\_\_

4) If SEM is used which mode was employed? \_\_\_\_\_

5) Was EDS used? Y or N. 6) How many photographs are being sent? \_\_\_\_\_

Comments:

-----  
**SPECIMEN #**

IDENTITY: \_\_\_\_\_ LOCATION: \_\_\_\_\_ SIZE: \_\_\_\_\_

1) Was the specimen cleaned prior to examination? Y or N. If yes, how was it cleaned? \_\_\_\_\_

2) Was the specimen coated prior to examination? Y or N. If yes, what is the coating and approximately how thick is it? \_\_\_\_\_

3) Circle the microscopic technique(s) used to characterize the origin?  
Optical SEM Other: \_\_\_\_\_

4) If SEM is used which mode was employed? \_\_\_\_\_

5) Was EDS used? Y or N. 6) How many photographs are being sent? \_\_\_\_\_

Comments:

### **Topic #3: Participants Evaluation Of Their Own Material**

**OBJECTIVE:** To determine the overall effectiveness and applicability of Military Handbook 790 "Fractography and Characterization of Fracture Origins in Advanced Structural Ceramics" to a variety of ceramic materials.

**GENERAL INFORMATION:** You can use any advanced ceramic material (long- or continuous-fiber reinforced ceramics can not be used) for this topic. It can be a commercial or an experimental ceramic material. It does not have to be a current vintage ceramic or one which you are presently examining. We recommend using a set of fast fracture specimens.

#### **INSTRUCTIONS:**

- 1) Apply the guidelines in Military Handbook 790 to a ceramic material of your choice.
- 2) Provide generic background information on the ceramic including a summary of the process and testing history.
- 3) Provide information on the fractographic analysis techniques which were used, especially any improvements or refinements to, or deviations from, Military Handbook 790.
- 4) Summarize the findings with a Weibull plot, the specimen data, appropriate photographs of the typical fracture origins, and a photograph of the microstructure.
- 5) Based on your experience make any suggestions on ways to improve Military Handbook 790.

## **APPENDIX 2: Factors Which Complicate The Comparison Of The Measured Fracture Origin Size To The Fracture Mechanics Size Estimate**

A number of material and microstructural factors can complicate the comparison of the measured fracture origin size to the size estimated by fracture mechanics (Equation 1b in Topic #1):

$$c = \{K_{Ic} / (Y \sigma)\}^2 \quad (1b)$$

where:  $c$  = the characteristic origin dimension, (e.g., depth, radius),  
 $K_{Ic}$  = fracture toughness,  
 $\sigma$  = stress at the fracture origin,  
and  $Y$  = stress intensity shape factor for the origin

It is difficult to make generalizations for all materials about how these factors can interfere with this comparison. Our purpose in using Equation 1b is to *help verify that the correct feature has been characterized as the fracture origin*. This verification will be considered adequate if the calculated and fractographically-measured sizes agree within a factor of two or three. If they disagree by a factor of more than 3, the fractographer should reconsider his or her characterization of the origin.

In the following sections some factors which can account for differences between the measured and calculated size values will be discussed. The fracture mechanics calculated origin size ( $c_{calc}$ ) from Equation 1b will be compared to the fractographically-measured size ( $c_{meas}$ ) for an origin.

We first discuss the factors that cause systematic differences.

### **Factors Which Cause The Calculated Origin Size To Be *Smaller Than* The Fractographically-Measured Origin Size**

**CRACK BLUNTING** - Crack tip blunting (from a thermal treatment, or an environmental-chemical reaction) will cause the calculated size ( $c_{calc}$ ) to be *smaller than* the measured crack size ( $c_{meas}$ ). The higher stress necessary to propagate a blunt crack (relative to a sharp crack) will lead to a smaller  $c_{calc}$  estimate. Set #1 (Zirconia/Alumina) in Topic #1 may be an example of this situation.

**USE OF 2-DIMENSIONAL CRACK MODELS** - It is common practice to model origins with circumscribed circles, ellipses, semicircles or semiellipses. This may be suitable for some origins such as machining damage. In general, however, the use of such two-dimensional penny-shaped models for real, three-dimensional origins is a gross oversimplification. Compendiums or collections of

stress intensity factors for more representative origin geometries such as References A2.1 - 4 may be consulted. (The new ASTM Standard Practice will list such sources in its Bibliography section, which has been expanded beyond that within MIL HDBK 790.)

A general rule of thumb is that an equiaxed three-dimensional origin model will have a Y factor that is less than or equal to the Y for a penny-shaped origin of the same cross sectional area. As a consequence, use of the two-dimensional circular or elliptical models (and their associated Y factors) can lead to a  $c_{calc}$  that is *smaller than*  $c_{meas}$ .

**SPECIMEN OR COMPONENT STRESS GRADIENTS** - The stress to be used in Equation 1b should be the stress at the fracture origin. This may or may not be the maximum stress in the specimen or component. For example, if the origin is located below the surface in a flexure specimen, the stress at the origin will be less than the maximum stress in the specimen. Erroneous usage of the maximum stress will cause  $c_{calc}$  to be *smaller than*  $c_{meas}$ .

### **Factors Which Cause The Calculated Origin Size To Be *Larger Than* The Fractographically-Measured Origin Size**

**STABLE CRACK EXTENSION - Environmentally Assisted** - Stable crack extension due to slow crack growth (SCG) from an origin can be an interfering factor. This phenomena is often environmentally assisted. Water in liquid or gaseous form can promote SCG in many ceramics. If the zone of SCG is readily apparent on a fracture surface and its size used in Equation 1b, the calculated and measured crack sizes may be very similar. If the crack extension is not detected,  $c_{calc}$  will be *larger than* the fractographically-measured crack size,  $c_{meas}$ . This is illustrated in Figure A2.1. Set #3 ( $Al_2O_3$ ) in Topic #1 appears to an example of this situation.

**STABLE CRACK EXTENSION - R Curve Phenomena** - Severe complications can arise if the material exhibits stable crack extension due to R-curve behavior (rising crack extension resistance with crack length) prior to fracture. In such cases, it may be a gross oversimplification to utilize a point value of fracture toughness ( $K_{Ic}$ ) in Equation 1b. Fracture may instead be dictated by the rate of rising stress intensity ( $K_I$ ) with crack extension versus the rate of toughening due to the R-curve effect. One should be very careful about the value of fracture toughness, " $K_{Ic}$ ", that one uses even for approximation purposes. The fracture toughness obtained from large-crack, conventional fracture toughness tests (double cantilever beam, double torsion, etc.) may be a value for a fully-developed crack which is centimeters long, and is at the high toughness plateau of an R-curve which may not be relevant to a small (e.g. 25 micrometers), naturally-occurring fracture origin. The local fracture toughness at the origin may be much less than the large-crack toughness. Using the plateau toughness

value will result in  $c_{calc}$  being *larger than*  $c_{meas}$ . It is recommended that whenever possible the fracture toughness value for small cracks be used in Equation 1b. Set #1 (Zirconia/Alumina) in Topic #1 could be an example of how the R-curve phenomenon effects this comparison.

If the material has only a shallow R-curve, then the effect may not be significant and Equation 1b may provide reasonable crack size estimates.

**SPECIMEN OR COMPONENT STRESS RAISERS** - Specimens with notches or shoulders may have stresses larger than the assumed stress. Specimen misalignments (flexure, tension, other) can also cause enhanced stresses at an origin. Since the stress at the origin may be underestimated,  $c_{calc}$  will be *larger than*  $c_{meas}$ .

**ORIGIN CAUSES A LOCAL FRACTURE TOUGHNESS DEGRADATION** - The origin may have a different composition than the bulk (i.e., an inclusion). A chemical reaction may occur between the origin and the surrounding matrix which causes a degradation of the local fracture toughness around the origin. Use of a bulk matrix  $K_{IC}$  would cause the  $c_{calc}$  value to be *larger than* the  $c_{meas}$  value.

**ORIGIN IS WITHIN A SINGLE GRAIN** - In coarse-grained ceramics the origin may be within a single grain. The single crystal fracture toughness for the appropriate cleavage plane, which is typically less than the polycrystalline fracture toughness, should be used in Equation 1b. If not, and the polycrystalline fracture toughness is used,  $c_{calc}$  will be *larger than*  $c_{meas}$ .

**ORIGIN LINK UP WITH OTHER DISCONTINUITIES OR A SURFACE** - If a primary origin is near another discontinuity or a free surface, it is conceivable that the ligaments between the discontinuities or the free surface may fracture prior to overall specimen fracture as shown in Figure A2.2. If the fractographer cannot discern the links, the measured critical crack size will be an underestimated and  $c_{calc}$  will be *larger than*  $c_{meas}$ .

### **Factors Which Cause The Calculated Origin Size To Be Either *Smaller Or Larger Than* The Measured Origin Size**

**CRACK NESTING OR INTERACTIONS** - Crack nesting (nearby origins in the same axis as the applied stress, see Fig. 1.8) usually causes the calculated origin size ( $c_{calc}$ ) to be *smaller than* the measured crack size ( $c_{meas}$ ). This occurs when the cracks shield each other from the stress field and is most pronounced when the cracks are lined up such that they overlap each other as shown in Figures 1.8 and A2.3. This might be expected to occur for closely spaced, periodic, and similar-sized surface cracks from machining damage. The Y factor

on the origin is reduced in this instance. Set #1 (Zirconia/Alumina) in Topic #1 may be an example of the effects of crack nesting on this comparison.

On the other hand, there are instances where cracks may be aligned or staggered in three dimensions in which case the stress intensity factor ( $Y$ ) at any one crack could be higher than the  $Y$  for a solitary crack. Figure A2.4 illustrates this case. The extra cracks may or may not be visible on the fracture surface. In such cases, the  $c_{calc}$  value will be *larger than* the  $c_{meas}$  value.

Nearby additional discontinuities whether they are sharp and crack-like or blunt (like spherical pores) can either cause the stress intensity factor ( $Y$ ) to be enhanced or diminished at the fracture origin, depending upon the specifics of their sizes, shapes and locations in relation to the fracture origin. Examples of interacting discontinuities are shown in Figure A2.5. Some of these extra discontinuities may not be on the plane of fracture, and thus will not be fractographically detected. Nearby discontinuities can cause  $c_{calc}$  to be either *larger or smaller than*  $c_{meas}$  on the fracture surface.

References A2.2 - A2.4 should be consulted for additional stress intensity factor solutions for interacting cracks.

**STABLE CRACK EXTENSION - High Temperature** - Stable crack extension from high-temperature crack growth phenomena may lead to similar differences between calculated and measured origin sizes. The slow crack growth zone will be readily apparent in many materials. It may be intergranular, heat tinted, and/or oxidized. Crack size at criticality will probably agree reasonably well with a prediction from Equation 1b, provided that the material is still elastic. If the crack growth is not discerned, then  $c_{calc}$  will be *larger than*  $c_{meas}$ .

If the crack extension is due to accumulated creep damage, linear elastic fracture mechanics and Equation 1b will no longer be applicable. (The crack size ( $c_{calc}$ ) predicted by Equation 1b, will be *smaller than* the measured size ( $c_{meas}$ ).)

**RESIDUAL STRESSES** - Residual stresses can result in  $c_{calc}$  being either *smaller or larger than*  $c_{meas}$ . They can arise from many sources. Residual stresses from grinding are usually compressive in the immediate surface region (0-5 micrometers deep), but change to tensile deeper into the bulk. The gradient can be very steep, with compression stresses well over 1 GPa at the surface. Tensile stresses can be of the order of a tens of MPa to several hundred MPa. Thus, the effect upon a surface crack will depend upon how large the crack is. If it is very shallow, it may be primarily under the influence of compression stresses. This will cause  $c_{calc}$  to be *smaller than*  $c_{meas}$  (if the compressive stresses are not taken into account). Conversely, if the crack is large, and the tip experiences a tensile stress, then  $c_{calc}$  will be *larger than*  $c_{meas}$ .



Residual stresses can arise from other sources such as surface transformation effects (e.g. in zirconia), surface oxidation reactions, thermal strains from nonuniform sintering, and thermal and elastic strain between grains in anisotropic ceramics. Generalizations about comparing  $c_{calc}$  to  $c_{meas}$  are difficult to make in these instances. It is often impossible to determine the local residual stresses at any specific origin.

**ORIGIN TRUNCATION ON THE FRACTURE SURFACE** - The fracture surface may not reveal the full origin. The fracture plane may cut through, or truncate the origin in a fashion that the full size is not seen, as illustrated in Figure A2.6. Examples are a machining crack that is at an angle to the principal stress direction, or a Hertzian cone crack that is cleaved by the final fracture surface. The calculated origin size ( $c_{calc}$ ) will be *larger than* the fractographically-measured origin size ( $c_{meas}$ ). A further complication is that the true shape may not be seen and estimates of the Y factor could be wrong in either direction.

**ORIGIN IRREGULARITY** - Some origins have very irregular shapes, and penny-shaped cracks are extremely poor models. Examples are Hertzian cone cracks, cracks at impact sites, or cracks under scratches.

**VARIATION IN THE PROPERTIES OF THE ORIGIN RELATIVE TO THE SURROUNDING MATRIX** - The origin itself may be an inclusion or second phase discontinuity which has thermal expansion, fracture toughness, or elastic moduli that are different than the surrounding medium. The thermal or elastic properties mismatches can cause very localized strains which can cause localized cracking. These scenarios are discussed in more detail in References A2.1 and A2.5.

## REFERENCES

A2.1 I. Bar-on, "Applied Fracture Mechanics," in Engineered Materials Handbook, Vol. 4, Ceramics and Glasses, ed. S. Schneider, ASM, Metals Park, OH, 645-661 (1991).

A2.2 Stress Intensity Factors Handbook, Vols. 1 and 2, ed. Y. Murakami, Pergamon Press, New York (1986).

A2.3 H. Tada, P.C. Paris and G.R. Irwin, The Stress Analysis of Cracks Handbook, Del Research Corp., St. Louis, (1973).

A2.4 D.P. Rooke and D.J. Cartwright, Compendium of Stress Intensity Factors, Her Majesty's Stationery Office, London (1976).

A2.5 A.G. Evans, "Structural Reliability: A Processing-Dependent Phenomenon," J. Am. Ceram. Soc., 65, 127-137 (1982).

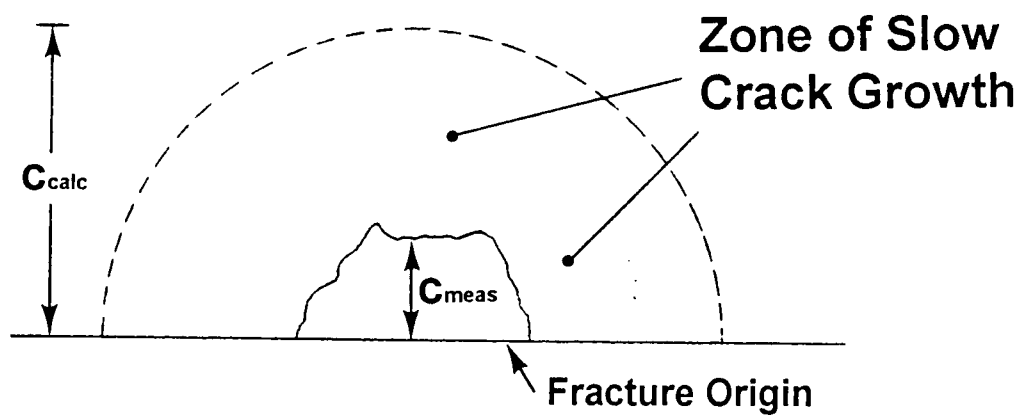


Figure A2.1 Slow crack growth may cause an origin to grow. Fracture occurs when the crack has extended to the critical size which should be the same as the size predicted from fracture mechanics ( $c_{calc}$ ). If the SCG zone is not detected, then it will appear that  $c_{calc}$  is larger than  $c_{meas}$ .

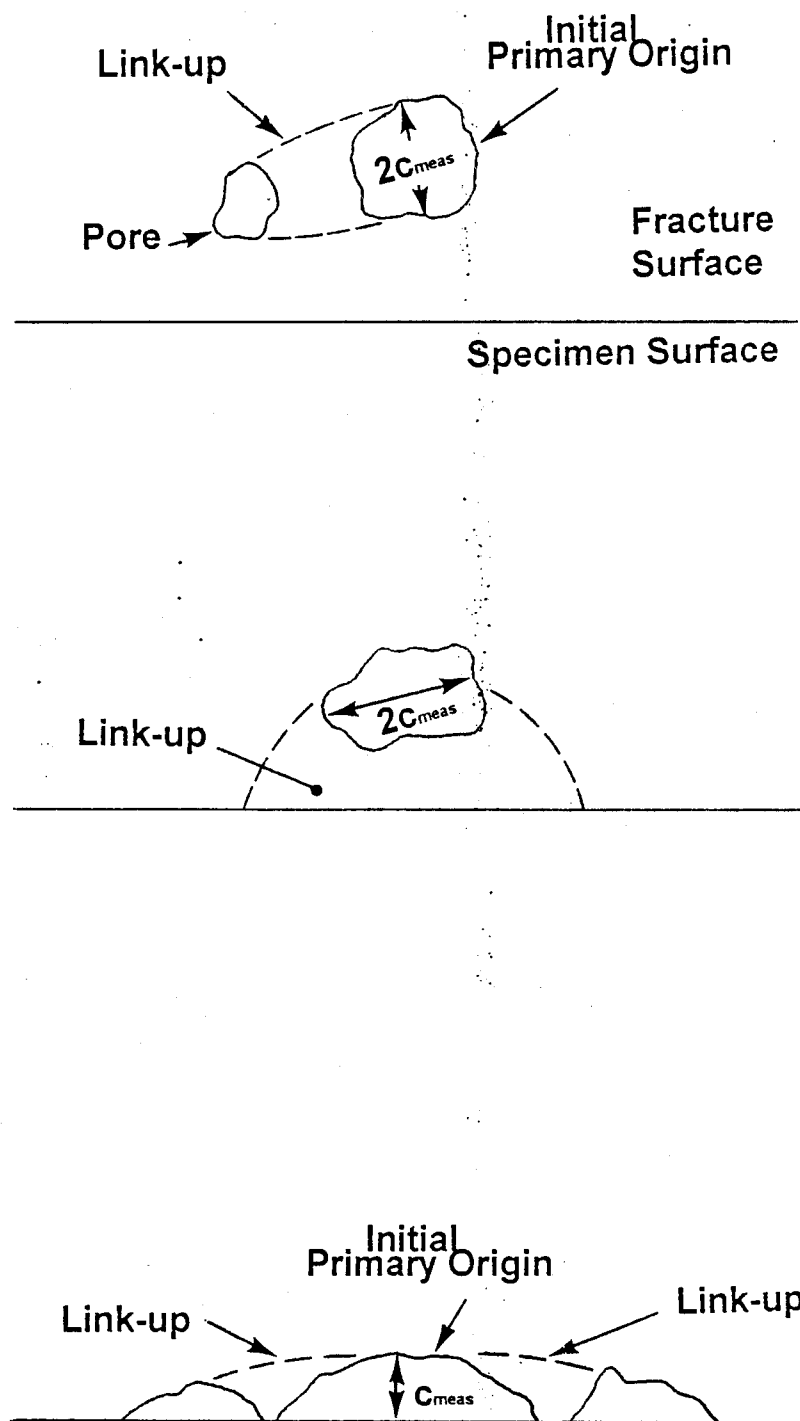


Figure A2.2 A origin can link-up with other discontinuities or with a free surface. The calculated size ( $c_{calc}$ ) will be larger than the size of the original or initially-obvious origin feature ( $c_{meas}$ ).

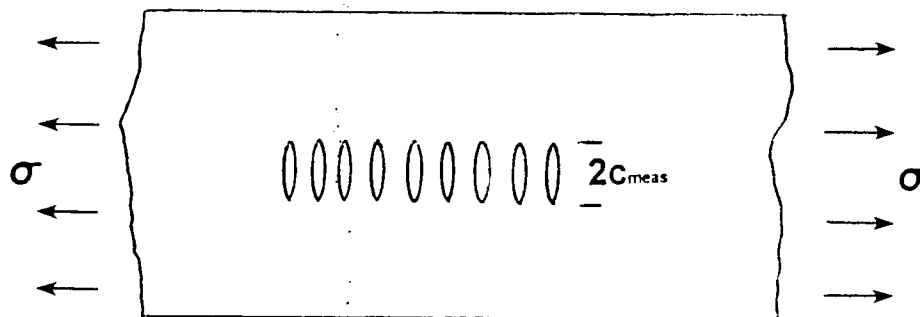


Figure A2.3 Nested, overlapping cracks can lead to a reduction in the stress intensity ( $\gamma$ ) at any single crack. In this case  $c_{calc}$  will underestimate the crack size measured on the fracture surface ( $c_{meas}$ ).

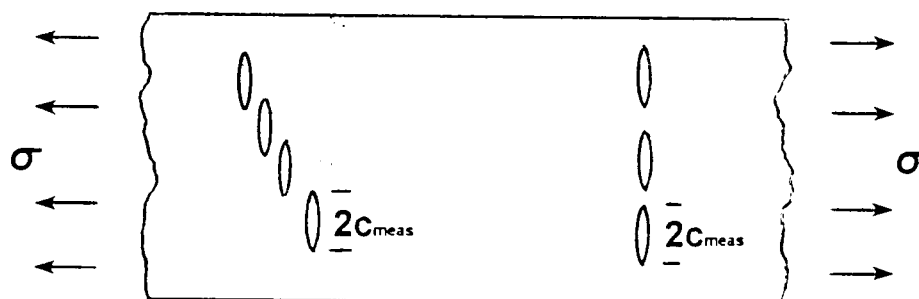


Figure A2.4 Staggered or aligned cracks can cause the stress intensity ( $\gamma$ ) to be magnified at the fracture origin.  $c_{calc}$  will overestimate the measured crack size ( $c_{meas}$ ).

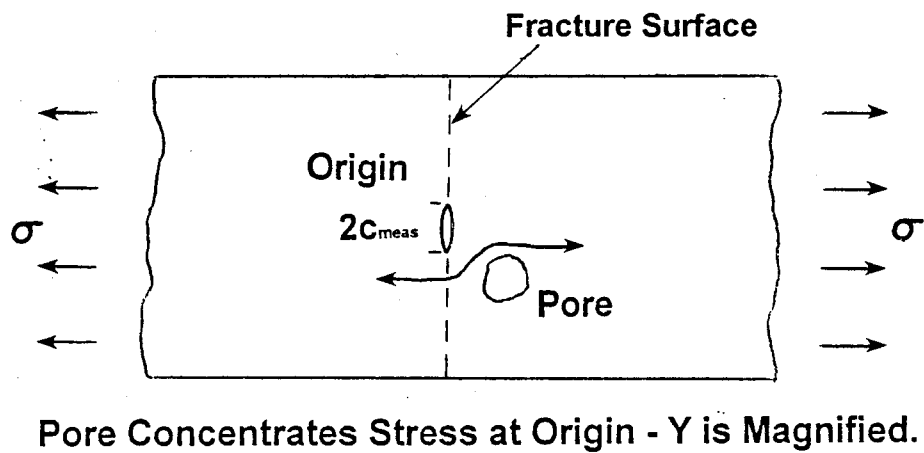
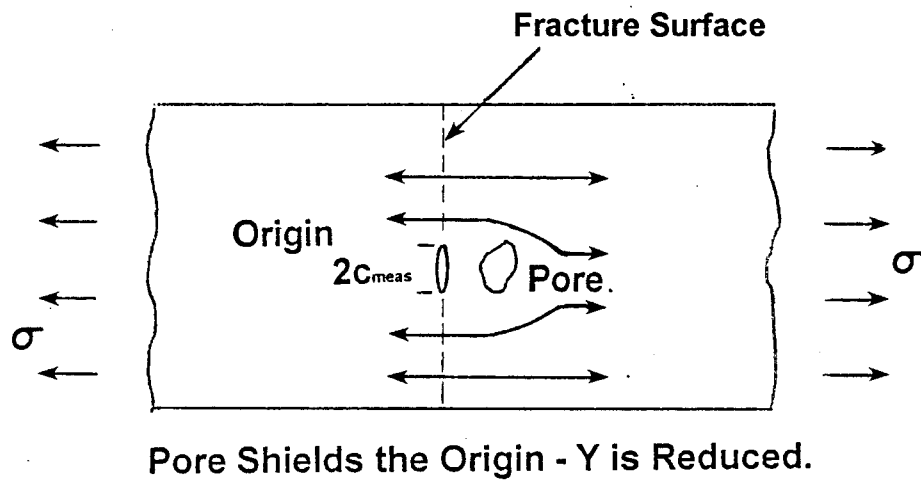


Figure A2.5 Discontinuities in the vicinity of the fracture origin can increase or decrease the stress intensity ( $Y$ ) and result in  $c_{calc}$  being either an over- or underestimate of  $c_{meas}$ .

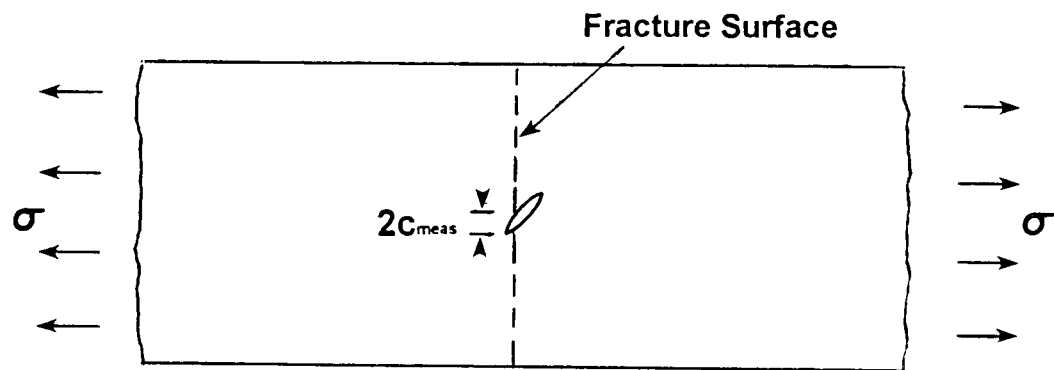


Figure A2.6 The origin may be truncated on the fracture surface, and its size,  $c_{meas}$ , may be underestimated during the fractographic analysis.

### **APPENDIX 3: Synopses Of Participants' Responses, Topics #1 And #2**

The fractographic results of each participating agency are summarized here with the following questions answered for each topic of the round robin. The organizers' comments are shown in *italics* at the end of each topic. There is no appraisal of Topic #3 due to the limited number of participants who chose to take part.

#### **TOPIC #1**

- a) Did the markings on the photographs clearly identify the fracture origin and the associated mirror?
- b) Were both halves of the photograph set marked?
- c) How was the origin and mirror size reported?
- d) Was the size of the origin and mirror estimated? If so, were they compared to measured values?

#### **TOPIC #2**

For each agency a table is provided indicating the participants' and the organizers' characterization of the origins within the specimen set the participant received. The organizers' characterization is immediately below the participants' for each specimen. EXCELLENT AGREEMENT means the participant and organizers agreed on at least the Identity and Location and that the photographs from each showed the same origin.

- a) Where the specimens cleaned prior to examination?
- b) Were coatings applied? If so what types and how were they applied?
- c) Were optical and scanning electron microscopy used?
- d) Which mode(s) of viewing in the SEM were used?
- e) Was elemental analysis (i.e., EDS) used?
- f) Did the agency examine the mating halves of the fracture surface? The external surfaces?
- g) Where the photographs marked to indicate the location and size of the origin?
- h) Was the size of the origin estimated? If so, was it compared to the measured value?

\*All single size values listed in the following tables are origin diameters (2c) unless noted and 2-dimensional values are depth x width for semiellipses and minor axis x major axis for ellipses.



## PARTICIPANT 1

### TOPIC #1

- a) Yes
- b) Only for set #3.
- c) For sets #1 & #2 the origin was represent by a width and for set #3 by depth x width. Mirror radius was reported.
- d) No.

*Focused on possible damage to the tensile surface which may indicate an unfamiliarity of how machining damage can be created and appear in ceramics.*

### TOPIC #2 - SPECIMEN SET: H

<u>No.</u>	<u>Identity</u>	<u>Location</u>	<u>Size (<math>\mu\text{m}</math>)</u>	<u>Comments</u>
1	PR w/LG	NS	80	45 $\mu\text{m}$ below tensile surface; Dark spot when viewed optically
	LG	S	70	
2	PS	S	11	Did not examine tensile surface. Size is scratch width
	HD	S	30	
3	P	S	56 x 68	EXCELLENT AGREEMENT
	P	S	50	
4	P	S	12 x 45	Did not take into account the history of the material.
	PT	S	30 x 275	
5	MD	E	530	Characterized properly but different site
	MD	E	?	
6	P/PR	V	230	EXCELLENT AGREEMENT; Location below surface is 211 $\mu\text{m}$ Located about 200 $\mu\text{m}$ below tensile surface
	PR	V	200	

- a) Sonicated in methanol, rinsed and blasted with canned air
- b) Yes, a Au coating  $\approx 4 \mu\text{m}$  thick
- c) Yes
- d) Secondary electron was used for all. Back scattered mode was also used on 1, 2 & 6
- e) EDS on 2 & 6
- f) Photographs and comments indicate that both fracture surfaces and the external surfaces were examined only for 4 & 5
- g) Yes
- h) No

*Examination of the external surfaces in 2 and the incorporation of the material history into the analysis of 4 may have changed the participants' characterization of these specimens.*

## PARTICIPANT 2

### TOPIC #1

- a) Yes
- b) Yes
- c) A width for sets #1 & #2 and a 2-dimensional value for set #3. Mirror radius was reported.
- d) No.

*Focused on possible damage to the tensile surface which may indicate an unfamiliarity of how machining damage can be created and appear in ceramics.*

### TOPIC #2 - SPECIMEN SET: K

<u>No.</u>	<u>Identity</u>	<u>Location</u>	<u>Size (<math>\mu\text{m}</math>)</u>	<u>Comments</u>
1	I	V/NS	60	Photos agree as does Location & Size; Did not use EDS; 20 $\mu\text{m}$ below surface
	LG	NS	30 x 65	About 20 $\mu\text{m}$ below surface
2	?	NS	?	Did not examine tensile surface
	HD	S	15	Size is scratch width
3	P	V/NS	90	EXCELLENT AGREEMENT; About 20 $\mu\text{m}$ below surface
	P	NS	60	Located about 20 $\mu\text{m}$ below tensile surface
4	SV	S	125	Did not take material history into account
	PT	S	20 x 200	Can not be surface void.
5	MD	S/E	?	EXCELLENT AGREEMENT
	MD	S/E		
6	P	V/NS	170	
	PR	S/NS	100 x 170	About 20 $\mu\text{m}$ below tensile surface

- a) Only air cleaned.
- b) No for 1, 4-6 and 10 nm of Au for 2 & 3
- c) Yes
- d) Secondary electron mode only
- e) No
- f) Only for 1 & 2. Photographs and comments do not indicate that both fracture surfaces or external surfaces were examined.
- g) Only the location.
- h) No

*Examination of the external surfaces in 2 and the incorporation of the material history into the analysis of 4 may have changed the participants' characterization of these specimens. Use of EDS may also have changed the characterization of some origins.*

### PARTICIPANT 3

#### TOPIC #1

- a) Yes
- b) Yes, sets #2 & #3 only
- c) Both had a single dimension: diameter for the origin and radius for the mirror
- d) No.

*Focused on possible damage to the tensile surface which may indicate an unfamiliarity of how machining damage can be created and appear in ceramics. Had difficulty seeing the mirror - "No distinct mirror" in sets #1 and #2*

#### TOPIC #2 - SPECIMEN SET: R

<u>No.</u>	<u>Identify</u>	<u>Location</u>	<u>Size (<math>\mu\text{m}</math>)</u>	<u>Comments</u>
1	LG/P	NS	40	ID'ed properly but ORG believe it is a different area; Origin listed as 5 $\mu\text{m}$ below surface
	LG	S	20 x 120	
2	CK	S	180	Notice HD but called is a CK; Photos do not show tensile surface
	HD	S	30	Size is scratch width
3	I	S	45	EDS reveals Si, Cl, K, Na, Al & S - labeled as I?; No EDS of bulk
	P	S	?	
4	MD?	E	20?	Did not take thermal history into account
	PT	E	20 x 100	
5	MD	S	50 - 75	EXCELLENT AGREEMENT
	MD	S	40 x 90	
6	PR	E	230	EXCELLENT AGREEMENT
	PR	E	100 x 250	

- a) Just "dusted off"
- b) 1 coated with Al, 2-4 with C and 5 & 6 with C + Au/Pd
- c) Yes
- d) Secondary electron mode.
- e) EDS only on 3
- f) Yes, both halves viewed simultaneously under the SEM. Photographs and comments do not indicate that the external surfaces were examined.
- g) Yes
- h) No

*Calibration photograph provided for the SEM. Reported mirror sizes but some of these values were only slightly larger than the origin size.*

## PARTICIPANT 4

### TOPIC #1

- a) Yes
- b) Yes
- c) Diameter for both except for the origin in set #3 which had a radius reported
- d) No\*

*Felt the origins in sets #1 & #2 were shallow half-penny shaped cracks emanating from machining grooves. \*The measured origin size in sets #1 & #2 was used to estimate the mirror constant. The mirror constant was then related to the toughness to obtain a  $K_{Ic}$  value. This value was compared to the provided toughness number. There was excellent agreement in both cases.*

### TOPIC #2 - SPECIMEN SET: J

<u>No.</u>	<u>Identity</u>	<u>Location</u>	<u>Size (<math>\mu\text{m}</math>)</u>	<u>Comments</u>
1	MD	S	3 - 7	Photos agree and show LG; No EDS; Size is very small.
	LG	S	25 x 200	
2	HD	S	c = 63	EXCELLENT AGREEMENT Size is scratch width
	HD	S	10	
3	P	S	100	EXCELLENT AGREEMENT; Could be located at S or E
	P	S/E	20 x 100	
4	I(?)	S	115	Photos agree; "EDS shows Si & O in cavity"
	PT	S	50 x 100	
5	HD	S	c = 91	Noted chipping on chamfer but did not equate to Machining
	MD	S/E		
6	A	NS	450	Agglomerate tends to be denser
	PR	S/NS	200 x 375	

- a) Ultrasonically cleaned 1-4 for 60 seconds in acetone then ethanol
- b) Only 3 was coated with 100 Å of Au/Pd
- c) Yes
- d) Secondary electrons on all. Back scatter was also used on 1 & 4.
- e) Yes, 4 only
- f) Yes, Yes
- g) Yes
- h) No

*Detailed analysis with many optical and SEM photographs.*

## PARTICIPANT 5

### TOPIC #1

- a) Markings were incomplete
- b) No
- c) Both were reported as a radius
- d) Origin size only. Yes, this estimated value was compared to the measured value. If these values did not agree then possible explanations were provided.

### TOPIC #2 - SPECIMEN SET: I

<u>No.</u>	<u>Identity</u>	<u>Location</u>	<u>Size (<math>\mu\text{m}</math>)</u>	<u>Comments</u>
1	?	S	?	Could not identify; Location could be S or NS?; Photos not clear
	LG	S	?	
2	HD	S	20 - 100	EXCELLENT AGREEMENT
	HD	S	30	Size is scratch width
3	PA	S	c = 25-30	Speculated on how origin came about
	P	S	30 X 40	
4	CHIP	E	c = 30 - 35	Did not take thermal history into account
	PT	E	?	
5	CHIP	E	c = 20	EXCELLENT AGREEMENT
	MD	E	125	
6	PA	V	c = 50	Labeled incorrect area
	PR/A	NS	100 x 150	

- a) No cleaning
- b) Yes, with 250 Å of Au.
- c) SEM only
- d) Secondary electron mode only
- e) No
- f) Yes, Yes
- g) No
- h) Yes, mechanical property data was used to estimate the size of the origin and this was compared to what was actually measured.

*SEM time was limited. Some identity codes are inconsistent with MIL HDBK-790. Reasonable agreement was obtained between the estimated origin size and the measured size.*

## PARTICIPANT 6

### TOPIC #1

- a) Yes
- b) No
- c) 2-dimensional values of depth x width in both cases
- d) No

### TOPIC #2 - SPECIMEN SET: P

<u>No.</u>	<u>Identity</u>	<u>Location</u>	<u>Size (<math>\mu\text{m}</math>)*</u>	<u>Comments</u>
1	?	S	30 x 70	Optically reported as "Dark Spot"; Si WDX map indicates depletion of SiC in area of origin
	LG	S	10 x 30	
2	MD	S	20 x 800	Issue of machining or handling damage
	HD	S	30	Size is scratch width
3	P	V	125 x 40	Examination of mating half may have changed Location to S
	P	S	110 x 40	
4	PT	S	40 x 300+	EXCELLENT AGREEMENT
	PT	S/E	25 x 100	
5	MD	E	20 x 65	EXCELLENT AGREEMENT
	MD	E	25	
6	PR	S	100 x 145	EXCELLENT AGREEMENT
	PR	S	80 x 140	

\* not certain if 2-dimensional values are depth x width or minor axis x major axis

- a) Ultrasonically cleaned for 5 minutes in acetone.
- b) 1-4 were coated with C and 5 & 6 with Au.
- c) Yes
- d) Secondary electron mode on all
- e) EDS used on all but 4, and WDX was used on 1
- f) SEM photographs are of only one half of the fracture surface - examined only one half of fracture surface? External surfaces?
- g) Location but not size
- h) No

*Good work by the participant. Examination of the mating half of the fracture surface may have proved to be beneficial to the characterization.*

## PARTICIPANT 7

### TOPIC #1

- a) Yes
- b) Yes
- c) Both were reported as a diameter (2c for origin and 2r for mirror)
- d) No

*Tended to focus on possible machining damage on the tensile surface.*

### TOPIC #2 - SPECIMEN SET: A

<u>No.</u>	<u>Identity</u>	<u>Location</u>	<u>Size (<math>\mu\text{m}</math>)</u>	<u>Comments</u>
1	PS	V	190 x 130	ID'ed as PS but noted presence of LG; Noted LG agrees with calculation of size
	LG	V	50	Located about 180 $\mu\text{m}$ below tensile surface
2	SD/PR	S	120	ID uncertain; Saw HD but seemed to focus on PR
	HD	S	5	Size is scratch width
3	P	E	42 x 100	EXCELLENT AGREEMENT, see Topic #2 for details on location
	P	V	40 x 65	Located $\approx$ 175 $\mu\text{m}$ below the tensile surface
4	PT	S	128	EXCELLENT AGREEMENT
	PT	S	120 x 178	
5	MD	S	30 x 190	Marks on photographs indicate E location
	MD	E	35	
6	PR/A	S	80 x 120	Agglomerate tends to be denser
	PR/PS	S	100 x 160	

- a) "Just blown clean"
- b) All specimens coated with 100 Å of Au/Pd
- c) Yes
- d) Secondary and back scatter modes used on all
- e) No
- f) Yes
- g) Yes
- h) Size estimates of the origin in 1 & 2 were made and compared to the measured value

*Would have had EXCELLENT AGREEMENT on specimen 5 if "Edge" location had been reported. Photographs clearly show the origin located at the edge.*

## PARTICIPANT 8

### TOPIC #1

- a) Identified clearly but not clear enough for the organizers to check the size measurements
- b) No
- c) Single dimension for each, depth for origin and radius for mirror
- d) No

### TOPIC #2 - SPECIMEN SET: B

<u>No.</u>	<u>Identity</u>	<u>Location</u>	<u>Size (<math>\mu\text{m}</math>)</u>	<u>Comments</u>
1	LG	V	30, 20	EXCELLENT AGREEMENT, EDS shows Al; Photos not good quality
	LG	V	50	
2	MD	S	?	Issue of machining or handling damage
	HD	S	15	Size is scratch width
3	P	NS	20 x 80	Location may be different if mating half was examined?
	P	S	30 x 75	
4	I	S	60 x 70	Did not account for thermal history; EDS shows Si - Inclusion?
	PT	S	100 x 120	
5	MD	E	?	EXCELLENT AGREEMENT
	MD	E	?	
6	I	S	230 x 400	Labeled incorrectly, EDS shows only Ti
	PR	S	240 x 380	

- a) Cleaned with compressed air
- b) No
- c) Yes
- d) Secondary electron mode on all
- e) Yes on 1, 4, & 6
- f) Yes? Photographs and comments do not indicate that the external surfaces were examined.
- g) Location - yes
- h) No

*Quality of photographs was below average. Examination of mating halves of the primary fracture surface may have been beneficial. Better interpretation of EDS results is needed.*



## PARTICIPANT 9

### TOPIC #1

- a) Yes
- b) No
- c) 2-dimensional value of depth x width for both
- d) Origin only. Measured the size of the origin and using the Newman-Raju analysis in Ref. 12 to calculate  $Y$ . Then estimated  $K_{Ic}$  and compared it to the  $K_{Ic}$  value provided.

*Calculated  $K_{Ic}$  for set #1 was high (7.3 MPa $\sqrt{m}$ ) and for set #3 is was low (2.7 MPa $\sqrt{m}$ ) when compared to the values proved. An indication that the measured origin size was off, especially for set #3. Good toughness agreement in set #2.*

### TOPIC #2 - SPECIMEN SET: Q

<u>No.</u>	<u>Identity</u>	<u>Location</u>	<u>Size (<math>\mu m</math>)</u>	<u>Comments</u>
1	LG	NE	$c \approx 150$	EXCELLENT AGREEMENT; NE is a possibility; $K_{Ic}$ agrees with origin size
	LG	NS	10 x 50	Located about 25 $\mu m$ below tensile surface
2	MD	S	73 x 217	$K_{Ic}$ agrees w/origin size; Issue of machining or handling damage
	HD	S	10	Size is scratch width
3	P	NS	35 x 80	EXCELLENT AGREEMENT; $K_{Ic}$ was not estimated
	P	NS	75 x 25	Origin may be connected to the surface
4	PT	S	57 x 170	EXCELLENT AGREEMENT
	PT	S	?	
5	MD	E	25 x 65	EXCELLENT AGREEMENT
	MD	E	60 x 100	
6	PR	S	50 x 100	EXCELLENT AGREEMENT
	PR	S	50 x 125	

- a) Ultrasonically in acetone prior to SEM analysis but not optical analysis
- b) Coated with 70nm of Au
- c) Yes
- d) Secondary and back scatter modes used on all
- e) No
- f) Yes, No
- g) Yes
- h) No, but the measured origin size in 1, 2, 4 & 5 was used to estimate the toughness and this was compared to the value provided

*Best agreement among all participants with the organizers. Very detailed effort with plenty of detailed analysis and high quality photographs. Effort and results belie the participants limited experience. Estimated  $K_{Ic}$  from origin size. These values agreed very well with the values provided. Examination of the external surfaces of 2 may have resulted in better agreement with the organizers' characterization.*

## PARTICIPANT 10

### TOPIC #1

- a) Location yes - but not size
- b) Yes, on sets #1 & #2
- c) Single dimension for both
- d) No

*Looked for cracks in the material.*

### TOPIC #2 - SPECIMEN SET: G

<u>No.</u>	<u>Identity</u>	<u>Location</u>	<u>Size (<math>\mu\text{m}</math>)</u>	<u>Comments</u>
1	LG	NS	$\approx 50$	EDS shows origin void of Si, interpreted as SiC LG?; about 20 $\mu\text{m}$ below surface
	LG	S	?	
2	PS	S	75 - 80	Did not look at tensile surface
	HD	S	10	Size is scratch width
3	P	NS	60 - 70	EXCELLENT AGREEMENT
	P	NS	20 x 40	About 5 $\mu\text{m}$ below tensile surface
4	MD	S	90	Did not account for thermal history
	PT	S	30 x 100	
5	CK	NS	5 - 10	Did not look at mating half or chamfer in detail
	MD	E/S	?	
6	A	S	$\approx 150$	"PR from uncrushed agglomerate"
	PR/PS	S	100 x 175	

- a) Ultrasonically in ethanol
- b) Coated with Au
- c) SEM only
- d) Secondary electron mode on all
- e) Only on 1
- f) No, No
- g) Location yes, size no
- h) No

*Examination of the mating halves of the fracture surface and further interpretation of the results from the EDS X-ray map may have resulted in a different characterization of specimen 1.*

## PARTICIPANT 11

### TOPIC #1

- a) Yes
- b) Yes
- c) Single dimension for both, depth? for origin and radius for mirror
- d) Origin only. Used the strength toughness values provided to estimate the origin size then compared this to what they actually measured. Provided detailed explanation if these values did not agree.

### TOPIC #2 - SPECIMEN SET: F

<u>No.</u>	<u>Identity</u>	<u>Location</u>	<u>Size (<math>\mu\text{m}</math>)</u>	<u>Comments</u>
1	I	S	300	"Black area"; Size estimated to be 144 $\mu\text{m}$ ; No EDS
	LG	S	170	
2	HD	S	?	EXCELLENT AGREEMENT; Optical analysis revealed more details than SEM Size is scratch width
	HD	S	30	
3	P/CK	S	$\approx 200$	Looked at only 1/2 of surface; Size estimate = 90 $\mu\text{m}$
	P	S	?	
4	P/MD	S	Depth = 68	Mentioned history in comments but did not tie together; Size estimate agrees
	PT	S	30 x 90	
5	M	V?	?	Very tricky; Possible microstructural feature?; SEM of only 1/2 of fracture surface
	MD	E	?	
6	PR	NS	150 x 400	EXCELLENT AGREEMENT; about 150 $\mu\text{m}$ below surface About 200 $\mu\text{m}$ below tensile surface
	PR	V	250 x 360	

- a) 2, 3 & 5 were cleaned in alcohol
- b) No, a field emission microscope was used
- c) Yes
- d) Secondary electrons on 1-3 and back scattered electrons on 4-6
- e) No
- f) Yes optically, but SEM photographs indicate the examination of only one half of fracture surface in all but 4, Yes
- g) Location yes
- h) Yes, Yes

*Estimated origin size from mechanical property data provided. If the estimated size disagreed with the measured size possible explanations were provided. Quality of photographs were inconsistent; some were too bright and others were too dark.*

## PARTICIPANT 12

### TOPIC #1

- a) Yes
- b) Yes
- c) 2-dimensional value of depth x width for both
- d) No

*Confused the meaning of edge and surface location. Did a credible job for first attempt at fractography.*

### TOPIC #2 - SPECIMEN SET: M

<u>No.</u>	<u>Identify</u>	<u>Location</u>	<u>Size (<math>\mu\text{m}</math>)*</u>	<u>Comments</u>
1	PR/A	NS	15 X 30	
	LG	E	25 x 80	
2	PR	NS	40 X 60	Did not look at tensile surface
	HD	S	10	Size is scratch width
3	P	NS	30 X 80	EXCELLENT AGREEMENT
	P	NS	40 x 75	
4	?	E	25 X 50	Confused meaning of E and S; Difficult to ID; Inexperience shows.
	PT	E	20 x 75	
5	CK/MD	E	10 X 50	Confused meaning of E and S
	MD	E	60 x 380	Difficult one to identify
6	PR	NS	120 X 160	EXCELLENT AGREEMENT
	PR	NS	120	

\* not certain if 2-dimensional values are depth x width

- a) Cleaned with compressed air
- b) No
- c) SEM only
- d) Secondary electron mode for all
- e) No?
- f) Yes, but external surfaces were not. Both halves of fracture surface were mounted tensile surface-to-tensile surface which did not permit the examination of the external surfaces
- g) Yes in some cases but not all
- h) No

*The agencies inexperience with fractography of ceramic materials is evident in this topic. This led to the examination of the wrong area of the fracture surface and misinterpretations in the origin characterization. Even so they did a credible job. Appears to have confused the meaning of edge and surface location.*

## PARTICIPANT 13

### TOPIC #1

- a) Yes
- b) No
- c) Single dimensions for both
- d) No

### TOPIC #2 - SPECIMEN SET: D

<u>No.</u>	<u>Identity</u>	<u>Location</u>	<u>Size (<math>\mu\text{m}</math>)</u>	<u>Comments</u>
1	LG	NS	23 - 75	EXCELLENT AGREEMENT; EDS shows Al in origin
	LG	NS	40	About 10 $\mu\text{m}$ below tensile surface
2	HD	S	?	EXCELLENT AGREEMENT
	HD	S	10	Size is scratch width
3	P	S	10 - 65	EXCELLENT AGREEMENT
	P	S	20 x 40	
4	SV	S	15	Thermal history not taken into account
	PT	S	20 x 25	
5	?	?	?	Examined incorrect region of fracture surface
	MD	S	50 x 85	
6	SV	S	50 - 250	
	LG/PR	S	140 x 170	

- a) Ultrasonically cleaned in ethanol
- b) No coatings on 1, 4 & 6, but 2, 3 & 5 were coated with 10-20  $\mu\text{m}$  of C
- c) SEM only
- d) Secondary and back scatter on 1, 4 & 6; Secondary only on the remainder
- e) Only on 1 & 3
- f) Photographs indicate that only one half of fracture surface was examined, but the external surfaces were examined
- g) In a few instances location only
- h) No

*Excellent quality photographs. Did not take the material history (4) and the origin definition (4 & 6) into account during characterization.*

## PARTICIPANT 15

### TOPIC #1

- a) Yes
- b) No
- c) 2-dimensional of depth x width for origin and radius for the mirror
- d) No

*Not certain about the sizes that were reported because these values could not be confirmed.*

### TOPIC #2 - SPECIMEN SET: C

<u>No.</u>	<u>Identify</u>	<u>Location</u>	<u>Size (μm)</u>	<u>Comments</u>
1	MD	E	Depth = 100	Saw LG zones but "probably not cause of fracture"
	LG	E	30 x 80	
2	HD	S	100 x 190	EXCELLENT AGREEMENT: Photo does not show HD Size is scratch width
	HD	S	25	
3	P	NS	46 x 170	EXCELLENT AGREEMENT
	P	NS	10 x 70	
4	PT	S	34 x 113	EXCELLENT AGREEMENT
	PT	S	?	
5	MD	E	?	EXCELLENT AGREEMENT
	MD	E	?	
6	A	S	160 x 80	ID might be different if mating half was examined
	PR/PS	S	160 x 100	

- a) No
- b) 2 & 3 coated with 20 nm of Au
- c) Yes
- d) Secondary only on all
- e) No
- f) Appears to have examined only one half of fracture surface. External surfaces?
- g) Yes, but markers were not always clear
- h) No

*Good work. Only one photograph was provided for all but specimen 4 and the participant had only one year of fractographic experience. Quality of photographs was not good. The lack of photographs made some of the interpretations and comparisons by the organizers extremely difficult.*

## PARTICIPANT 16

### TOPIC #1

- a) No. The participant marked the plastic holders that the photographs came in, thus it was difficult for the organizers to determine what they were indicating.
- b) Yes.
- c) Single dimension for both
- d) No

*Appears to be a rushed effort.*

### TOPIC #2 - SPECIMEN SET: L

<u>No.</u>	<u>Identify</u>	<u>Location</u>	<u>Size (<math>\mu\text{m}</math>)</u>	<u>Comments</u>
1	LG	NE	40	Appears to have picked one LG as origin; About 75 $\mu\text{m}$ below surface
	LG	NS	35 x 120	About 50 $\mu\text{m}$
2	LG	S	50 - 70	Did not see HD but it can be seen on low magnification photo
	HD	S	30	Size is scratch width
3	P	S	Depth = 38	EXCELLENT AGREEMENT
	P	S	45 x 100	
4	?	?	?	
	PT	S	35 x 75	
5	?	?	?	No origin detected
	MD	E	?	
6	PR	S	Depth = 125	EXCELLENT AGREEMENT
	PR	S	160 x 220	

- a) ?
- b) ?
- c) Appears to be SEM only?
- d) Appears to be secondary electron mode?
- e) No
- f) Appears to have examined only one half of fracture surface? External surfaces?
- g) Sometimes, there were no micrometer markers on many of the photographs
- h) No

*A rushed effort or a lack of experience? Many questions on the data sheet went unanswered. Provided three photographs (as outlined in MIL HDBK-790) of all but specimen 5. Specimens were returned unwrapped and still attached to the SEM stub, but there was no indication of which specimen was which on the stub.*

## PARTICIPANT 17

### TOPIC #1

- a) Yes
- b) Yes, but only sets #1 & #3
- c) Size ranges (max/min) were reported for #1 & #2 and a single dimension for set #3
- d) No

*Focused on possible damage to the tensile surface which may indicate an unfamiliarity of how machining damage can be created and appear in ceramics.*

### TOPIC #2 - SPECIMEN SET: S

<u>No.</u>	<u>Identity</u>	<u>Location</u>	<u>Size (<math>\mu\text{m}</math>)</u>	<u>Comments</u>
1	PR	E	256 !	Did not mention presence of LG
	LG	E	?	
2	A	S	238 !	Did not examine tensile surface Size is scratch width
	HD	S	30	
3	P	S	585 !	EXCELLENT AGREEMENT
	P	S	?	
4	P	S	251 x 46	Did not take thermal history into account
	PT	S	?	
5	MD	E	411 !	EXCELLENT AGREEMENT
	MD	E	?	
6	P/A(?)	S	85 x 89	Examination of mating half may change ID
	PR	S	100 x 75	

! size is the mirror radius rather than the origin size

- a) No
- b) All but 5 were coated with Au
- c) Yes, optical to determine the location of the origin
- d) Secondary electron mode for all
- e) Yes, on 1 & 2. Remainder?
- f) Appears to have examined only one half of the fracture surface with the SEM and none of the external surfaces
- g) Yes
- h) No

*Provided detailed photographs and markings for each specimen. Did not examine the mating half of the fracture surface or the external surfaces, and did not take the material history into account. This may have affected some of the characterizations. Reported mirror radius rather than origin size for all but specimens 4 & 6.*



## PARTICIPANT 18

### TOPIC #1

- a) Markings clearing identified the origin in sets #1 and #2. Origin not marked in set #3
- b) Only for set #2 and #3
- c) Single dimension for origin and radius for the mirror
- d) No

*"Interpretation of several observers did not agree." - participants' comment made about set #2.*

### TOPIC #2 - SPECIMEN SET: E

<u>No.</u>	<u>Identify</u>	<u>Location</u>	<u>Size (<math>\mu\text{m}</math>)</u>	<u>Comments</u>
1	2P	NS	Depth = 58	"Microstructural irregularity"- "very large region w/o SiC whiskers"
	LG	S	35	
2	PR/MD(?)	NS/V	65 (29)	Did not examine tensile surface; MD can not be NS or V Size is scratch width
	HD	S	10	
3	MD	E	60	
	P	E	100	
4	PT	S	50	EXCELLENT AGREEMENT
	PT	S	?	
5	PR/MD	NS/E	15	
	MD	S/E	60	
6	PR	S	81	EXCELLENT AGREEMENT; "Easiest material to deal with"
	PR/PS	S	270 x 150	

- a) Ultrasonically cleaned in acetone
- b) No
- c) Yes
- d) The back scattered electron mode was used for 1 & 2 while the rest were examined using secondary electrons
- e) EDS only on 1 & 2
- f) SEM photographs indicate only one half of the fracture surface was examined. Does not appear that the external surfaces were examined
- g) Yes
- h) No

*Examination of the external surfaces in 2 and the incorporation of the material history into the analysis of 4 may have changed the participants' characterization of these specimens. Use of EDS may also have changed the characterization of some origins.*

# DISTRIBUTION LIST

No. of Copies	To
1	Office of the Under Secretary of Defense for Research and Engineering, The Pentagon, Washington, DC 20301
	Director, U.S. Army Research Laboratory, 2800 Powder Mill Road, Adelphi, MD 20783-1197
1	ATTN: AMSRL-OP-SD-TP, Technical Publishing Branch
1	AMSRL-OP-SD-TA, Records Management
1	AMSRL-OP-SD-TL, Technical Library
	Commander, Defense Technical Information Center, Cameron Station, Building 5, 5010 Duke Street, Alexandria, VA 23304-6145
2	ATTN: DTIC-FDAC
1	MIA/CINDAS, Purdue University, 2595 Yeager Road, West Lafayette, IN 47905
	Commander, Army Research Office, P.O. Box 12211, Research Triangle Park, NC 27709-2211
1	ATTN: Information Processing Office
	Commander, U.S. Army Materiel Command, 5001 Eisenhower Avenue, Alexandria, VA 22333
1	ATTN: AMCSCI
	Commander, U.S. Army Materiel Systems Analysis Activity, Aberdeen Proving Ground, MD 21005
1	ATTN: AMXSY-MP, H. Cohen
	Commander, U.S. Army Missile Command, Redstone Arsenal, AL 35809
1	ATTN: AMSMI-RD-CS-R/Doc
	Commander, U.S. Army Armament, Munitions and Chemical Command, Dover, NJ 07801
1	ATTN: Technical Library
	Commander, U.S. Army Natick Research, Development and Engineering Center Natick, MA 01760-5010
1	ATTN: SATNC-MI, Technical Library
	Commander, U.S. Army Satellite Communications Agency, Fort Monmouth, NJ 07703
1	ATTN: Technical Document Center
	Commander, U.S. Army Tank-Automotive Command, Warren, MI 48397-5000
1	ATTN: AMSTA-ZSK
1	AMSTA-TSL, Technical Library
	President, Airborne, Electronics and Special Warfare Board, Fort Bragg, NC 28307
1	ATTN: Library
	Director, U.S. Army Research Laboratory, Weapons Technology, Aberdeen Proving Ground, MD 21005-5066
1	ATTN: AMSRL-WT
2	Technical Library

No. of Copies	To
1	Commander, Dugway Proving Ground, UT 84022 ATTN: Technical Library, Technical Information Division
1	Commander, U.S. Army Research Laboratory, 2800 Powder Mill Road, Adelphi, MD 20783 ATTN: AMSRL-SS
1	Director, Benet Weapons Laboratory, LCWSL, USA AMCCOM, Watervliet, NY 12189 ATTN: AMSMC-LCB-TL
1	AMSMC-LCB-R
1	AMSMC-LCB-RM
1	AMSMC-LCB-RP
3	Commander, U.S. Army Foreign Science and Technology Center, 220 7th Street, N.E., Charlottesville, VA 22901-5396 ATTN: AIFRTC, Applied Technologies Branch, Gerald Schlesinger
1	Commander, U.S. Army Aeromedical Research Unit, P.O. Box 577, Fort Rucker, AL 36360 ATTN: Technical Library
1	U.S. Army Aviation Training Library, Fort Rucker, AL 36360 ATTN: Building 5906-5907
1	Commander, U.S. Army Agency for Aviation Safety, Fort Rucker, AL 3636 ATTN: Technical Library
1	Commander, Clarke Engineer School Library, 3202 Nebraska Ave., N., Fort Leonard Wood, MO 65473-5000 ATTN: Library
1	Commander, U.S. Army Engineer Waterways Experiment Station, P.O. Box 631, Vicksburg, MS 39180 ATTN: Research Center Library
1	Commandant, U.S. Army Quartermaster School, Fort Lee, VA 23801 ATTN: Quartermaster School Library
1	Naval Research Laboratory, Washington, DC 20375 ATTN: Code 6384
1	Chief of Naval Research, Arlington, VA 22217 ATTN: Code 471
1	Commander, U.S. Air Force Wright Research and Development Center, Wright-Patterson Air Force Base, OH 45433-6523 ATTN: WRDC/MLLP, M. Forney, Jr.
1	WRDC/MLBC, Mr. Stanley Schulman
1	U.S. Department of Commerce, National Institute of Standards and Technology, Gaithersburg, MD 20899 ATTN: Stephen M Hsu, Chief, Ceramics Division, Institute for Materials Science and Engineering

No. of Copies	To
1	Committee on Marine Structures, Marine Board, National Research Council, 2101 Constitution Avenue, N.W., Washington, DC 20418
1	Materials Sciences Corporation, Suite 250, 500 Office Center Drive, Fort Washington, PA 19034
1	Charles Stark Draper Laboratory, 555 Technology Square, Cambridge, MA 02139
1	General Dynamics, Convair Aerospace Division, P.O. Box 748, Fort Worth, TX 76101
1	ATTN: Mfg. Engineering Technical Library
1	Plastics Technical Evaluation Center, PLASTEC, ARDEC, Bldg. 355N, Picatinny Arsenal, NJ 07806-5000
1	ATTN: Harry Pebly
1	Department of the Army, Aerostructures Directorate, MS-266, U.S. Army Aviation R&T Activity - AVSCOM, Langley Research Center, Hampton, VA 23665-5225
1	NASA - Langley Research Center, Hampton, VA 23665-5255
1	U.S. Army Vehicle Propulsion Directorate, NASA Lewis Research Center, 2100 Brookpark Road, Cleveland, OH 44135-3191
1	ATTN: AMSRL-VP
1	Director, Defense Intelligence Agency, Washington, DC 20340-6053
1	ATTN: ODT-5A, Mr. Frank Jaeger
1	U.S. Army Communications and Electronics Command, Fort Monmouth, NJ 07703
1	ATTN: Technical Library
1	U.S. Army Research Laboratory, Electronic Power Sources Directorate, Fort Monmouth, NJ 07703
1	ATTN: Technical Library
1	Dr. Roger Morrell, Building 13, National Physical Laboratory, Teddington, Middlesex, TW11 0LW, UNITED KINGDOM
1	Prof. Dietrich Munz, Kernforschungszentrum Karlsruhe, Postfach 3640, D-7500 Karlsruhe 1, GERMANY
1	Dr. Theo Fett, Kernforschungszentrum Karlsruhe, Postfach 3640, D7500 Karlsruhe 1, GERMANY
1	Dr. Marc Steen, JRC Petten, P.O. Box 2, 1755 ZG Petten, THE NETHERLANDS
1	Dr. P. Moretto, JRC Petten, P.O. Box 2, 1755 ZG Petten, THE NETHERLANDS
1	Dr. W. Vandermeulen, V.I.T.O., Borestang 200, B 2400 MOL BELGIUM
1	Mr. Jakob Kubler, EMPA Dubendorf, Uberlandstrasse 129, CH 8600 Dubendorf, SWITZERLAND
1	Dr. Lennart Carlsson, Swedish National Testing & Research Institute, Box 857, S-501 15 Boras, SWEDEN

No. of Copies	To
1	Dr. Bernard Cales, Ceramiquee Techniques Desmarquest, Z 1. No. 1, Rue de l'industrial, 27025 Evreux Cedex, FRANCE
1	Mr. Jonathan Salem, NASA-Lewis Research Center - 5250, 21000 Brook Park Road, Cleveland, OH 44135
1	Dr. James Wimmer, Allied Signal/Garrett Auxiliary Power Co., 2739 East Washington Street, P.O. Box 5227, Phoenix, AZ 85010-5227
1	Prof. James Varner, Alfred University, NYS College of Ceramics, Alfred, NY 14802
1	Dr. Thomas Hollstein, Fraunhofer, Institut für Werkstoffmechanik, Wohlerstrabe 11, D-7800 Freiburg, GERMANY
1	Dr. Christian Ullner, BAM, Fachgruppe 1.2, Unter den Eichen 87, D-1000 Berlin 45, GERMANY
1	Dr. Kristin Breder, Oak Ridge National Laboratory - HTML, Building 4515, P.O. Box 2008, Oak Ridge, TN 32831-6062
1	Ms. Gail Meyers, GTE Products Corporation, Hawes Street, Towanda, PA 18848
1	Mr. James Edler, Eaton Corporation, P.O. Box 766, Southfield, MI 48037
1	Mr. Reginald Stannard, Morgan Materials Technology Ltd, Bewdley Road, Stourport-on-Severn, Worcestershire DY13 8QR, UNITED KINGDOM
1	Mr. Roy Rice, 5411 Hoport Drive, Alexandria, VA 22310
1	Mr. Michael Foley, Sr. Gobain/Norton Industrial Ceramics, Goddard Road, Northboro, MA 01532
1	Dr. M. Ferber, Oak Ridge National Laboratory - HTML, P.O. Box 2008, MS 6064, Oak Ridge, TN 32831-6062
1	Prof. J. Mecholsky, University of Florida, 256A Rhines Hall, Gainesville, FL 32611
1	Dr. Jill Glass, Sandia National Laboratories, Dept. 1845, MS 0607, Albuquerque, NM 87185-5100
1	Dr. Edwin Beauchamp, Sandia National Laboratories, P.O. Box 5800, Albuquerque, NM 87185-5800
1	Dr. John Helfinstine, Corning Incorporated, SP-FR-4, Corning, NY 14831
1	Dr. George Sines, UCLA, 6532BH, Los Angeles, CA 90024
1	Dr. Richard C. Bradt, University of Nevada-Reno, Mackay School of Mines, Reno, NV 89557-0047
1	Dr. V. D. Frechette, NYS College of Ceramics at Alfred University, Binne-Merrill Hall, Alfred, NY 14802
1	Dr. Steve Freiman, NIST, Bldg. 223, Room A215, Gaithersburg, MD 20899-0001

No. of Copies	To
1	Dr. David Green, Penn State University, 118 Steidle, University Park, PA 16802
1	Dr. Arvid Pasto, Oak Ridge National Laboratoy, P.O. Box 2008, MS 6064, Oak Ridge, TN 37830
1	Dr. Albert Segall, Penn State University-CAM, 511 Deike Building, University Park, PA 16802
	Director, U.S. Army Research Laboratory, Watertown, MA 02172-0001
2	ATTN: AMSRL-OP-WT-IS, Technical Library
10	Authors